CONTROL STRATEGIES FOR SOLAR WATER HEATING SYSTEMS

by

UWE T. HIRSCH

A thesis submitted in partial fulfillment of the
requirements for the degree of

MASTER OF SCIENCE

(Chemical Engineering)

at the

UNIVERSITY OF WISCONSIN-MADISON

1985

CONTROL STRATEGIES FOR SOLAR WATER HEATING SYSTEMS

Uwe T. Hirsch

Under the Supervision of Professor John A. Duffie

In many recent publications, a low collector flowrate strategy for solar domestic hot water (SDHW) systems is recommended; improvements of 10-20% resulting from enhanced tank stratification at reduced flowrates are predicted for these systems. The performance of SDHW systems was investigated using simulations. The effects of collector design, heat exchangers for freeze protection and control alternatives on the predicted system performance improvement were investigated.

Results of detailed TRNSYS simulations were compared with data of field experiments conducted by the National Bureau of Standards. The comparisons were done for side-by-side high and low flowrate SDHW systems in single and double tank configurations. Good agreement between predicted and measured performance indicated that TRNSYS computer simulations are adequate to investigate the behavior of SDHW systems. The optimal collector flowrate for these systems was found to be approximately 10 $l/hr\text{-}m^2$ for the single and the double tank system instead of the originally recommended flowrate of 75 $l/hr\text{-}m^2$.

Flowrate distributions in a collector and in an array were calculated to study the sensitivity of the collector heat removal factor, F_R, (as used in the Hottel-Whillier equation) to nonuniform

flow. The nonuniform flowrate distribution within a collector was found to be negligible, whereas the nonuniform flowrate distribution in an array of three parallel collectors (18 parallel risers) was significant. This was found for a typical collector design with manifold and risers at high and at low flowrates. The distribution is strongly dependent on the number of parallel risers. No significant dependence of F_R was found at either the high or the low collector flowrates, which indicates that the typical design is appropriate for use with the reduced collector flowrate strategy.

Investigations of SDHW systems with heat exchangers showed a reduction of system performance when the flowrate was reduced from standard values on either side of the heat exchanger. The penalty of a reduced heat transfer coefficient at lower flowrate generally outweighs the advantage of a stratified storage tank so that performance improvements for systems with collector storage heat exchangers at reduced flowrates are not likely.

The design of on/off controllers was studied for the reduced flowrate strategy. The turn-off temperature difference ΔT_{off} is calculated according to a design rule which relates the useful energy gain to the pump power consumption. Another control objective is to restrict cycling during periods of low radiation level (start-up, cloud cover, shut-down). With these design rules, the previously used controller settings were recalculated assuming that the set-point for ΔT_{off} was correct for the high collector flowrate. The

calculated controller set-points were significantly different from the ones used in experiments. Simulations with these set-points resulted in a reduction of the solar fraction for systems operated at high collector flowrate, but the effects were found to be insignificant at low collector flowrates. The performance of the base case system decreased steadily with increasing ΔT_{off}.

Simulations with a combined proportional controller and an on/off controller resulted in an increased solar fraction of 2 and 0.5 percentage points for the single and double tank systems, respectively. The proportional controller was set to adjust the flowrate so that the collector outlet temperature did not exceed the supply set temperature.

Another control strategy in which the flowrate was increased to reach a controller set-point for the ratio of total collector flow to load flow did not result in further improvement. Generally the on/off controller is appropriate for the low collector flowrate strategy in SDHW sytems.

APPROVED:

Dec 16, 1985
Date

John A. Duffie, Professor
Chemical Engineering

ACKNOWLEDGEMENTS

I thank Professor John A. Duffie, Jack, who supported me with his guidance and advice for my research, and Professor Sanford A. Klein, Sandy, who always had another idea, question or answer keeping my mind open for new problems. I am very grateful that both Jack and Sandy were advisors and friends, who helped me enjoy my stay and work. I also thank my fellow graduate students and the whole "Solar Lab" staff; without them many problems would have found no answer and many questions would not have been raised. I am glad that I could work in such a supportive environment.

For their personal support I thank my friends Karla and Uta, all the friends I have found here, and my friends in Germany for their "keeping in touch". Particularly I thank my parents, brother and sister who gave me hope, help and determination during the ups and downs of my stay.

Furthermore, I thank Professor Michael Zeitz, the organizer of the successful and unique exchange program between the University of Stuttgart and the Chemical Engineering Department at the University of Wisconsin in which I participated. I appreciate the advice, support and information Professor Zeitz supplied.

Although they influenced my work in many different ways it would not have been possible without the help of any of the persons mentioned. They were all vital to me.

The financial support for this work was supplied during the first two semesters by the German taxpayers through the German Academic Exchange Service (DAAD). During the remaining time funds were made available through the Department of Energy supplied by the American taxpayers.

Finally I dedicate this work to: Horst, Maria, Anette, Peter und meinen Freund Kai. DANKE!

TABLE OF CONTENTS

LIST OF TABLES

LIST OF FIGURES

NOMENCLATURE

This list contains the symbols use in the text. All symbols are also explained the first time they occur in a chapter.

A = tank gross section

A = pipe crossectional area

A_c = collector area

A_w = wall area

b_o = incidence angle modifier coefficient

C_i = constant

C_{min} = minimum capacitance rate in a heat exchanger

C_{max} = maximum capacitance rate in a heat exchanger

C_{hot} = hot side capacitance rate in a heat exchanger

C_{cold} = cold side capacitance rate in a heat exchanger

c_p = specific heat capacitance

D = tank diameter

D = averaged hydrolic diameter of the collector loop

D_p = pipe diameter

DS = controller decision parameter

F' = collector efficiency factor

F_R = collector heat removal factor

f = friction factor

G_T = incident radiation

h_{ft} = heat transfer coefficient to the wall

$K_{\tau\alpha}$ = incidence angle modifier

k_t = tank contents energy transport coefficient

k_w = wall energy transport coefficient

L = length of the total collector flowpath

L_p = pipe length

M_l = total daily load draw

$\overline{M}_c/M_l$ = monthly average daily collector flow over total daily load draw

$(\overline{M}_c/M_l)$ = requested $\overline{M}_c/M_l$ ratio

m_n = mass of individual node

$\dot{m}$ = absolute mass flowrate in tank

$\dot{m}$ = mass flowrate through pipe

$\dot{m}_c$ = collector flowrate

$\dot{m}_{c,P}$ = collector flowrate, proportional controller

$\dot{m}_{c,I}$ = collector flowrate, integral controller

Nu = Nusselt number

n = number of nodes

Pr = Prandtl number

Δp = frictional pressure drop

Δp = pressure drop of the whole system

$\dot{Q}_u$ = rate of useful energy gain

Q_{aux} = energy supplied by auxiliary heater

Q_{load} = energy supplied to load

Q_{cload} = conventional energy supplied to load

Re = Reynolds number

r = ratio

s = tank wall thickness

T = local time-dependent tank temperature

T_a = ambient temperature

$\overline{T}_a$ = mean ambient temperature during operation time

T_{Ci} = collector inlet temperature

T_{Co} = collector outlet temperature

TCT = total daily collection time

T_{ci} = cold side of heat exchanger inlet temperature

T_{co} = cold side of heat exchanger outlet temperature

T_{hi} = hot side heat exchanger inlet temperature

T_{ho} = hot side heat exchanger outlet temperature

T_i = tank temperature in node i

$\overline{T}_p$ = mean pipe temperature during operation time

T_{set} = water supply set-temperature

T_{Ti} = tank return inlet temperature

T_{To} = tank outlet temperature

t = actual time

t_n = node time constant

ΔT = temperature difference

$\Delta T_{measured}$ = temperature difference measured by controller

UA_{HX} = heat exchanger overall heat transfer coefficient

U_L = overall collector loss coefficient

U_p = pipe loss coefficient

U_pA_{pi} = overall loss coefficient of collector inlet pipe

U_pA_{po} = overall loss coefficient of collector outlet pipe

$UA_{loss,i}$ = overall loss coefficient of node i

$\dot{V}$ = highest volume flow through storage tank

$\dot{V}$ = volume flowrate

V_n = node volume

V_t = tank volume

v = fluid velocity in pipe

ε = heat exchanger effectiveness

λ_c = effective thermal conduction coefficient

λ_t = thermal conduction coefficient of tank contents

λ_w = thermal conduction coefficient of tank wall

η_p = collector efficiency

η_p = pump efficiency

ρ = fluid density

ρ = water density

$(\tau\alpha)$ = transmittance absorptance product

Δt = simulation timestep

Δt = timestep of available data

I. INTRODUCTION

In recent publications solar researchers [1-6] suggested to reduce the collector flowrate for solar domestic hot water (SDHW) systems stratifying the solar storage tank and thereby to enhance system performance. These suggestions found a widely positive response and are now introduced to industrial designs. SDHW systems accounted for more than 70% of the solar industries production in 1984 [7]. They are used throughout the United States and have to face extreme climates and very different owner needs. The reduced collector flowrate raises questions of applicability in already installed systems, of the need for new control strategies and of compatibility of low collector flowrate with standard system components. Comparisons for one- and two-tank SDHW system simulations with side-by-side experiments, the problem of flowrate distribution in collectors at reduced collector flowrate, the system performance of SDHW systems with heat exchangers and the effect of controllers with proportional and integral criteria on the system performance at reduced collector flowrates are presented. The first chapter gives general descriptions of the type of systems used, a brief discussion of published results and an outline of this investigation.

I.1 System Description

Two SDHW systems are of general interest: one-tank and two-tank systems. A one tank system integrates solar preheating and auxiliary heating in one storage tank. The obvious advantages are reduced in-

vestment and a smaller tank surface area resulting in lower tank losses. A disadvantage is that solar preheated water can mix with the tanks auxiliary heated portion, thereby increasing the operation time of the auxiliary heater. A two-tank setup will prevent this, because the auxiliary and solar heating are separated. The larger surface area of the storage accounts for increased losses. These losses usually result in lower solar fractions for two-tank systems than for otherwise identical one-tank systems. It is still useful to have a two-tank system, especially if the losses are accounted towards the heating of the building.

Parts of this investigation are comparisons between experimental data from Fanney [8] and simulations. Therefore the base case systems used in the simulation studies were chosen to correspond to the experimental systems investigated by Fanney. A schematic of the NBS systems in one-tank and two-tank modes is shown in Figures I.1 and I.2. The parameters used in the simulations are, unless otherwise noted, in Table I.3. All simulations conducted were done with TRNSYS [9].

To have uniform system parameters for simulation comparisons the experimentally measured parameter data had to be reduced. With the method outlined by Duffie and Beckman [10] six flowrate dependent collector efficiency curves were recalculated at an average flowrate of 35.5 $l/hr\text{-}m^2$ Pipe losses, which were computed from two sets of nine day experimental data, were then accounted for in the averaged $F_R(\tau\alpha)$ and F_RU_L values with a scheme outlined by Duffie and Beckman. They

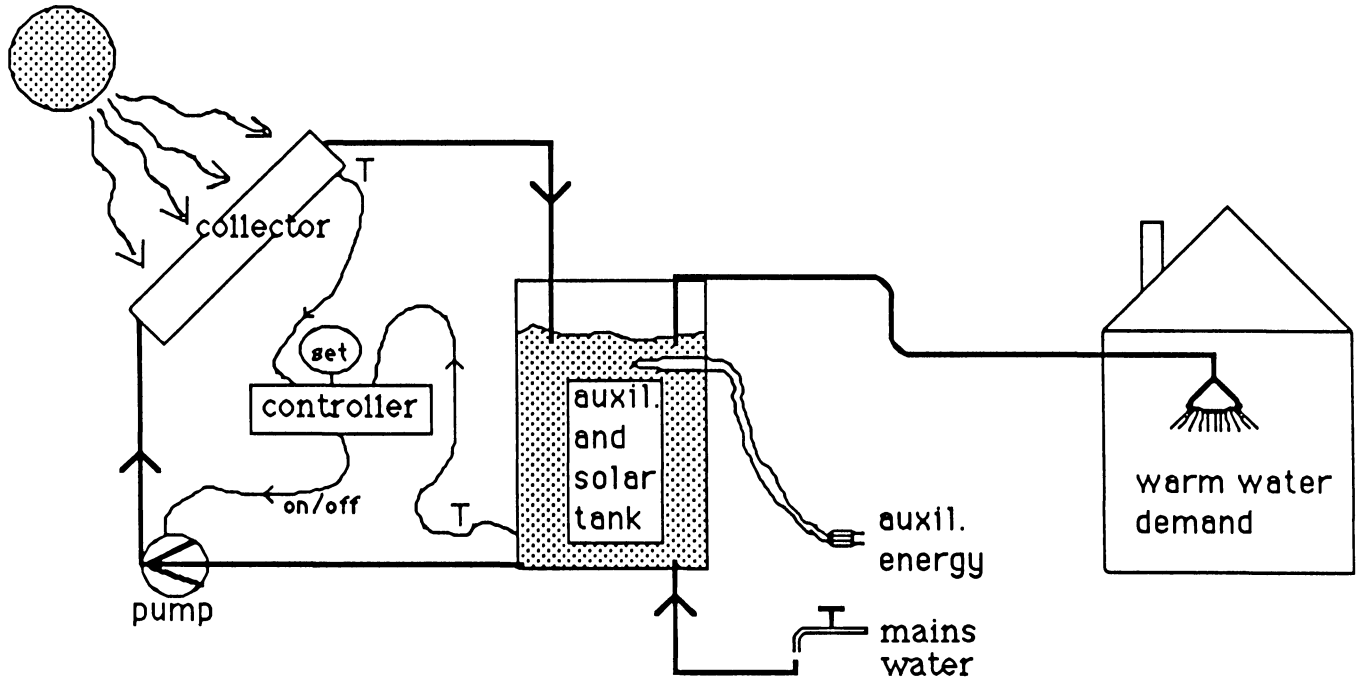

Figure I.1. Single-tank solar domestic hot water system. Schematic of the system setup used for simulations and experiments.

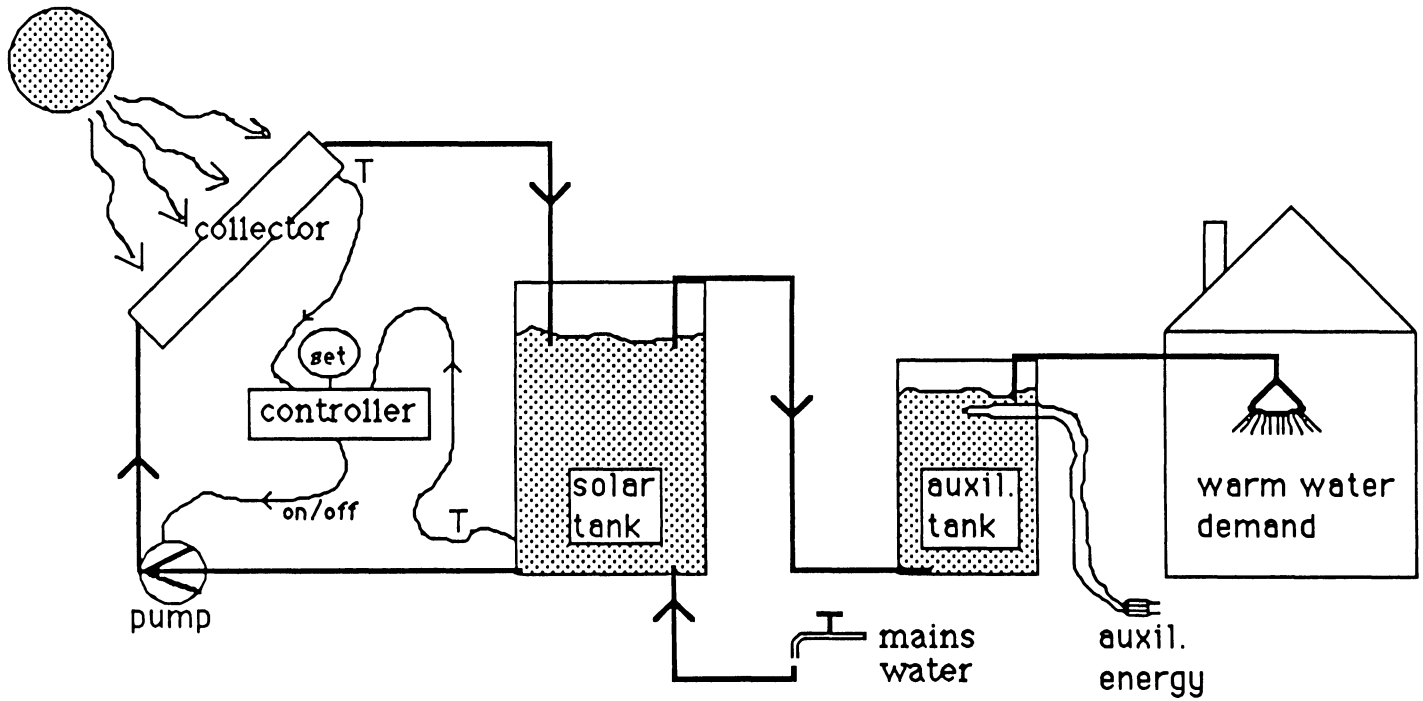

Figure I.2. Double-tank solar domestic hot water system. Schematic of the system setup used for simulations and experiments.

Parameter	Value
Collector:	
area	4.2 m^2
$F_R(\tau a)_n$	.763
$F_R U_L$	5.139 W/°C-m^2
test flowrate	150 l/hr
incidence angle modifier coefficient b_o	.1
tilt ß	43°
Pipes:	
diameter	12.7 mm
length to collector	7.85 m
length from collector	8.96 m
Pipe UA	2.77 W/°C
Tanks:	
solar tank volume, height	275 l, 1.5 m
UA	2.78 W/°C
auxil.tank volume, height	135 l, 1.4 m
UA	1.95 W/°C
max. auxil. power	3.5 kW
T_{set} , $\Delta T_{deadband}$	60 °C , 5 °C
Pump Controller:	
ΔT_{on}	11.1 °C
ΔT_{off}	2.8 °C
high flowrate	300 l/hr
low flowrate	37.5 l/hr
Load:	260 l/day, RAND distributed

Table I.3. System parameters used in TRNSYS simulations. From the parameter specifications of the experimental NBS system for single- and double-tank systems.

were combined to an average efficiency curve at the flowrate of 35.5 $l/hr\text{-}m^2$. In all simulations this efficiency curve was input to the TRNSYS collector model routine.

The two-tank and one-tank system are identical except for the second tank. In the experimental tests of the two-tank system, the heating element in the preheat tank was disconnected. The outlet of the preheat tank was connected to the inlet of the auxiliary tank. The upper and lower temperature deadbands shown in Table I.3 for the on-off controller are identical with those used in the experimental setup of Fanney.

I.2 Low Collector Flowrates And Stratified Tanks

The idea of low collector flowrates is not all new. Thermosyphon SDHW systems performed better than active SDHW systems in several cases [11,12] or they are at least comparable to the active SDHW system performance [13]. Low collector flowrates are inherent in these systems, which implies that active SDHW system performance can be improved by reducing the collector flowrate. That this idea did not advance as fast as the high flowrate approach is mainly due to the effort to increase the collector efficiency. This effort leads to a high flowrate because of the relation between collector efficiency and collector flowrate as derived from the Hottel-Whillier equation [10].

That a stratified tank enhances system performance is well known. Many publications deal with the questions on how to enhance stratification. Two main aspects are: to achieve any stratification

a driving force, the temperature difference over the collector, has to be sufficiently high, and second to use this temperature difference, internal tank mixing has to be minimized.

VanKoppen, Sharp, Veltcamp, Cole, Lavan and others [2,5,14-16] suggested that the optimum collector flowrates are significantly lower than the flowrates recommended to achieve high collector efficiencies, because they enhance the stratification of storage tanks. In an extensive simulation study, Wuestling [1] found that the system performance can be improved by 10 to 15 percent. This is consistent with results of vanKoppen [2] and Sharp [5] and somewhat less than Lunde [3] and Veltcamp [15] predicted. The optimum flowrate Wuestling found is at about 10 $l/hr\text{-}m^2$ or about one for $\overline{M}_c/M_l$, the ratio of monthly average daily collector flow and daily load flow, for a variety of two-tank SDHW systems. The base case system described by Wuestling has a storage tank sized to have a volume of the total daily load draw. Therefore, the recommended reduced collector flowrate coincides with other recommendations of an average once-a-day tank turnover [3,14].

Low collector flow SDHW systems are a significant step towards higher active system performance. The number of publications reflects the impact low collector flowrates can have. Collector design changes for reduced collector flowrates are now introduced to commercial users by collector manufacturers [17], which underlines the importance of the reduced collector flowrate strategy.

I.3 Objectives

The objectives of this work are to verify simulation results of SDHW system performance at low collector flowrates to explore the following four points concerning the operation of SDHW systems at low collector flowrates.

I.3.1 First, Comparison of Simulation Results with Experimental Data

Fanney [8] provided hourly experimental data from simultaneous high and low collector flowrate tests. With these data a comparison between experimental data and TRNSYS simulation results was conducted and used for verification of the simulation. They were for one-tank and two-tank SDHW systems for a nine day period each. The tests were done in August 1984 for the two-tank system and in September 1984 for the one tank system at the NBS facility in Gaithersburg, MD. Weather data measurements, a detailed system description and system parameters were provided.

I.3.2 Second, Compatibility of Low Collector Flowrates and Collector Design

At a reduced collector flowrate the question whether the flowrate distribution in solar collectors has a significant effect on the collector heat removal factor F_R is of interest. Most commercial collectors for SDHW systems are manufactured for high flowrates, which provide a high collector heat removal factor F_R. At high flowrates (about 75 $l/hr\text{-}m^2$) collector design has a significant impact on the frictional pressure drop. Because of easy manufacturing collectors usually feature a lower and upper header with a number of risers

between them. Experimental experience [18-21] indicate that the collector flow distribution becomes more uneven with reduced collector flowrates. This does not agree with calculations of collector flow distributions as described in Chapter III. The discrepancy may be explained by differences between individual risers, which account for a superimposed pressure drop. This additional pressure drop disturbs the collector flow distribution more at low than at high collector flowrates, which explains experimental experiences. Identical risers produce collector flow distributions which become more even with reduced collector flowrates. Comparison of a collector pressure drop and flow distribution computation routine with analytical work of Dunkle and Davey [22,23] is presented. The calculation routine allows the input of individual effective riser lengths. Furthermore it is not restricted to laminar riser and turbulent header flow, which was assumed in the analytical solution of Dunkle and Davey.

One question arises from the degree of collector flow distribution: how is the F_R value affected, if the difference between the real collector flow distribution and the assumed even distribution increases. The effect on F_R determines whether the performance of already installed systems of standard design can be improved by reducing the collector flowrate and whether major collector design changes are necessary.

I.3.3 Third, Compatibility of Low Collector Flowrates and Heat Exchangers

Since SDHW systems are used in all kinds of climates, freezing conditions have to be taken into account for many systems. Three basic freeze protection methods are possible: removal of water from the collector at temperatures below a set freeze temperature or as the response to another control action (drain down or drain back systems), heating of the collector at freezing conditions (auxiliary and recirculation systems) and the use of a heat removal fluid, which does not freeze at the lowest expected temperature. The first two methods use water but need a special freeze control feature (except shut off drain back systems), whereas the latter works without additional control but employs a heat exchanger between the collector and solar storage tank. The collector heat removal fluid is usually an ethylene-glycol/water mixture. Glycol/water SDHW systems are widely used but to date no investigation of possible collector flowrate strategies has been conducted for a system with this freeze protection method. The best combination of collector and tank side flowrate for a given SDHW heat exchanger system is not obvious, but has to be thoroughly investigated by experiments or simulations. Detailed measurements for different collector and tank side flowrates for a heat exchanger have been made by Fanney and the test data are available. The heat exchanger tested will be used in similar side by side experiments as described in I.3.1. The test data were input to a series of TRNSYS simulations revealing the performance of a

glycol/water SDHW system with a heat exchanger at a wide range of possible collector and tank side flowrate combinations. Direct comparison with the same weather data base have not been conducted. Nevertheless, a comparison of trends was made and is outlined.

I.3.4 Fourth, Changes in the Control Strategy for Low Collector Flowrates

After determining that low collector flowrates enhance the performance of SDHW systems, the question remains as to what is the best control strategy and the best controller setpoints for SDHW systems. From a control point of view, there are a lot of differences for a low collector flowrate SDHW system. Increased delay times are due to piping and collector time constants. The ratio of the thermal mass of system components and the capacitance rates increases. The increased time constants are proportional to the flowrate reduction. Pumping power requirements are reduced to a fraction of what they were at a high collector flowrate. This parasitic power reduction alone could justify the reduction of the collector flowrate, even without other performance gains. An on/off controller, designed to control the energy collection of the SDHW system, might not be appropriate. Proportional or integral control strategies for the low collector flowrate systems may enhance the performance.

Economic reasons do not allow expensive controllers and reliability dictates simple controllers with a small number of sensors. These are the reasons to prevent complex sophisticated controllers. The effect of low collector flowrates on pump cycling at various

temperature deadbands was investigated for an on/off controller. Results for a control strategy, which allows to increase the flowrate to prevent temperatures higher than the tank set temperature, are presented. A control strategy to meet Wuestlings criteria of $\overline{M}_c/M_1$ of approximately one is also included.

II. VALIDATION OF TRNSYS SIMULATION RESULTS WITH NBS EXPERIMENTAL DATA

An important step when using computer simulation routines is a validation of its computations. This point is particularly critical for investigations of small changes compared to overall results. The best validation of simulations is comparison with experimental field data. This chapter describes TRNSYS simulations and comparisons of simulations with experiments.

II.1 System Parameter Determination

TRNSYS [9] (TRaNsient SYStem) is a modular structured digital simulation program featuring many standard modules containing descriptions of (energy) system components. An executive program handles energy, mass and information flows through a system. Simulations are initiated by setting up a simulation deck. The TRNSYS deck is a simulation and system description. It tells TRNSYS which component output to use as an input to another component and contains the component parameters for each module in the simulation. It also contains other information such as the simulation-time length, start time, timestep etc. Time-dependent forcing functions such as weather data, pure algebraic computations and Input/Output are treated like modular components of a system. At each time step, inputs of interconnected modules are checked for convergence by the executive routine at a user specified tolerance. Internal loops are therefore executed until they converge or reach an iteration limit. After a

user-specified number of unsuccessful attempts to reach convergence the simulation will be terminated to prevent output of incorrect simulation results.

The original purpose of TRNSYS and its main use is the simulation of energy flow systems such as SDHW systems. The performance of SDHW system components depends on a time dependent input (e.g., radiation data, ambient temperature, etc.) and constant characterizing parameters such as area, volume etc.

II.1.1 Collector Efficiency Data Reduction

As shown in [10] the instantaneous collector efficiency equation can be derived from the Hottel-Whillier equation

$$\dot{Q}_u = A_c[F_R(\tau\alpha)G_T - F_R U_L(T_i - T_a)] \qquad (II.1)$$

by dividing by the product of incident radiation and collector area to yield

$$\eta = \frac{\dot{Q}_u}{G_T A_C} = F_R(\tau\alpha) - F_R U_L \frac{(T_i - T_a)}{G_T} \qquad (II.2)$$

where: $\dot{Q}_u$ = rate of useful energy gain

A_c = collector area

F_R = collector heat removal factor

$(\tau\alpha)$ = transmittance absorptance product

U_L = overall collector loss coefficient

T_i = collector heat removal fluid inlet temperature

T_a = ambient temperature

G_T = incident radiation

A linear efficiency is ordinarily derived from measurements according to the ASHRAE 93-77 Test Procedure [24].

$F_R(\tau\alpha)$ and F_RU_L are functions of the collector flowrate. Therefore, a conversion from the collector flowrate at test conditions to the operating flowrate is necessary. The correction factor, r, derived by Duffie and Beckman [10] for $F_R(\tau\alpha)$ and F_RU_L is

$$r = \frac{\left[\dot{m}_c c_p / A_c F'U_L \left(1 - \exp\left(-\frac{A_c F'U_L}{\dot{m}_c c_p}\right)\right)\right]_{\text{operation condition}}}{\left[\dot{m}_c c_p / A_c F'U_L \left(1 - \exp\left(-\frac{A_c F'U_L}{\dot{m}_c c_p}\right)\right)\right]_{\text{test condition}}} \qquad \text{(II.3)}$$

where: F' = collector efficiency factor

c_p = specific heat of fluid

$\dot{m}_c$ = collector flowrate

Assuming $F'U_L$ does not change between the test and the operating conditions,

$$F'U_L = -\frac{\dot{m}_c c_p}{A_c} \ln\left(1 - \frac{F_R U_L A_c}{\dot{m}_c c_p}\right) \qquad \text{(II.4)}$$

can be used in Eq. (II.3) for test and operating conditions.

Collector efficiency tests require that the collector be (nearly) perpendicular to the incident radiation. The dependence of $(\tau\alpha)$ on the angle of incidence, θ, as noted in [10] can be accounted for

by the use of a linear incidence angle modifier

$$K_{\tau\alpha} = \frac{(\tau\alpha)}{(\tau\alpha)_n} = 1 - b_o\left(\frac{1 - \cos\theta}{\cos\theta}\right) \qquad \text{(II.5)}$$

This linear expression is sufficient for angles of up to 60°. For angles between 60° and 90° a linear decrease to zero is used in TRNSYS. The incidence angle modifier coefficient b_0 is also determined according to the ASHRAE 93-77 standard. Equation (II.5) shows good agreement with the first part of the curve of $(\tau\alpha)$ vs. angle of incidence. The error in $K_{\tau\alpha}$ caused by the nonlinear dependence of $K_{\tau\alpha}$ on Θ at large angles of incidence is not significant, because radiation levels at large Θ are low. This is true provided that collectors are orientated toward the equator with a tilt approximately equal to the latitude. The incidence angle modifier is independent of collector flowrate, therefore b_0 from Table I.3 can be used at any collector flowrate.

Fanney provided six linear efficiency functions for the collectors used in NBS experiments. The parameters of these efficiency curves are given in Table II.1. The collectors were evaluated at different flowrates between 71.5 l/hr-m^2 and 11.9 l/hr-m^2. The efficiency at 8.93 l/hr-m^2 for the low collector flowrate experiments could not be measured because of an excessive time constant at that flowrate. To exclude experimental uncertainties for simulation comparisons at various collector flowrates an efficiency curve was calculated by combining the measured efficiency curves. The collec-

specific flowrate	$F_R(\tau\alpha)$	F_RU_L	r
[1/hr-m^2]	[-]	[W/ °C]	[-]
71.28	.81	5.12	.97
53.46	.79	4.51	.98
35.64	.77	4.19	1
26.73	.76	4.36	1.02
17.82	.73	4.36	1.06
11.88	.67	4.07	1.16
average specific flowrate	average $F_R(\tau\alpha)$	average F_RU_L	
35.64	.775	4.56	

Table II.1. Measured efficiency curves of collectors used by Fanney at various collector flowrates. Averaged efficiency without pipe losses.

tor flowrate correction factor was calculated using Eq. (II.3) for a mean collector flowrate of 35.5 $l/hr\text{-}m^2$. Then, the average $F_R(\tau\alpha)$ and F_RU_L were calculated using the individual correction factors as weighting functions so that

$$\overline{F_R(\tau\alpha)} = \frac{1}{N} \sum_{i=1}^{N} r_i[F_R(\tau\alpha)]_i \qquad \text{(II.6)}$$

and

$$\overline{F_RU_L} = \frac{1}{N} \sum_{i=1}^{N} r_i[F_RU_L]_i \qquad \text{(II.7)}$$

where N is the number of collector efficiency curves. With these values a standard efficiency curve for simulations is found. The averaged values are in Table II.1 not including pipe losses.

II.1.2 Pipe Loss Estimation

Pipe losses can be significant for the performance of a system and should therefore be taken into account. The parameter information from Fanney did not include pipe heatloss coefficients. However, the hourly data did include the collector outlet, tank inlet, and ambient temperature, as well as the collector flowrate and pump operating time. These data can be used to estimate the energy loss of the pipe Q_{pl}. Q_{pl} is calculated as

$$Q_{pl} = \sum_{\substack{\text{operating} \\ \text{time}}} \dot{m}_c c_p (T_{Co} - T_{Ti})\, \Delta t \qquad \text{(II.8)}$$

where: T_{Co} = collector outlet temperature

T_{Ti} = tank return inlet temperature

Δt = timestep of available data

With pipe surface area A_p, expressed by pipe length L_p and pipe diameter D_p, Q_{pl} also is

$$Q_{pl} = (\pi D_p L_p)\, U_p (\bar{T}_p - \bar{T}_a) \sum_{\text{operating time}} \Delta t \qquad \text{(II.9)}$$

where: U_p = pipe loss coefficient

$\bar{T}_p$ = mean pipe temperature during operation time

$\bar{T}_a$ = mean ambient temperature during operation time

Combination of Eqs. (II.8) and (II.9) yields U_p

$$U_p = \frac{\sum_{\text{operating time}} \dot{m}_c c_p (T_{Co} - T_{Ti})\, \Delta t}{(\pi D_p L_p)(\bar{T}_p - \bar{T}_a) \sum_{\text{operating time}} \Delta t} \qquad \text{(II.10)}$$

All of the data needed to compute U_p with Eq. (II.10) for the collector→tank pipe were supplied; however, the data for the tank→collector pipe were not available.

To integrate the pipe losses into the collector efficiency function, two factors derived in [10] were used

$$\frac{(\tau\alpha)'}{(\tau\alpha)} = \frac{1}{1 + \dfrac{U_p A_{po}}{\dot{m}_c c_p}} \qquad \text{(II.11)}$$

and

$$\frac{U_L'}{U_L} = \frac{(\tau\alpha)'}{(\tau\alpha)} \left(1 - \frac{U_p A_{pi}}{\dot{m}_c c_p} + \frac{U_p A_{pi} + U_p A_{po}}{A_c F_R U_L}\right) \qquad \text{(II.12)}$$

with: U_pA_{pi} = overall loss coefficient of collector inlet pipe

U_pA_{po} = overall loss coefficient of collector outlet pipe

Setting

$$U_pA_{pi} = 0$$

for the pipe from tank to collector and with the averaged collector efficiency curve parameters of Table II.1 the final values of $F_R(\tau\alpha)$ and F_RU_L are

$$F_R(\tau\alpha) = 0.763 \; ; \quad F_RU_L = 5.139 \; W/(°Cm^2)$$

at a collector flowrate of 35.64 l/hr-m^2.

II.1.3 Thermal Conduction in Solar Storage Tanks

For standard operating conditions, i.e. high collector flowrate, thermal conduction is negligible in active SDHW storage tanks. They operate at high collector flowrates resulting in a large number of daily tank turnovers so that mixing of collector return and stored water substantially degrades the temperature gradient in the tank and thermal conduction effects. Low collector flowrate SDHW systems, however, achieve a much higher degree of stratification so that thermal conduction effects could be significant.

For thermosyphon systems, Morrison and Braun [12] point out that for a height-to-diameter ratio, H/D of 2.7, the conduction related decrease in system performance is small, but it becomes significant for H/D = 1. Simulations and estimations were used to determine the

effects of thermal conduction in the water and in the tank wall on long-term system performance.

A multi-node model of a tank with thermal conduction between nodes was developed by extending the one dimensional multi-node tank currently included in the TRNSYS library [9]. The energy balance for tank node i is

$$A H \rho c_p \frac{dT_i}{dt} = [\dot{m} c_p T_{i-1} + \frac{\lambda_c}{H} A(T_{i-1} - T_i)] - [UA_{loss,i}(T_i - T_a) + \dot{m} c_p T_i + \frac{\lambda_c}{H} A(T_i - T_{i+1})] \quad \text{(II.13)}$$

with: A = tank gross section

H = height of node

ρ = fluid density

T_i = temperature of node i

λ_c = effective thermal conduction coefficient

$UA_{loss,i}$ = overall loss coefficient of node i

If thermal conduction is neglected ($\lambda = 0$) Eq. (II.13) is identical with the standard TRNSYS tank model. The overall tank height divided by the number of nodes determines the distance for the conductive energy transport which is a parameter in Eq. (II.13). Simulation results were obtained with a 10 node model since significant changes could not be observed with more nodes.

The ratio of conductive energy flow through the tank wall to that through the water is

$$\frac{\dot{Q}_{c,wall}}{\dot{Q}_{c,tank}} = \frac{k_w A_w \Delta T}{k_t A \Delta T} \tag{II.14}$$

with

$$k_w = \left(2\,\frac{1}{h_{ft}} + \frac{H}{\lambda_w}\right)^{-1} \tag{II.15}$$

$$A_w = \pi(D + s)s \approx \frac{4\,s}{D}\,A \tag{II.16}$$

$$k_t = \frac{\lambda}{H} \tag{II.17}$$

$$h_{ft} = \frac{Nu}{H}\,\lambda \tag{II.18}$$

$$\Rightarrow k_w = \frac{1}{H}\left(\frac{Nu\,\lambda\,\lambda_w}{2\lambda_w + Nu\lambda}\right) \tag{II.19}$$

$$Nu = 3.66 + \frac{0.0677(Pr\ Re\ D/H)^{1.33}}{1 + 0.1\ Pr(Re\ D/H)^{0.83}} \tag{II.20}$$

where:

k_w = wall energy transport coefficient

k_t = tank contents energy transport coefficient

A_w = wall area

ΔT = temperature difference

λ_w = thermal conduction coefficient of wall

λ_t = thermal conduction coefficient of tank contents

h_{ft} = heat transfer coefficient to the wall

D = tank diameter

s = wall thickness

Pr = Prandtl number

Re = Reynolds number

Nu = Nusselt number

Combination of Eqs. (II.14)-(II.20) yields

$$\frac{\dot{Q}_{c,wall}}{\dot{Q}_{c,tank}} = \frac{4s\ Nu\ \lambda_w}{D(2\lambda_w + Nu\lambda)} \qquad (II.21)$$

This ratio is listed in Table II.2 for typical tank designs and flowrates. The thermal conduction through the tank wall is less than 10% of the conduction through the water for all cases. Therefore, an upper limit on the real conduction value can be conservatively estimated by increasing the thermal conduction coefficient of the tank

flowrate [1/hr]	steel	plastic
300	.05	<.01
225	.04	<.01
150	.04	<.01
75	.03	<.01
37.5	.02	<.01

Table II.2. $Q_{c,wall}/Q_{c,tank}$ for various flowrates. With: D = 0.5 m; s = 5 mm; λ_{steel} = 50 W/m-°C; $\lambda_{plastic}$ = 0.36 W/m-°C.

contents by 10%. Including this increase, the conduction coefficient of water is 0.7 [W/m-°C] at 50°C [25].

The solar fraction f from monthly simulations was chosen to measure the effect of thermal conduction on SDHW system performance.

$$f = 1 - \frac{Q_{aux}}{Q_{load}} \qquad \text{(II.22)}$$

where: Q_{aux} = energy supplied by auxiliary heater

Q_{load} = energy supplied to load

In Figures II.3-II.5, f for SDHW systems of different height-to-diameter ratios is plotted with thermal conductivity as a parameter. The results verify that for height-to-diameter ratios of more than three, thermal conduction effects are negligible. In simulations of SDHW systems with height-to-diameter ratios of less than one, thermal conduction should not be neglected. In Figure II.6, the ratio of solar fractions of a 0.7 W/m-°C and a zero conduction case are plotted. Values of this solar fraction ratio for the SDHW system described in chapter I (H/D = 3.1) are within 1% of unity so that thermal conduction is neglected for simulations of this SDHW system.

II.2 Experimental Data Analysis

The experimental data used for the validation of simulations were taken by Fanney at the NBS Gaithersburg facility and supplied as hourly printouts. An example of these data is in Appendix C. Only the system description and weather data are necessary for simulations therefore only weather data and values to compute the pipe loss coef-

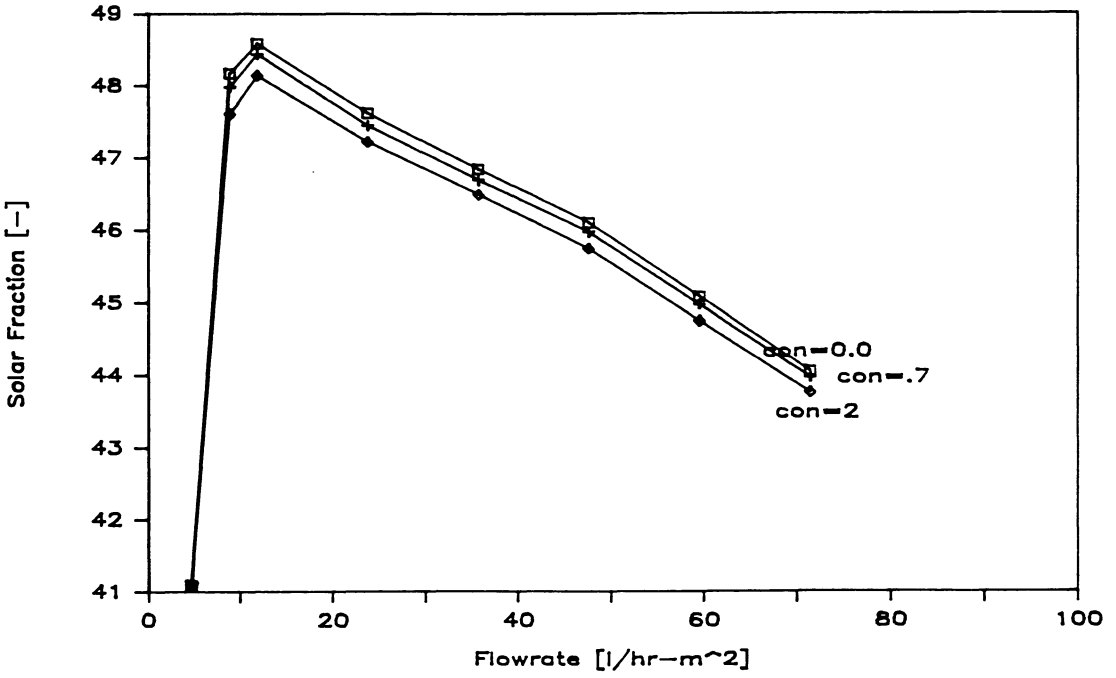

Figure II.3. Solar fraction vs collector flowrate. Tank with H/D = 3.1, conduction coefficient λ_c = con in [W/m-°C].

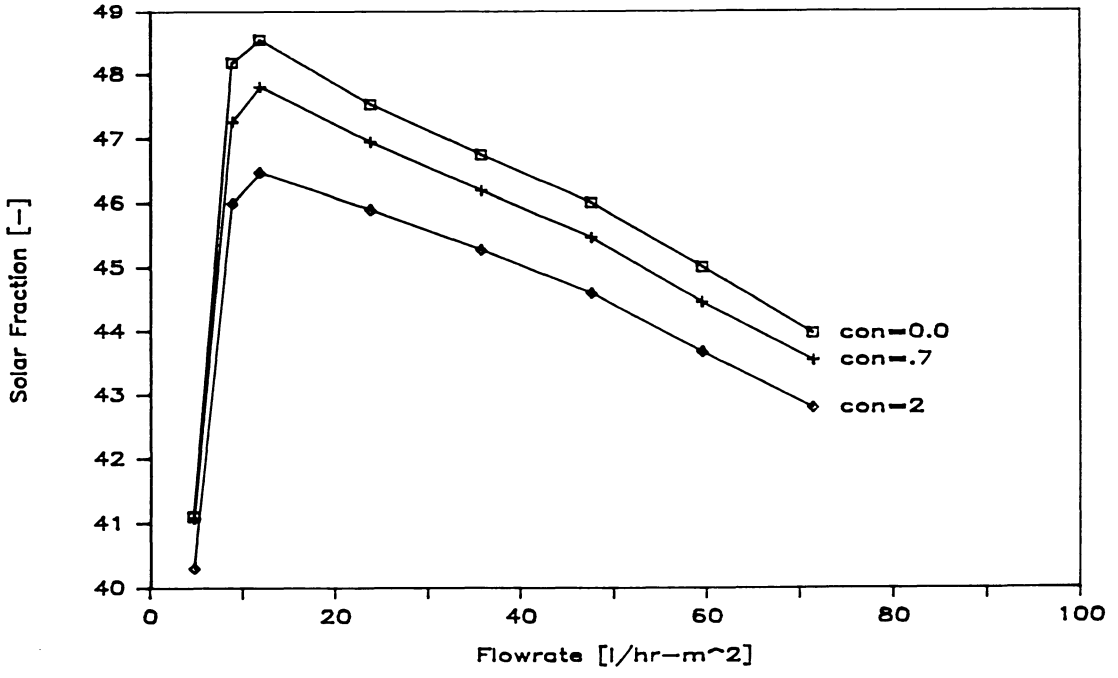

Figure II.4. Solar fraction vs collector flowrate. Tank with H/D = 1.0, conduction coefficient λ_c = con in [W/m-°C].

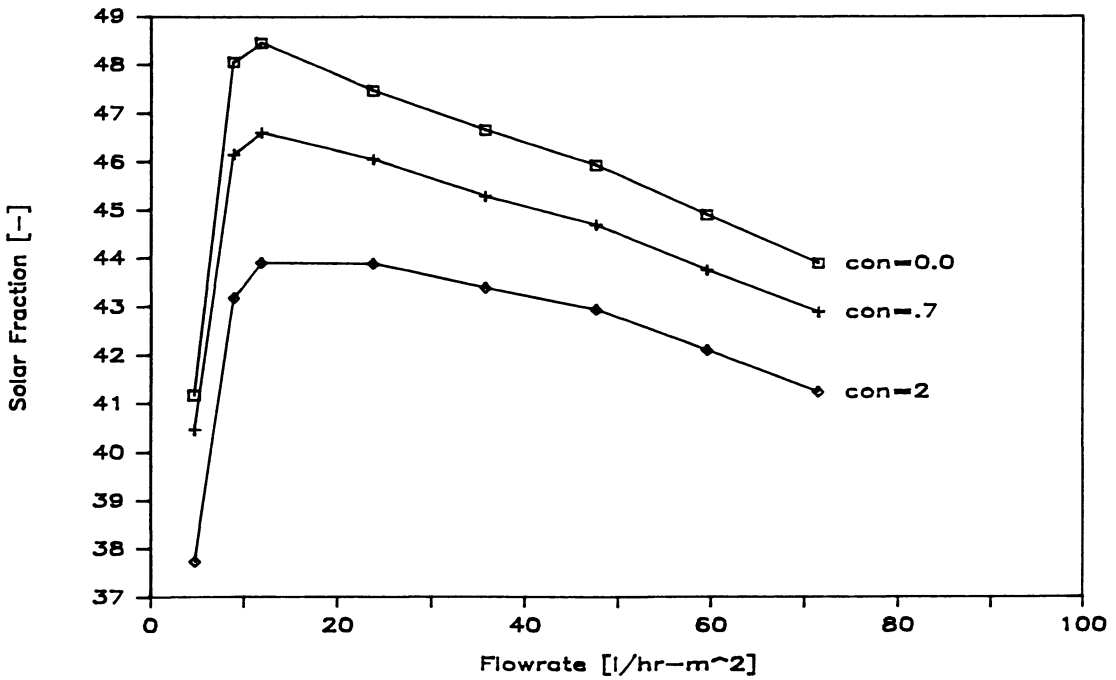

Figure II.5. Solar fraction vs collector flowrate. Tank with H/D = 0.5, conduction coefficient λ_c = con in [W/m-°C].

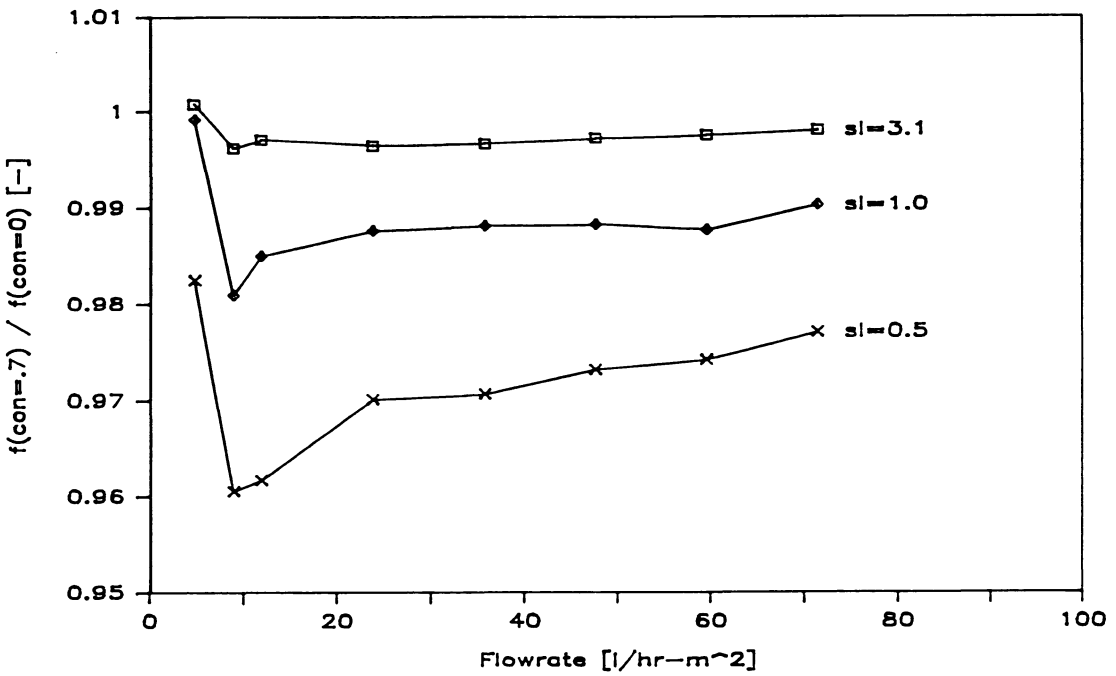

Figure II.6. Ratio of solar fraction with λ_c = 0.7 W/m-°C and λ_c = 0 vs. collector flowrate for different H/D values.

ficient were entered. The data files also included summaries for each day and both nine day periods.

Inspection of the data led to the conclusion that pipe losses had to be included in the simulation. Overall energy balances for each set of data and for each system showed fairly good results for high collector flowrate systems, but did not close well for the low collector flowrate systems. In Table II.7, the results of energy balances are listed as ΔQ_{sys}

$$\Delta Q_{sys} = \sum Q_{sys,input} - \sum Q_{sys,output} - Q_{stored\ sys} \quad (II.23)$$

and its fraction of the measured energy input to the SDHW system. Although these discrepancies exist the data are believed to be the best available. They represent only a 9-day period so that minor measurement problems may result in large differences for the overall energy balances. This has to be taken into account for comparisons with simulations. Nevertheless a high degree of agreement for the overall system performance between the simulations and the experiments lends confidence that the simulations incorporate the important heat transfer mechanisms of the simulated systems.

II.3 Comparison of TRNSYS Simulations and Experimental Results

II.3.1 Simulation Deck and Simulation Timestep

Listings of the TRNSYS simulation decks are included in Appendix A for the systems described in Chapter I. A flow diagram of the one-tank systems is in Figure II.8 showing the inputs, outputs and inter-

	1 Tank system		2 tank system	
	high collector flowrate	low collector flowrate	high collector flowrate	low collector flowrate
ΔQ_{sys} [kWhr]	9.54	19.9	4.16	12.7
$\frac{\Delta Q_{sys}}{\Sigma Q_{in}}$	.074	.137	.030	.085

Table II.7. Energy balances for the NBS systems. For two nine-day periodes of experimental data at collector flowrates of 71.5 l/hr-m^2 (high) and 9 l/hr-m^2 (low).

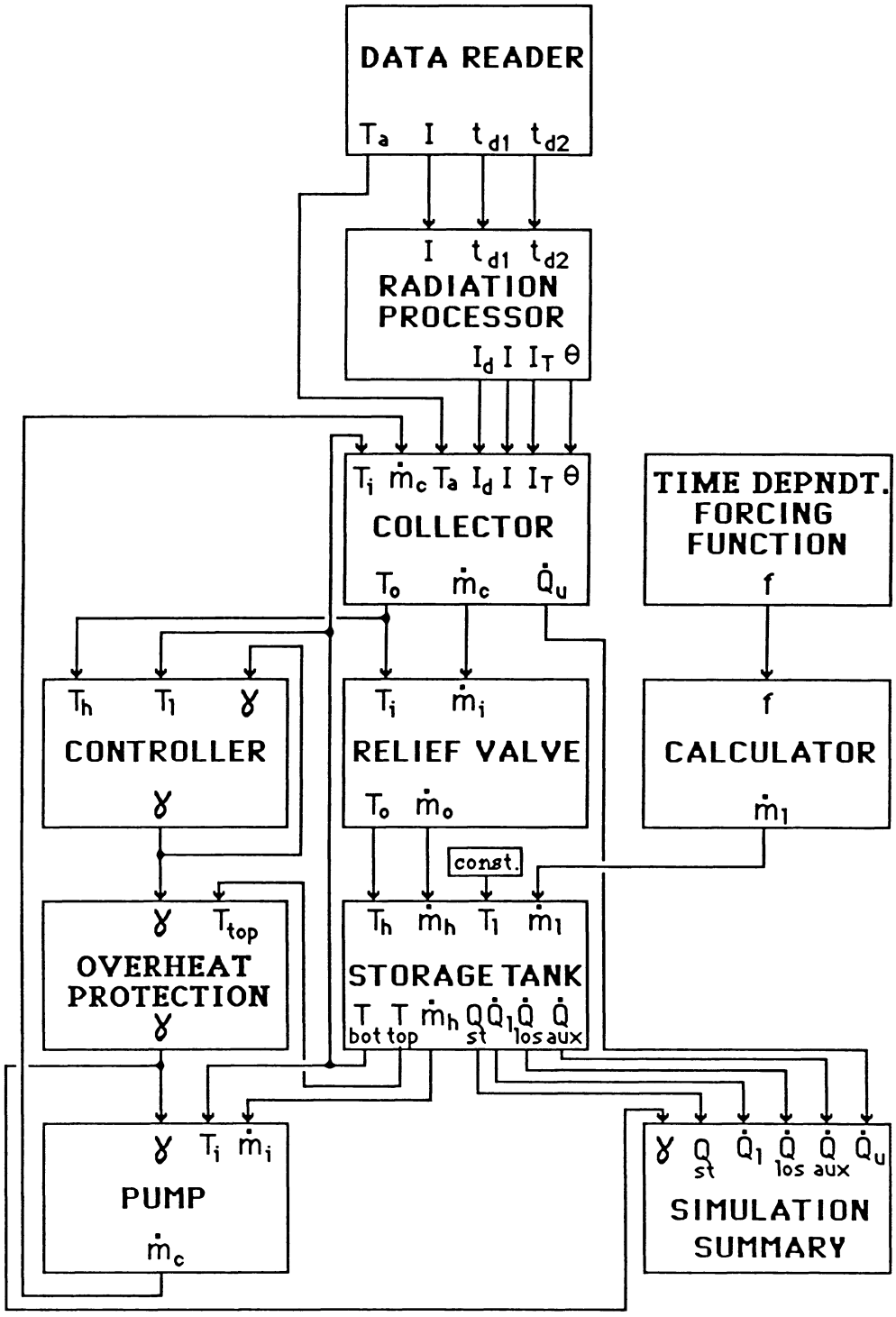

Figure II.8. Flow diagram of the singletank SDHW experimental system as developed for TRNSYS simulations.

connections of the system components. The simulation time and the component parameters are determined by the experimental system, whereas the simulation time step is a parameter to be chosen.

To solve differential equations, the simulation time step Δt has to be less than the smallest system time constant. For the storage tank, the time constant is

$$t_n = \frac{V_n}{\dot{V}} \qquad \text{(II.24)}$$

with: V_n = volume of a node

$\dot{V}$ = highest volume flow through storage tank

Zeitz [26] recommends to use 1/5 of the smallest system time constant for good agreement between system and simulations. Therefore simulations of the high collector flowrate experiments should have a time step Δt of

$$\Delta t = \frac{30\ \ell}{300\ \ell/\text{hr}} \frac{1}{5} = 0.02\ \text{hr} \approx 1\ \text{min}$$

To keep simulations of high and low collector flowrates comparable, this time step was used for all simulations. Further reasons for the chosen time step are provided in Appendix B. The tank model used for simulations was the one-dimensional multi-node model that is included in the TRNSYS library. The model generates a solution of the one-dimensional partial differential equation [Eq. (II.25)], which de-

scribes the storage tank, by solving n local ordinary differential equations [Eq. (II.26)] for n nodes along the tank axis.

$$\frac{\partial T}{\partial t} = \frac{4\dot{m}}{\pi\rho D^2}\frac{\partial T}{\partial x} - \frac{4U}{\rho c_p D}(T - T_a) \qquad \text{(II.25)}$$

$$\frac{dT_i}{dt} = \frac{\dot{m}}{m}(T_{i-1} - T_i) - \frac{UA_{los,i}}{\dot{m}c_p}(T_i - T_a) \qquad \text{(II.26)}$$

where: T, T_i = local time-dependent tank temperature

$\dot{m}$ = absolute mass flowrate in tank

m = mass of individual node

Another model generating an algebraic solution for the tank temperature, a plugflow model, is also included in the TRNSYS library. Although Wuestling [1] found good agreement between the two models and the multi-node model requires more computer time, the plugflow model was rejected, because its simulation of temperature distributions in the tank is not consistent at various flowrates. In Appendix B a detailed explanation is provided.

II.3.2 Simulation Results

In Figures II.9 to II.12 the results of the simulations and Fanney's experiments for both 9-day periods are shown. Values of the conventional load to calculate the fractional energy savings as used by Fanney are also included. Conventional load is the measured or simulated load plus conventional tank losses of 3.1 kWhr/day [8]. With this load, fractional energy savings can be defined replacing

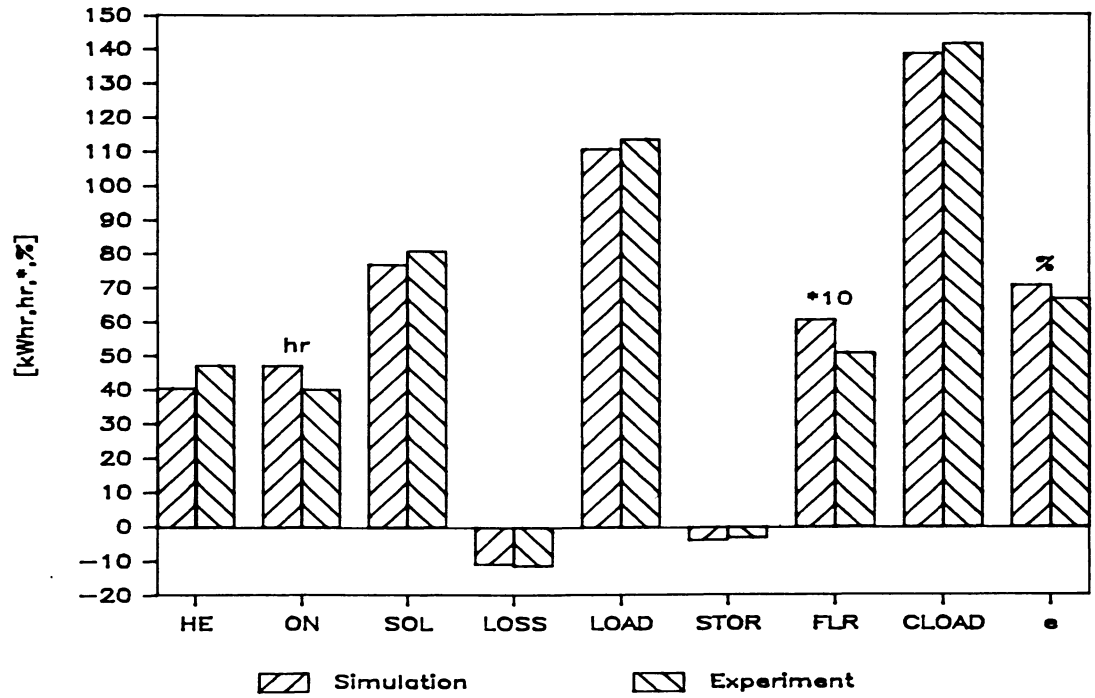

Figure II.9. Comparisons for nine days of simulations with experiments. For the single-tank SDHW system at a collector flowrate of 71.5 l/hr-m^2.

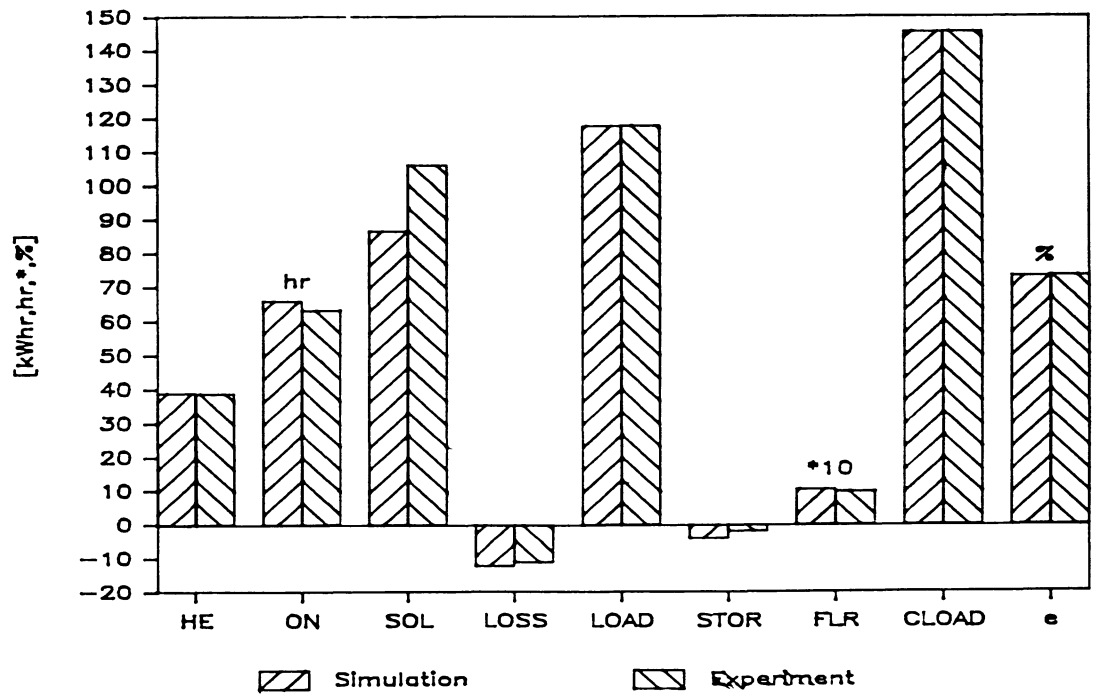

Figure II.10. Comparisons for nine days of simulations with experiments. For the single-tank SDHW system at a collector flowrate of 9.0 l/hr-m^2.

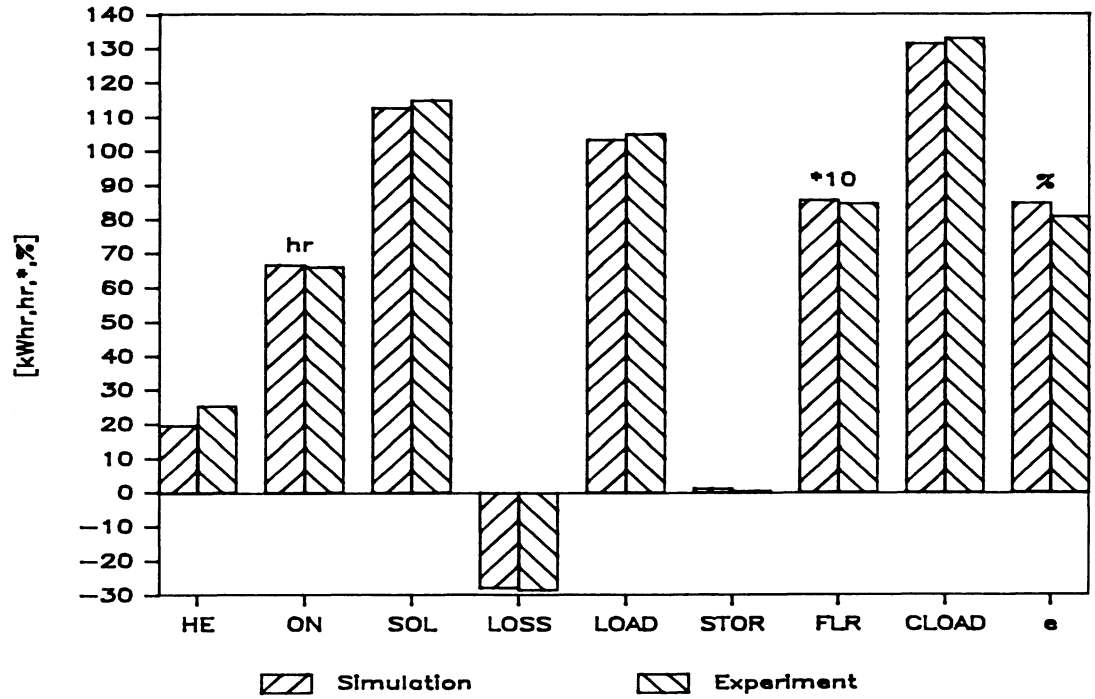

Figure II.11. Comparisons for nine days of simulations with experiments. For the double-tank SDHW system at a collector flowrate of 71.5 l/hr-m^2.

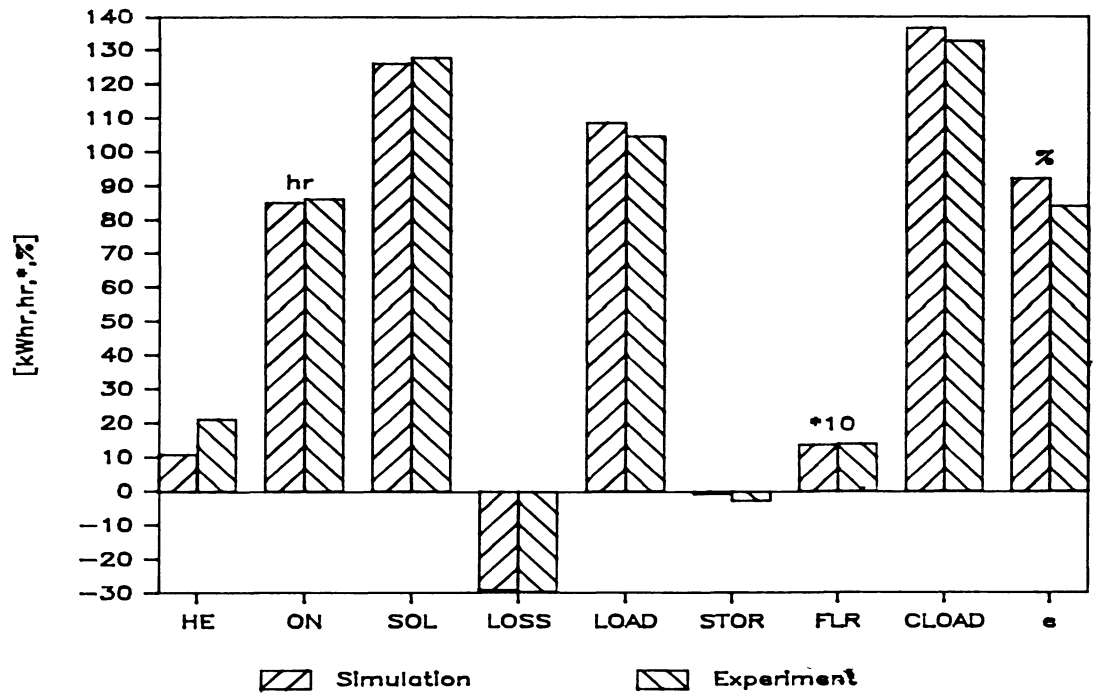

Figure II.12. Comparisons for nine days of simulations with experiments. For the double-tank SDHW system at a collector flowrate of 9.0 l/hr-m^2.

the load in Eq. (II.22) by the conventional load

$$e = 1 - \frac{Q_{aux}}{Q_{C,load}} \qquad \text{(II.27)}$$

Other values are: HE = heater energy [kWhr]

ON = operating time [hr]

SOL = collected solar energy [kWhr]

LOSS = tank losses [kWhr]

LOAD = supplied load energy [kWhr]

STOR = energy stored in tank [kWhr]

FLR = flowratio times ten [-]

The comparisons are satisfactory. The largest discrepancies between experiments and simulations are found for pump operating time and collected solar energy in the low collector flowrate one tank system. It should be noted that the differences between experiment and simulation have opposite directions. In the experiments, less operating time results in a higher useful energy gain. The explanation for this discrepancy is the lack of closure of in the energy balances of the experimental system as shown in Table II.7. The measured value of collected solar energy was too high, which was confirmed by Fanney [27].

Another discrepancy between experiments and simulations is that the improvement of the one tank SDHW system due to the reduced collector flowrate is higher than the improvement of the two tank SDHW system, whereas the simulation indicate the opposite effect. Reasons

to account for this are: (1) The tank model used for the one tank SDHW system puts the collector return water below the heating element. At high collector flowrates in the one tank experimental system, some auxiliary-heated water may be mixed with the solar preheat part of the storage tank, thereby increasing the demand for auxiliary energy while raising the collector inlet temperature, which degrades the performance of the experimental system. TRNSYS does not mix auxiliary with solar-heated water except for temperature inversions. Therefore the system performance of the one tank system at high flowrate may be overpredicted by the simulations. (2) The lack of closure in the experimental energy balances is larger than the discrepancy, which indicates that the problem may be due to experimental errors.

With the lack of closure in the energy balances for the experiments it is impossible to achieve exact agreement between the simulations and the experiments. TRNSYS simulations cannot have a lack of closure in their energy balances. However, the good overall agreement for essentially different systems validates the simulations, so that the TRNSYS simulation SDHW system can be used for further investigations.

II.4 Base Case: Climate and Load Variations

II.4.1 Performance Dependence on Location

Standard procedure is to run simulations for a variety of locations to determine the effect of changes in the weather on system performance. For the four essentially different climates of

Albuquerque, NM, Sterling, VA, Madison, WI, and Seattle, WA, the solar, auxiliary, loss and load energies as well as annual solar fractions are provided in Figures II.13 to II.16. The annual simulations for these climates show that the behavior of both the one-tank and the two-tank systems is consistent in its relations between high and low collector flowrate on an annual bases. This demonstrates that comparisons of system behavior are not strongly dependent on location. Therefore it is sufficient to concentrate on one single location for comparisons of simulations. The solar fraction for Madison and Sterling is about 50% and corresponds well to the design suggestion of Duffie and Beckman [10]. For that reason, and because of a familiarity with Madison weather data, Madison was chosen as the location for further simulations, unless otherwise noted.

The annual and monthly solar fractions vs. collector flowrates in Figure II.17 and II.18 of the one-tank and two-tank systems described above are for Madison weather data. Figures II.19 and II.20 show solar fraction vs. the ratio of monthly average collector flow over monthly load flow, $\overline{M_c}/M_l$. The maximum occurs at a flowrate of about 10 l/hr-m^2 for all months, but $\overline{M_c}/M_l$ varies between 0.5 and 1.7 at the highest solar fraction. The curves for March are nearly identical to the annual solar fraction curves. This has also been observed by Wuestling [1], who used simulations with March weather data for simulation comparisons instead of annual weather data. Because of this good correspondence, the simulation time can be

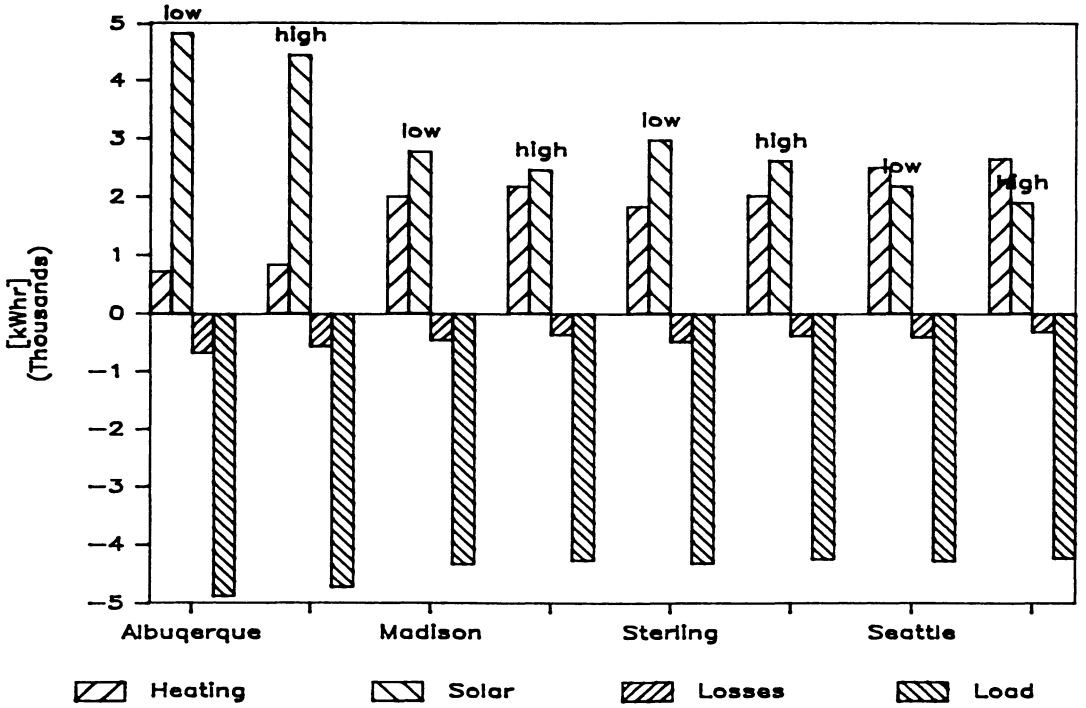

Figure II.13. Energy input and output for annual simulations in four locations. For the base case single-tank system at collector flowrates of 71.5 l/hr-m^2 (high) and 9 l/hr-m^2 (low).

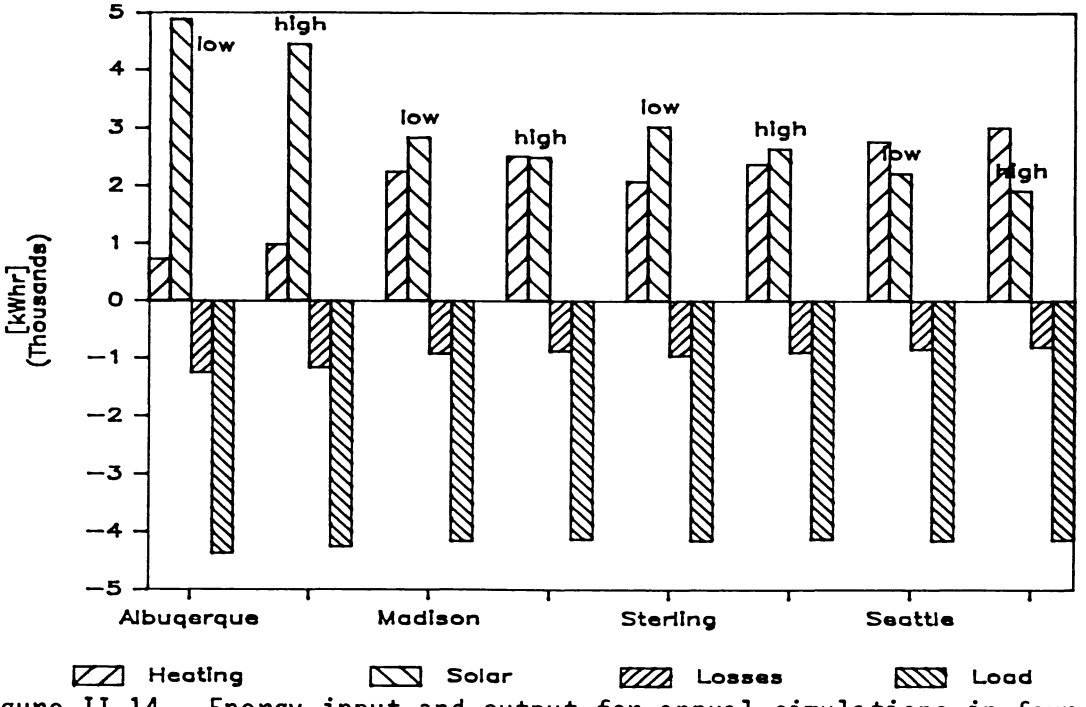

Figure II.14. Energy input and output for annual simulations in four locations. For the base case double-tank system at collector flowrates of 71.5 l/hr-m^2 (high) and 9 l/hr-m^2 (low).

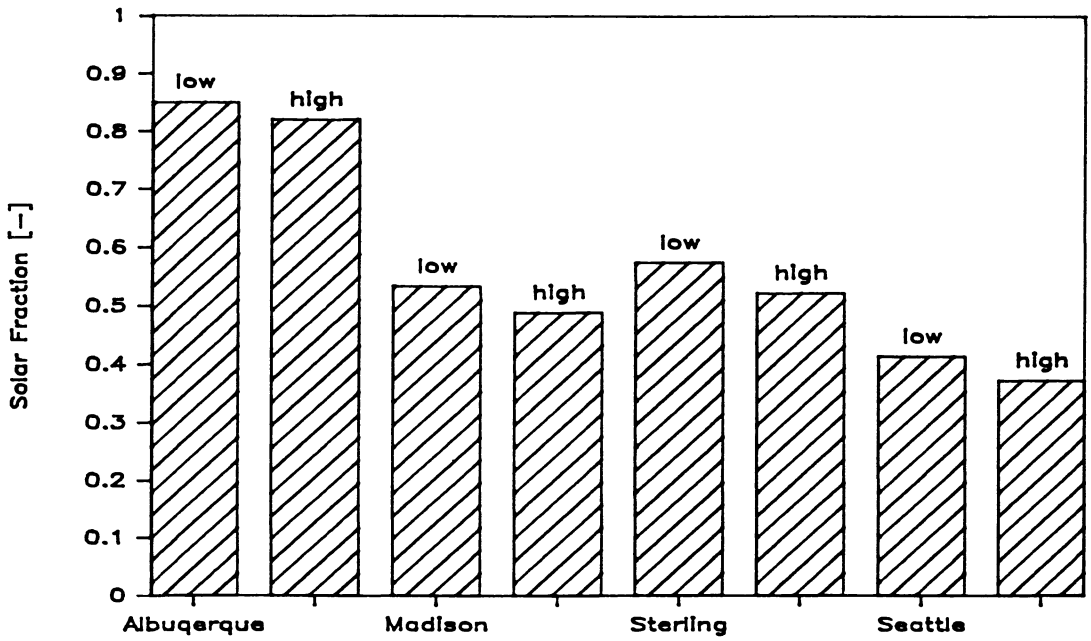

Figure II.15. Solar fraction for annual simulations in four locations. For the base case single-tank system at collector flowrates of 71.5 l/hr-m^2 (high) and 9 l/hr-m^2 (low).

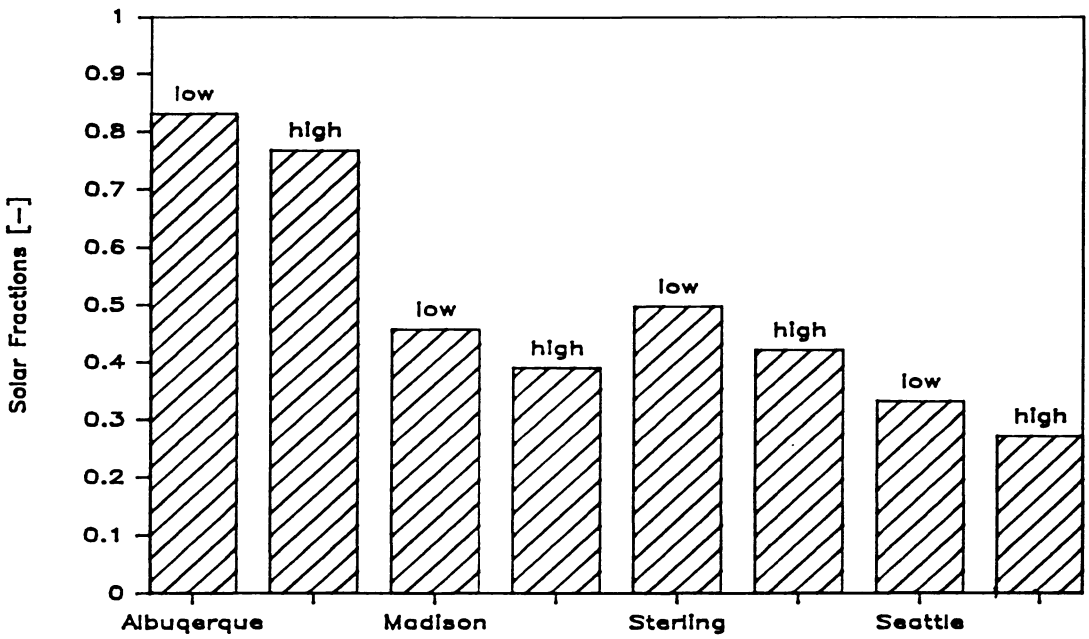

Figure II.16. Solar fraction for annual simulations in four locations. For the base case double-tank system at collector flowrates of 71.5 l/hr-m^2 (high) and 9 l/hr-m^2 (low).

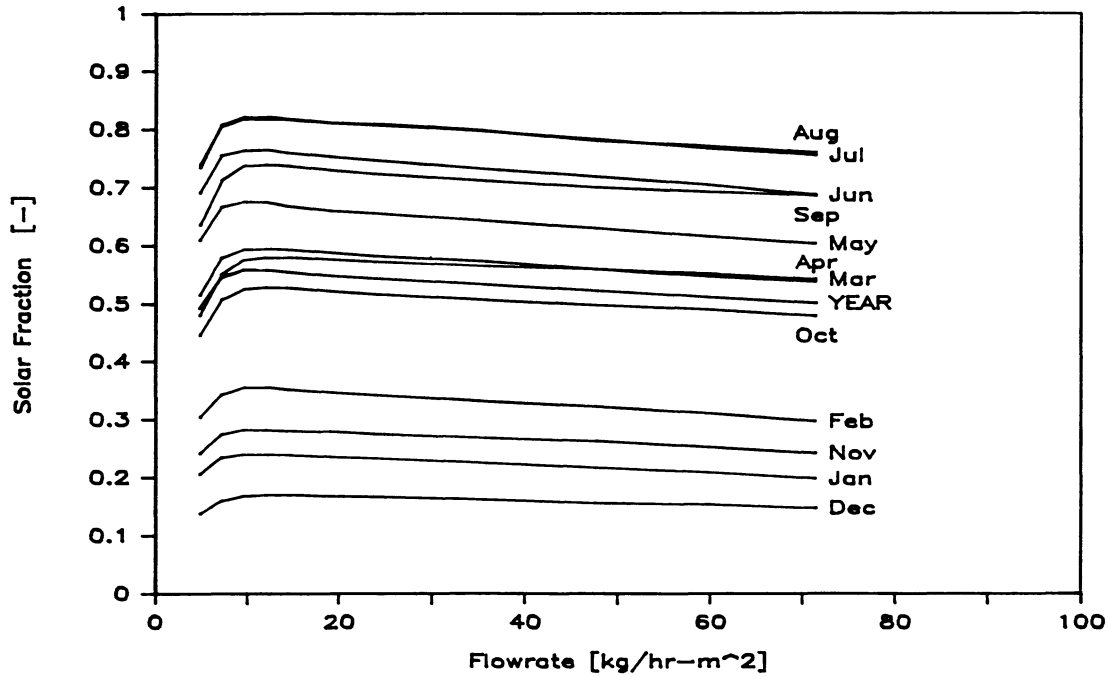

Figure II.17. Solar fraction vs. collector flowrate. For the single-tank base case system for monthly and annual simulations for Madison.

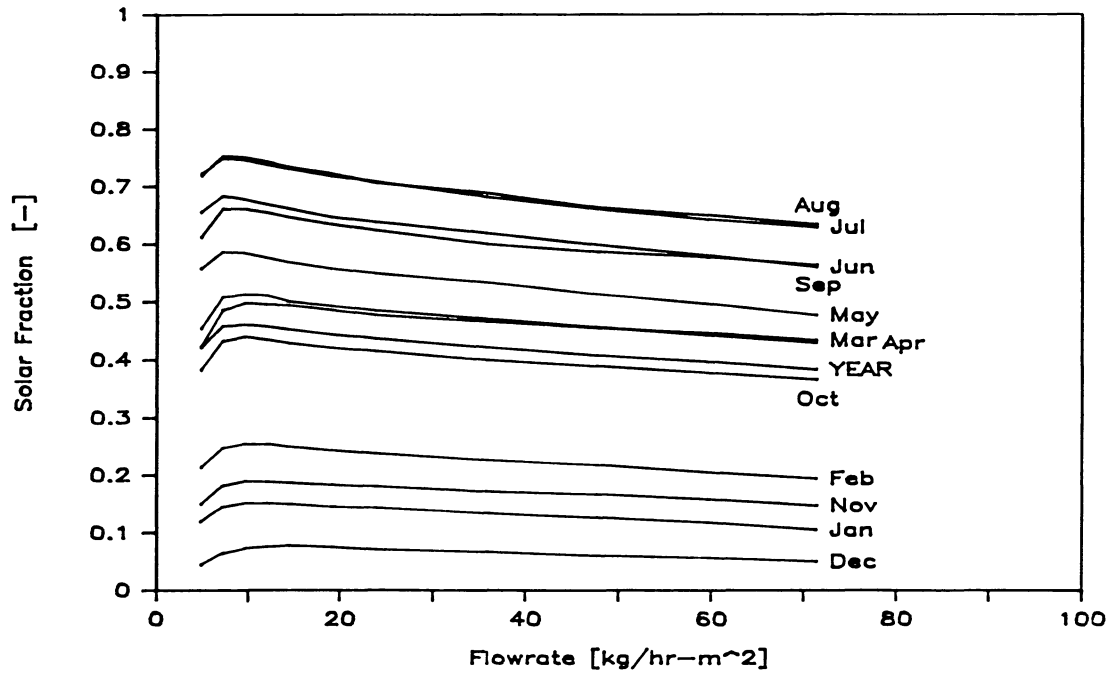

Figure II.18. Solar fraction vs. collector flowrate. For the double-tank base case system for monthly and annual simulations for Madison.

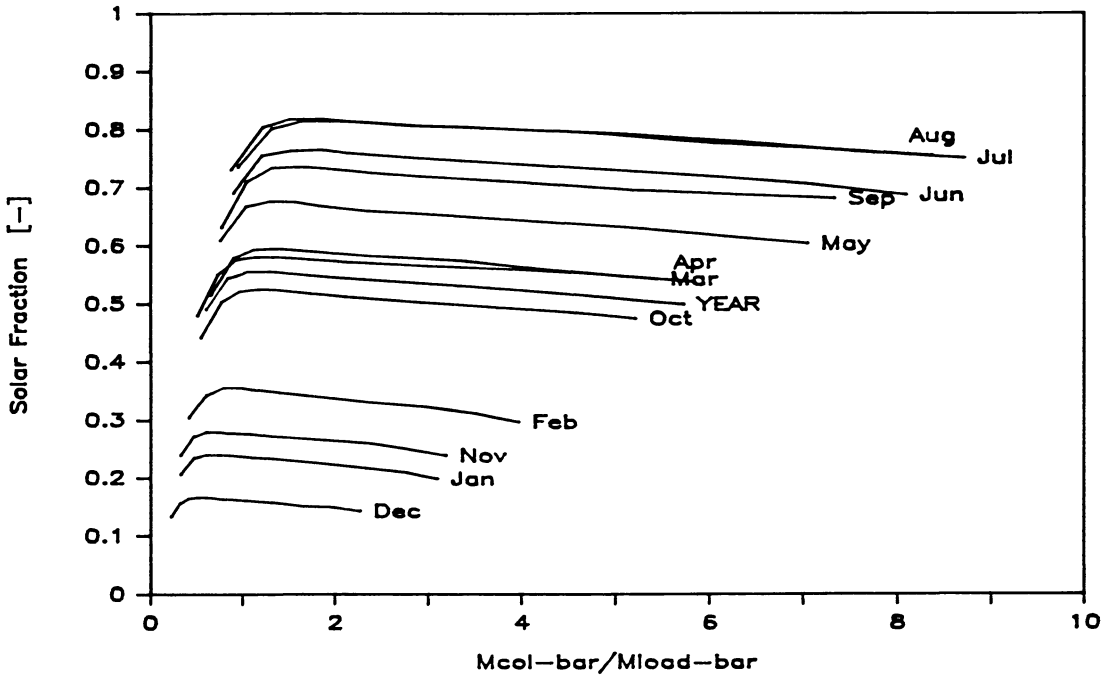

Figure II.19. Solar fraction vs. $\overline{M}_c/M_l$ (monthly average collector flow/monthly load flow). For the single-tank base case system for monthly and annual simulations for Madison.

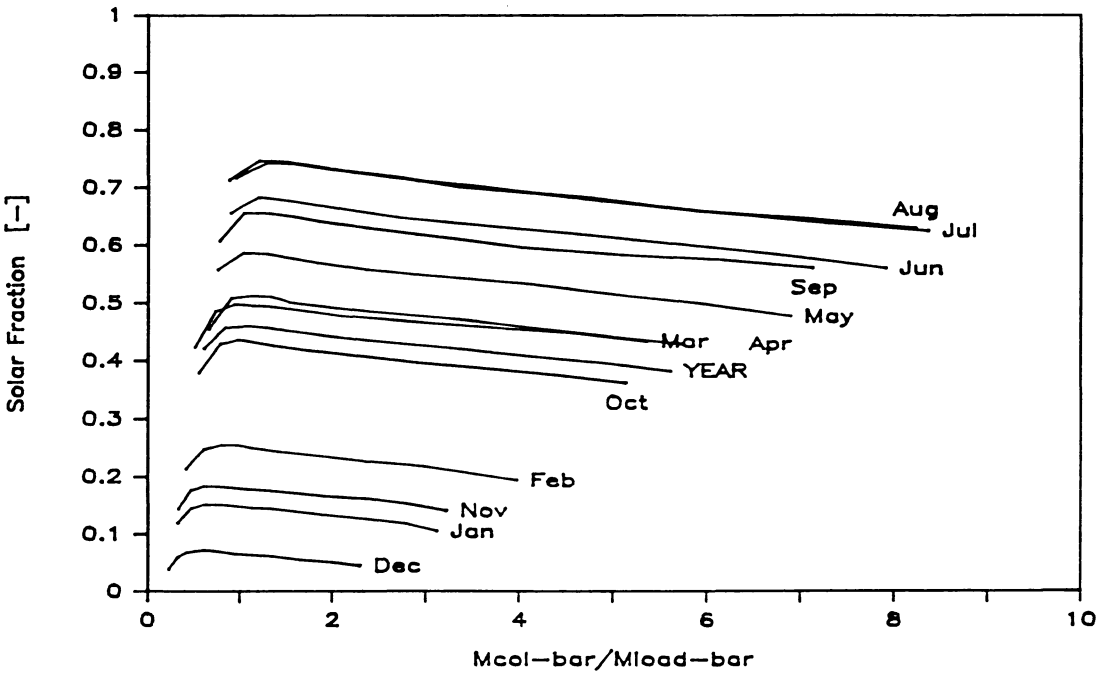

Figure II.20. Solar fraction vs. $\overline{M}_c/M_l$ (monthly average collector flow/monthly load flow). For the double-tank base case system for monthly and annual simulations for Madison.

confined to March for Madison weather data. This is an important simplification, since the small simulation time step of one minute results in large amounts of computer time per simulation.

II.4.2 Performance Dependence on Load Variations

The performance of SDHW systems depends strongly on the amount but also on the distribution of the load demand. In [1,10] and other publications the effect of the magnitude and distribution of the load demand is discussed in detail. The RAND hot water demand distribution is used by Wuestling [1] for simulation studies and Fanney [8] for experiments. It is the standard load distribution for studies of SDHW systems. Therefore the RAND profile was selected to allow comparisons, particularly with the supplied experimental data.

For practical reasons Fanney used the RAND load schedule at a constant flowrate, adjusting the time for the draw to reach the daily demand of 260 l. The flowrate of 3.79 l/min was large enough to draw the highest hourly load demand within ten minutes at the beginning of the hour.

It is impossible to follow this time-varying load demand without reducing the simulation time step to an unreasonably small value. Three kinds of load draws were simulated: (1) a constant load flowrate over the whole hour, i.e. the flowrate was varied from hour to hour to attain the required total demand for that hour; (2) a load flowrate of 12 times the one used for (1) but within the first five minutes of the hour; and (3) a schedule designed to stay as close as possible to the experimental load flowrate of 3.79 l/min while vary-

ing the load draw duration according to the limits of the simulation time step. The first kind of load draw was used, unless otherwise noted, throughout all simulations because of its simplicity, independence of simulation time step, and correspondence to other simulations.

The first and second load draw schedule over 24 hours are plotted in Figure II.21. Figure II.22 contains the solar fractions of annual simulations with all three kinds of schedules. The solar fractions of schedule two and three are nearly identical because there is no significant difference in their schedules. The difference between the constant load flowrate over the hour and the constant load flowrate over the first five minutes is considerable. A high load flow at the beginning of the hour forces the whole solar tank profile to shift upwards, thereby bringing cooler water to the tank thermostat and turning the auxiliary heater on. Simultaneously, cold mains water is mixed into the bottom portion of the solar tank resulting in a higher supply temperature to the collector, which reduces the collector efficiency.

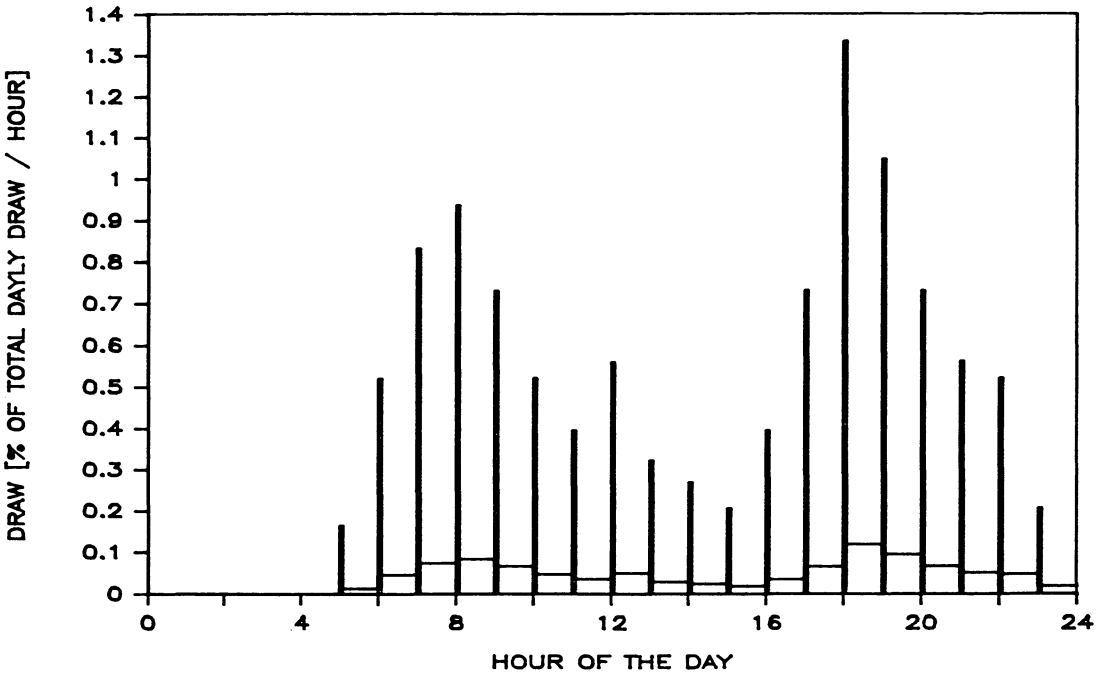

Figure II.21. Profiles for load draw over 24 hours. Hourly constant draw and draw in the first five minutes, for the same total amount and the RAND distribution.

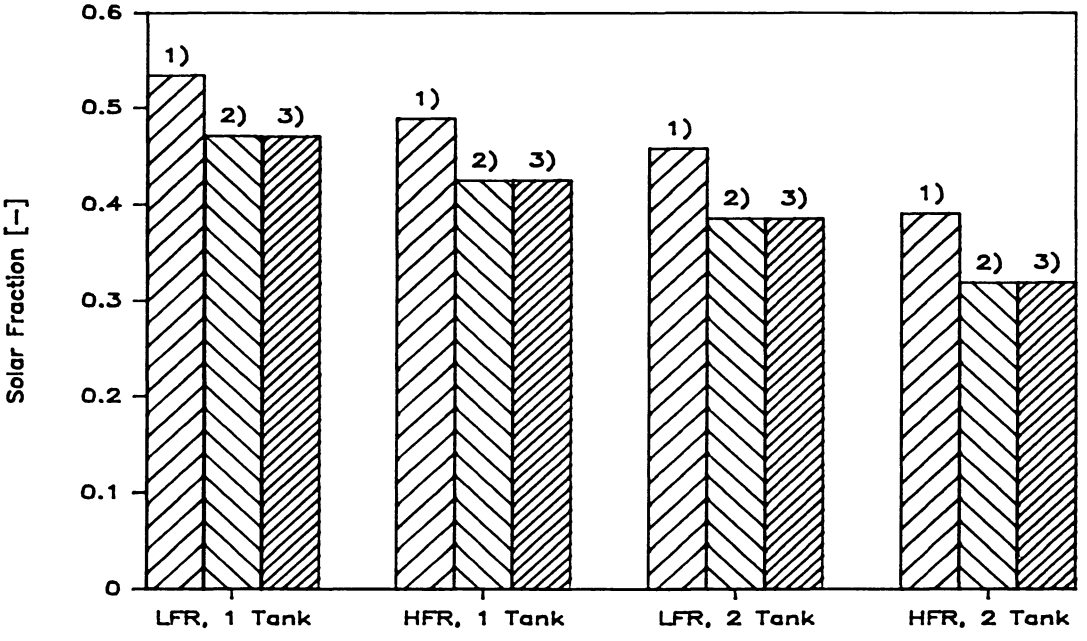

Figure II.22. Solar fraction of annual simulations. At flowrates of 71.5 l/hr-m^2(HFR) and 9 l/hr-m^2 (LFR), for the single-tank and double-tank base case systems.
Load draw schedules 1), 2), 3) as explained in text.

III. COMPATIBILITY OF LOW COLLECTOR FLOWRATE WITH STANDARD COLLECTOR DESIGN

In this chapter the flowrate distribution in a collector and collector array is analyzed. The collector heat removal factor F_R and its dependence on flowrate distribution is calculated for a typical collector at standard and reduced collector flowrates.

III.1 Flowrate Distribution in Solar Collectors and Arrays

The system performance improvement realized by reducing the collector flowrate is mainly due to enhanced temperature stratification in the solar storage tank. The low collector flowrate suppresses mixing in the tank and thereby allows a temperature gradient between tank top and bottom. The penalty of a reduced collector flowrate, the reduction in collector efficiency, can be offset by a lower collector inlet temperature to result in a reduction in auxiliary heating. In the instantaneous collector efficiency as defined in Eq. (II.22), η is proportional to the heat removal factor F_R. F_R is a function of collector flowrate $\dot{m}_c$, collector overall loss coefficient U_L and collector efficiency factor F'. The latter two are also weakly dependent on collector flowrate. F_R is usually calculated assuming a uniform flowrate distribution over the collector. For a standard collector design with risers running between a lower and an upper manifold, Dunkle and Davey [22] showed that the flowrate distribution is not necessarily uniform. Therefore, the effect of operating a standard collector, designed for a high collector flow-

rate, at reduced flowrate is of interest. If the flow distribution as indicated by experience [18-21] becomes more uneven F_R could be lower than expected and the reduction of collector flowrate not as advantageous as originally thought.

III.2 Collector Flowrate Distribution and Heat Removal Factor

III.2.1 Collector Flowrate Distribution

To quantify the effect of collector flowrate distribution in a collector on F_R this distribution has to be known. For a collector design and array arrangement as shown in Figure III.1 and with known pipe diameters, the flowrate distribution can be calculated. The flow through a pipe is derived from the pressure drop Δp

$$\Delta p = f \frac{L}{D} \frac{\rho}{2} v^2 \qquad \text{(III.1)}$$

with

$$v = \frac{\dot{V}}{A} = \frac{4\dot{m}}{\pi \rho D^2} \qquad \text{(III.2)}$$

to give

$$\dot{m} = \left(\frac{\pi^2 \rho D^5}{8fL} \Delta p\right)^{1/2} \qquad \text{(III.3)}$$

where: Δp = frictional pressure drop

f = friction factor

L = pipe length

D = pipe diameter

ρ = fluid density

v = fluid velocity in pipe

A = pipe cross sectional area

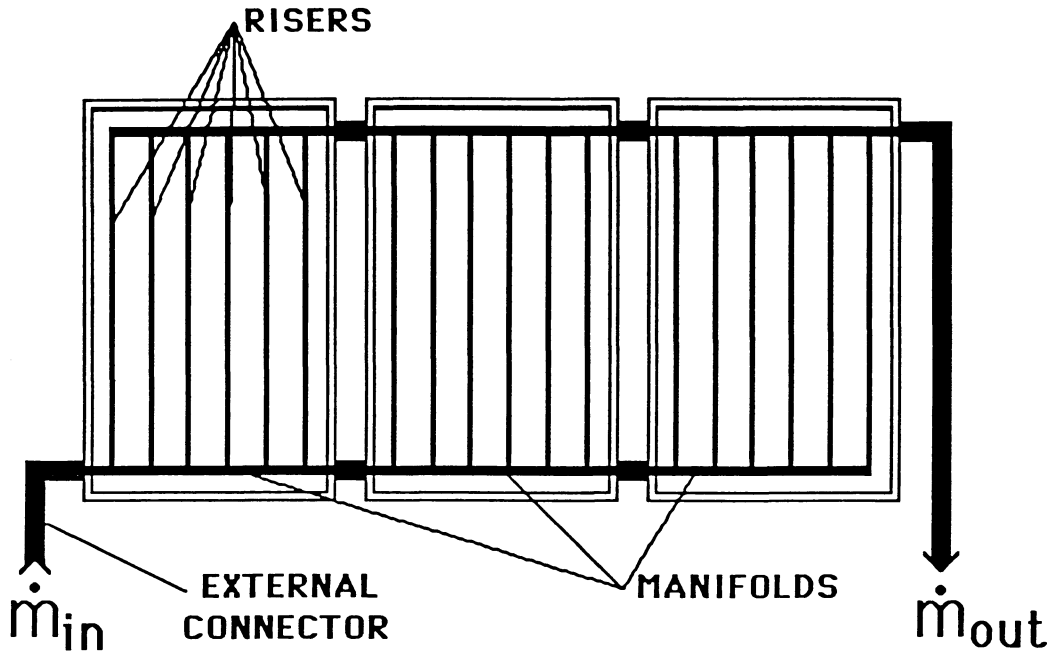

Figure III.1. Schematic of array of three collectors. Typical parallel arrangement for SDHW systems.

$\dot{m}$ = mass flowrate through pipe

The friction factor is dependent on the flow condition:

for laminar flow

$$f = \frac{64}{Re} \tag{III.4}$$

and for turbulent flow

$$f = \left[2 \log \left(\frac{Re \sqrt{f}}{2.51}\right)\right]^{-2} \tag{III.5}$$

Equation (III.5) from Prandtl and Karman is valid over the whole turbulent region ($Re > Re_{crit} = 2320$) [28] and has been solved by successive substitution. With these equations, iterative solutions for the flowrate distribution for a given total collector flowrate are calculated using the following five steps:

1) Guess the pressure drop of the first riser and calculate the flowrate through it.
2) Calculate the pressure drop in the upper and lower manifold for the part to the next riser. The flowrate is known from the flowrate in the previous riser. This results in the pressure of upper and lower manifold at the next riser.
3) Compute the flowrate through the next riser using the pressure difference between upper and lower manifold. Then continue with (2) for all risers.

4) The summation of the flow through all risers minus the total collector flowrate gives a flowrate deviation. A new guess of the pressure at the top of the first riser is calculated with the secant method from the flowrate deviation.

5) Repeat steps (1)-(4) until the flowrate deviation is sufficiently small.

By specifying an effective length of individual risers, disturbances such as surface roughness or cross-sectional area differences can be taken into account. Properties of the heat removal fluid are input to these calculations. However, an isothermal collector or collector array was assumed in the following results. This is a conservative assumption because buoyancy forces resulting from higher temperatures tend to equalize the flowrate distribution.

The analytical solution of Dunkle and Davey for the flowrate distribution cannot be used for the calculation at low collector flowrates. A basic assumption of their solution is violated: the flow in the upper and lower manifold cannot be assumed to be turbulent. Even for the high collector flowrate the flow in the first section of the upper manifold and the last section of the lower manifold are laminar.

III.2.2 Collector Heat Removal Factor Calculation

The purpose of computing the flowrate distributions in a collector or array was to calculate its effect on F_R compared to an even flowrate distribution. Specifications of the collectors and array used for the analysis are given in Table III.2. A wide variety of

Number of collectors	3
Number of risers per collector	6
Length of risers	1.87 m
Length of manifolds	0.89 m
Diameter of risers	6.35 mm
Diameter of manifolds	12.70 mm
External connection length	0.10 m
Absorber: copper, thickness	0.80 mm
absorptance	0.95
emissivity	0.12
Cover: single glass low iron	3.30 mm
transmittance	0.90
reflectance	0.03
Insulation: conductivity	0.05W/m°C
back thickness	75.9 mm

Table III.2. Design parameters of collector and array. For calculation of flowrate distribution and optical properties for F_R.

collector designs with various optical properties is commercially available. The collector installed on the CSU-Solar-House III, CO, was chosen for three reasons: (1) An available collector description; (2) its typical design; and (3) the optical values were used because aging tests did not show negative effects on the collector performance [29], so that they were assumed to be conservative. No attempt was made to investigate other designs, collector arrangements or optical properties because the results indicated that only significantly different collectors or array arrangements would have an effect on F_R.

The thermal analysis of a collector is outlined in detail by Duffie and Beckman [10]. To calculate the collector heat removal factor F_R it is necessary to know the collector efficiency factor F' and the overall loss coefficient U_L at the particular flowrate.

$$F_R = \frac{\dot{m}c_p}{A_c U_L}\left(1 - \exp\left(-\frac{A_c U_L F'}{\dot{m}c_p}\right)\right) \qquad \text{(III.6)}$$

If the collector efficiency in Eq. (II.2) is known at the particular flowrate for equal inlet and ambient temperature F_R can be derived as

$$F_R = \frac{\eta(T_{in} = T_a)}{(\tau\alpha)} = \frac{F_R(\tau\alpha)}{(\tau\alpha)} \qquad \text{(III.7)}$$

To evaluate either Eqs. (III.6) or (III.7) a thermal analysis of the collector is necessary. Based on the analysis of Duffie and

Beckman a program Analysis of Collector Efficiency (ACE) by Braun [30] was available. It applies a two-dimensional finite difference method with one dimension in flow direction. The other dimension refers to the calculation of temperatures of the cover, plate, fluid and backside of the collector. Figure III.3 shows the two directions in which temperatures are calculated. With the temperatures the collector efficiency is calculated for a specified flowrate and inlet temperature. ACE implicitly assumes an evenly distributed flowrate. With $(\tau\alpha)$ derived from optical properties F_R was then calculated with Eq. (III.7) and the efficiency for the particular flowrate.

For a collector with n risers and a flowrate distribution of $\dot{m}_1$, $\dot{m}_2$, ..., $\dot{m}_n$, n equivalent collector flowrates can be defined as

$$\dot{m}_{i,equi} = n \cdot \dot{m}_i \qquad \text{(III.8)}$$

A collector analysis with these flowrates yields n individual collector heat removal factors F_{R_i}. F_R for the whole collector is then given by the average value of F_{R_i}

$$F_R = \frac{1}{n} \sum_{i=1}^{n} F_{R_i} \qquad \text{(III.9)}$$

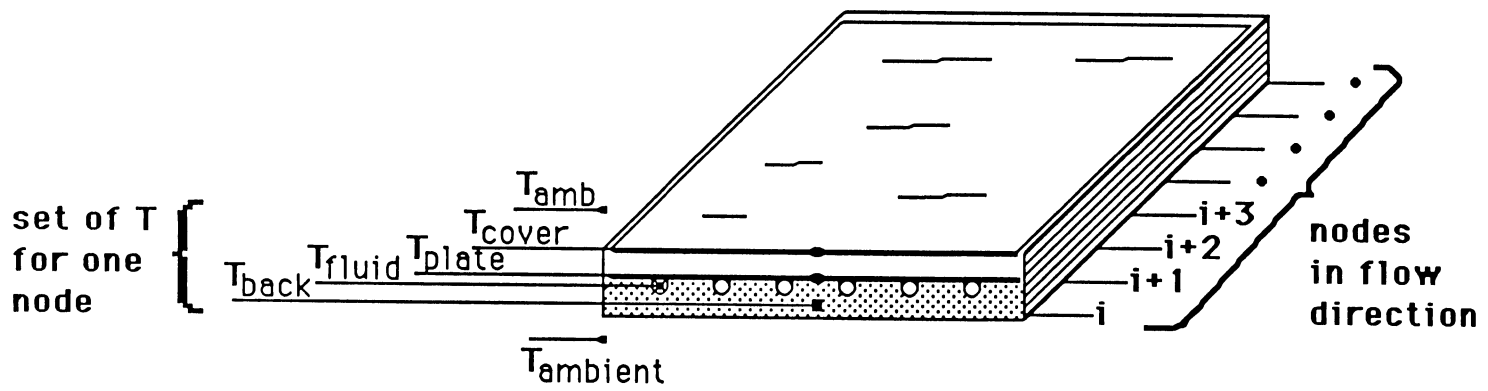

Figure III.3. The two-dimensional thermal network of a collector. Thermal analysis was done in both directions to result in the collector heat removal factor F_R.

III.3 Effects of Collector Flowrate Distribution on the Collector Heat Removal Factor F_R

III.3.1 Flowrate Distribution

The flowrate distribution for a collector and an array consisting of three collectors in parallel is plotted in Figures III.4 and III.5 at collector flowrates of 75 l/hr-m^2 and at 9.375 l/hr-m^2. The distribution is plotted as percent of deviation from the average flowrate.

$$D_i = \frac{\dot{m}_i - \dot{m}_c/n}{\dot{m}_c/n} 100 \qquad \text{(III.10)}$$

With $\dot{m}_c$ = total collector flowrate. This flowrate distribution is caused by the pressure drop across the manifolds. The ratio of pressure drop in a riser to pressure drop in the manifold determines the magnitude of the deviation. For the limiting case of infinitely long risers, a uniform flowrate distribution is reached, whereas the limiting case of risers of zero length results in the most uneven flowrate distribution.

Figure III.4 shows that the flowrate deviation for a single collector is lower than ±3% The explanation for this very even distribution is the small ratio of manifold pressure drop to riser pressure drop. For collectors installed in series the distribution of flowrate will be negligible.

Most collectors, however, are installed in parallel banks using a common manifold. Dunkle and Davey [22] recommended banks with up

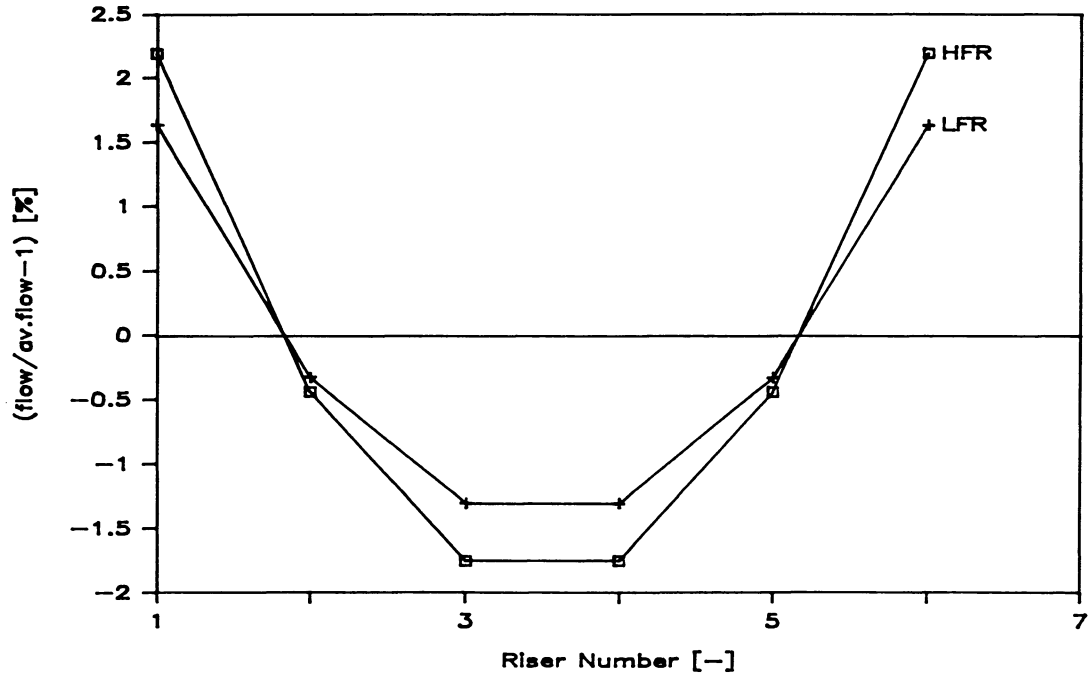

Figure III.4. Flowrate distribution in a collector. Calculalated for 6 risers; isothermal temperature = 75°C; water as collector fluid. At flowrate of 75 l/hr-m^2 (HFR) and 9.375 l/hr-m^2.

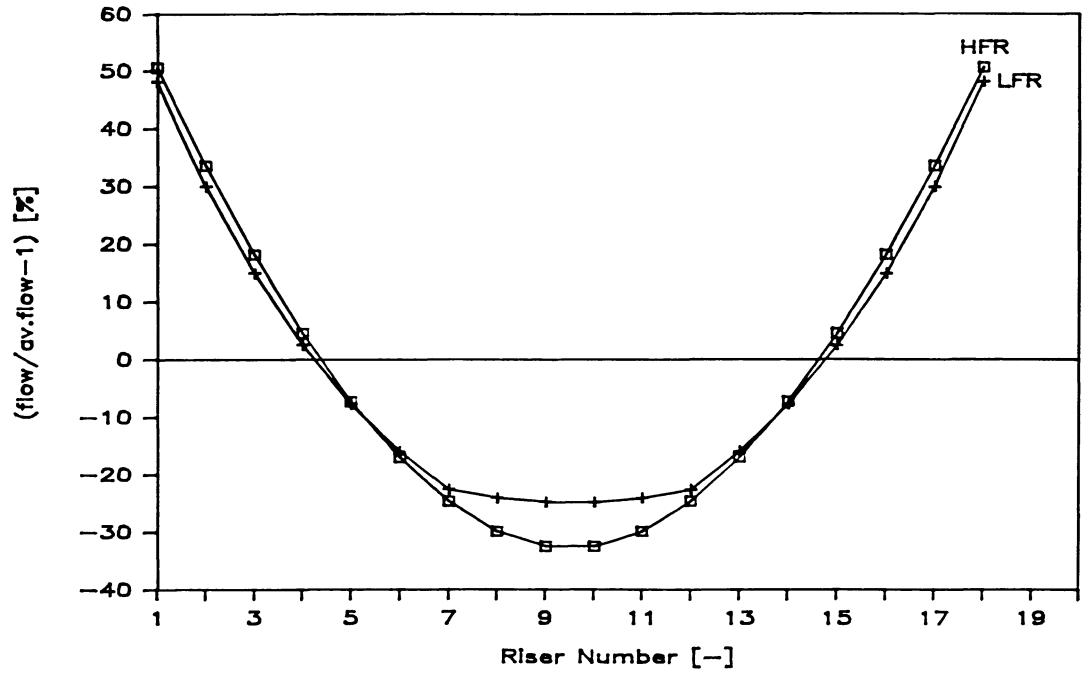

Figure III.5. Flowrate distribution in an collector array. Calculated for 18 risers; isothermal temperature = 75°C; water as collector fluid. At flowrate of 75 l/hr-m^2 (HFR) and 9.375 l/hr-m^2 (LFR).

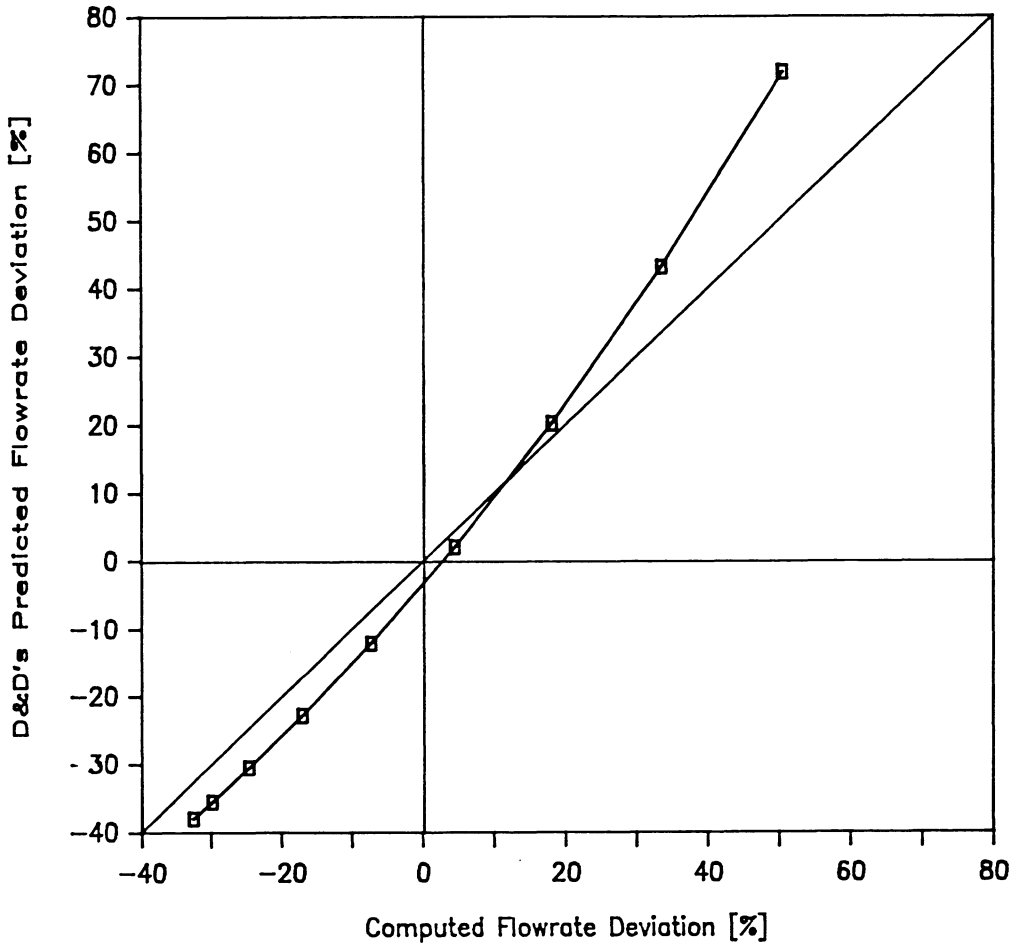

Figure III.6. Comparison of flowrate deviation predicted by Dunkle and Davey vs flowrate deviation calculated as outlined.

to 16 parallel risers. An array of three collectors specified in Table III.2 results in 18 parallel risers, which is close to Dunkle and Davey's recommendation and a common size for SDHW applications. Figure III.5 shows a large deviation from the average flowrate for 18 parallel risers. In the first and last riser the flowrate is as high as 1.5 times the average flowrate and it decreases to 65% of the average flowrate in the middle.

The significant difference between a collector and an array is due to the increase in the ratio of manifold to riser pressure drop. The average flowrate in the risers and their average pressure drop is the same for a single collector or an array, but the manifold flowrate for the array is three times as high and the pressure drop increases as the square of flowrate for turbulent flow. Note that the deviation in Figure III.4 and III.5 decreases with reduced flowrate.

In Figure III.6, the calculated flowrate distribution is compared with the one found by Dunkle and Davey [22] for the high collector flowrate. Comparison at the low collector flowrate is not included because the assumption of turbulent flow in the manifolds does not hold anymore. The differences in the distributions between the method outlined here and Dunkle and Davey's method are relatively small and can be attributed to their assumption of turbulent flow in the manifolds.

The flowrate distribution shown in Figure III.7 is for an array of three collectors in parallel. It is the same arrangement as for the flowrate distribution in Figure III.5 except for a doubling of

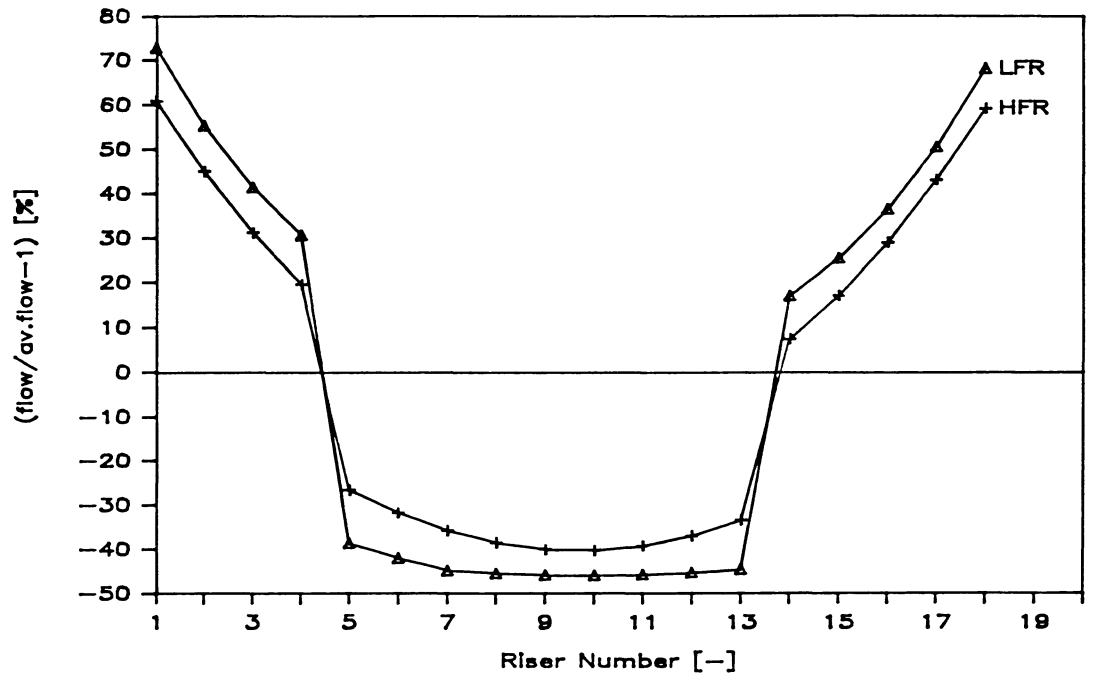

Figure III.7. Flowrate distribution in an collector array for non ideal risers. Calculalated for 18 risers; isothermal temperature = 75°C; water as collector fluid. Risers 6-13 with twice the effective length. At flowrate of 75 l/hr-m^2 (HFR) and 9.375 l/hr-m^2 (LFR).

the effective riser length for nine center risers. This effective length accounts for disturbances in the risers which are not equally distributed over all risers. The expected increase in nonuniformity of the flowrate distribution is found.

The different effective lengths represent differences between risers such as uneven diameters or surface roughness, i.e. the effective length accounts for nonideal risers. This results in a superimposed pressure drop which decreases the uniformity of the flowrate distribution at low more than at high collector flowrates.

III.3.2 Collector Heat Removal Factor F_R

The collector heat removal factor F_R averaged with Eq. (III.9) is plotted in Figure III.8 for collector flowrates of 71.5 l/hr-m^2 (high) and 9.375 l/hr-m^2 (low) vs. the average flowrate deviation D_a. The average flowrate deviation was defined as

$$D_a = \frac{1}{n} \sum_{i=1}^{n} |D_i| = \frac{1}{\dot{m}_c} \sum_{i=1}^{n} |\dot{m}_i - \frac{\dot{m}_c}{n}| \qquad \text{(III.11)}$$

The reduction of F_R for the high collector flowrate is negligible. This is supported by Duffie and Beckman [10]. The reduction of F_R in the parts with a lower flowrate than the average is made up for to some extent by parts of the collector with a higher flowrate than the average flowrate. For the low collector flowrate F_R decreases from 0.615 to 0.590 over the average collector flowrate deviation in the investigated range. The change in F_R of 0.025 is not significant.

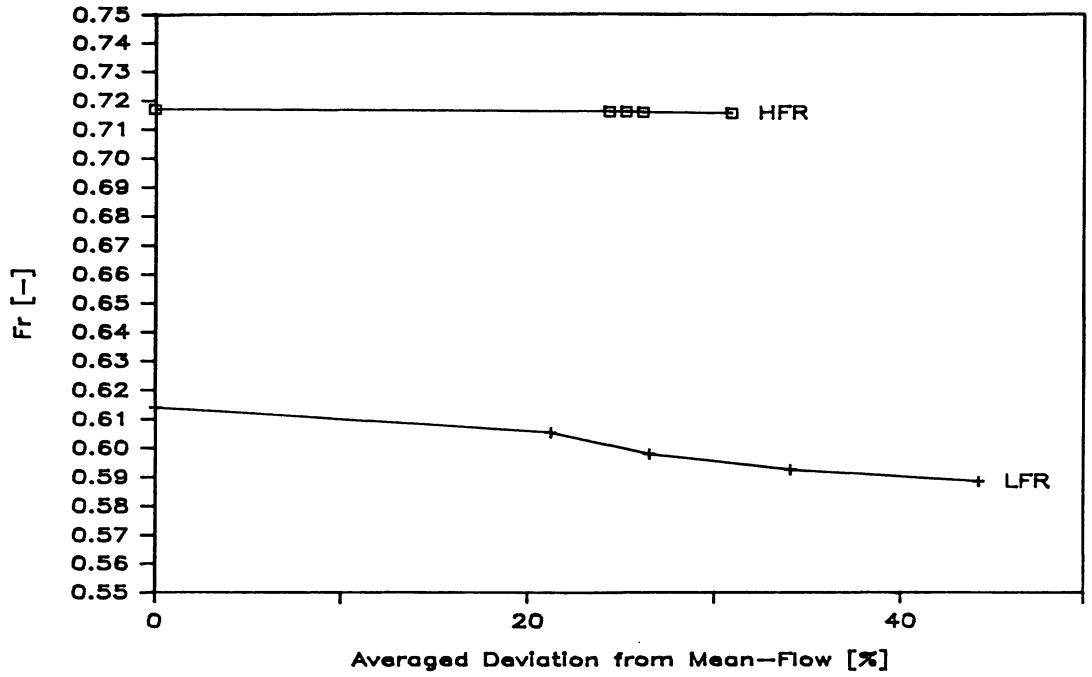

Figure III.8. Collector heat removal factor F_R vs. average absolute flowrate deviation. At flowrate of 75 l/hr-m^2 (HFR) and 9.375 l/hr-m^2 (LFR).

Measured flowrate distributions at reduced collector flowrates were unavailable for comparison with the calculated results.

The conclusion is that for collectors of the typical design shown in Figure III.1 no significant reduction in F_R as a result of low collector flowrate should be expected. Therefore systems with collectors of this design are well-suited for modification to operate at low collector flowrate, and improved performance can be expected.

IV. LOW COLLECTOR FLOWRATE COMPATIBILITY WITH A COLLECTOR-SIDE HEAT EXCHANGER

Collector-side heat exchangers are widely used as a means of freeze protection. Their compatibility with a reduced collector flowrate is investigated in this chapter.

IV.1 Heat Exchanger in a SDHW System

In all climates with temperatures occasionally below freezing liquid-based solar energy collection systems need freeze protection. One method of freeze protection is to ensure that the fluid running through the collector cannot freeze at the lowest temperature encountered in that climate. The liquids in all parts exposed to temperatures below freezing are antifreeze solutions such as ethylene-glycol/water mixtures.

A heat exchanger is needed to separate the collector loop from the solar storage tank containing the potable water. In SDHW systems, heat exchangers are widely used for freeze protection. The heat exchanger between the collector and tank may be located inside (internal) or outside (external) of the solar storage tank.

An external heat exchanger is investigated since detailed overall heat transfer coefficient data for such a heat exchanger were available. A schematic of a single tank SDHW system with external heat exchanger is in Figure IV.1. An ethylene-glycol water solution of 50% (by weight) was used in detailed measurements of heat exchanger UA_{HX} values by Fanney [31]. Four basic control strategies

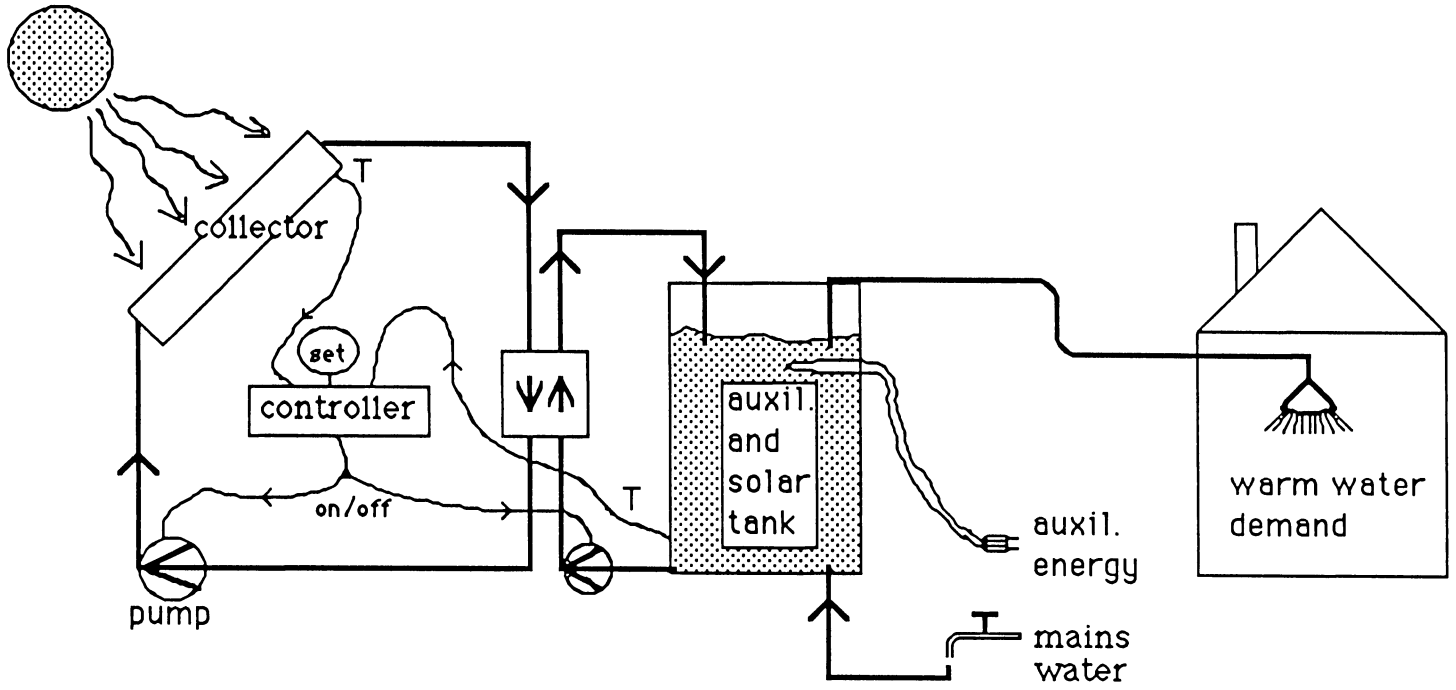

Figure IV.1. Single-tank solar domestic hot water system with heat exchanger. Schematic of the system setup used in simulations.

are possible for such a system:

1) high capacitance flow on both sides of the heat exchanger,
2) high capacitance flow on the collector-side and low capacitance flow on the tank-side of the heat exchanger,
3) low capacitance flow on both sides of the heat exchanger,
4) low capacitance flow on the collector-side and high capacitance flow on the tank-side of the heat exchanger.

The question, which of these strategies does result in the best system performance, does not have an obvious answer. Strategy one is the standard operating condition for SDHW systems with heat exchanger. It has a high collector efficiency and the best heat transfer coefficient for the heat exchanger of all four strategies because of the high flowrates on both heat exchanger sides. The high flowrate on the tank-side, however, prevents stratification in the storage tank. Strategy two also has a high collector efficiency. The heat exchanger UA_{HX} is lower because of the low flowrate on the tank-side of the heat exchanger. On the other hand this lower flowrate increases the stratification in the tank. Strategy three has the reduced collector efficiency of low collector flowrate systems and the lowest heat exchanger UA_{HX} value. The low tank flowrate prevents mixing in the tank and the low collector flowrate results in a large temperature difference for thermal stratification. Strategy four results in a low collector efficiency and mixing in the tank but it has a higher heat exchanger UA_{HX} value than strategy three.

IV.2 Simulation Setup for a SDHW System with Heat Exchanger

To answer the question, "which strategy reveals the highest system performance?", the base case simulations of systems without heat exchangers were repeated with a heat exchanger between the collector and the tank. The results of heat exchanger heat transfer coefficient measurements over a wide range of Reynolds numbers on either side of the heat exchanger were obtained from Fanney [31]. Curves fitted to the measured values were input to a modified TRNSYS heat exchanger subroutine. The measured UA_{HX} values and the curves are shown in Figure IV.2. The modification was necessary to allow flowrate and temperature dependent UA_{HX} values to be used. The UA values were supplied to the program as a table and linearly interpolated when necessary. For a counter-flow heat exchanger and known inlet conditions the transferred energy is

$$\dot{Q}_{trans} = \varepsilon C_{min}(T_{hi} - T_{ci}) \qquad \text{(IV.1)}$$

where TRNSYS uses

$$\varepsilon = \frac{1 - \exp\left(-\frac{UA_{HX}}{C_{min}}\left(1 - \frac{C_{min}}{C_{max}}\right)\right)}{1 - \frac{C_{min}}{C_{max}}\exp\left(-\frac{UA_{HX}}{C_{min}}\left(1 - \frac{C_{min}}{C_{max}}\right)\right)} \qquad \text{(IV.2A)}$$

for $0.01 < (C_{min}/C_{max}) < 0.99$

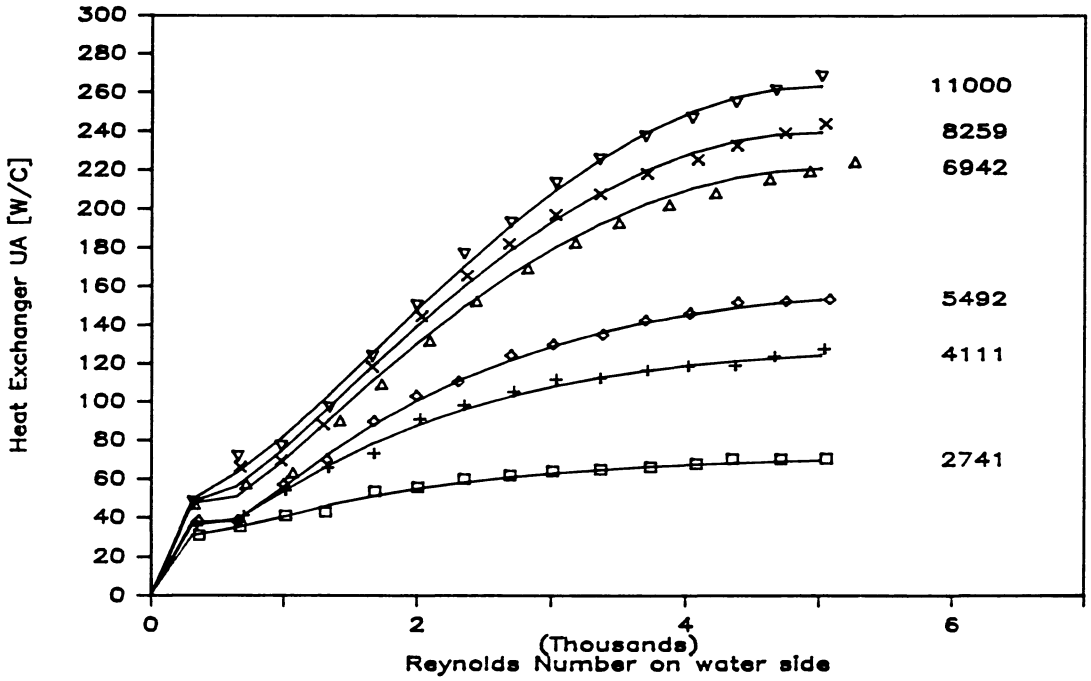

Figure IV.2. Heat exchanger UA values. Curves are Values used in TRNSYS, points are measured values. Parameter is the collector side Reynolds number.

$$\varepsilon = 1 - \exp\left(-\frac{UA_{HX}}{C_{min}}\right) \qquad \text{(IV.2B)}$$

for $(C_{min}/C_{max}) < 0.01$

$$\varepsilon = \frac{\frac{UA_{HX}}{C_{min}}}{1 + \frac{UA_{HX}}{C_{min}}} \qquad \text{(IV.2C)}$$

for $0.99 < (C_{min}/C_{max})$

where: ε = heat exchanger effectiveness

C_{min} = minimum capacitance rate

C_{max} = maximum capacitance rate

T_{hi} = hot side fluid inlet temperature

T_{ci} = cold side fluid inlet temperature

UA_{HX} = heat exchanger overall heat transfer coefficient

The cold and the hot side outlet temperatures are then

$$T_{ho} = T_{hi} - \varepsilon \frac{C_{min}}{C_{hot}} (T_{hi} - T_{ci}) \qquad \text{(IV.3)}$$

$$T_{co} = T_{ci} + \varepsilon \frac{C_{min}}{C_{cold}} (T_{hi} - T_{ci}) \qquad \text{(IV.4)}$$

where: T_{ho} = hot side outlet temperature

T_{co} = cold side outlet temperature

C_{hot} = hot side capacitance rate

C_{cold} = cold side capacitance rate

IV.3 Simulation Results for a SDHW System With Heat Exchanger

Simulations were done with the base case SDHW system setup for both the one and the two-tank systems. Investigations with twice the collector area of the base case system were conducted and systems with a heat exchanger having higher overall heat transfer coefficients were simulated.

IV.3.1 Base Case System Performance Results

To include all possible control strategies, simulations were run with various flowrates on both sides of the heat exchanger. The solar fraction vs. the flowrate on the tank-side of the heat exchanger is shown in Figures IV.3 and IV.4. Curves are drawn for a variety of specific flowrates through the collector array. The curves show a decrease in system performance as the flowrate on either side of the heat exchanger decreases. No significant differences between one and two-tank SDHW systems as a result of the heat exchanger were observed. With the flowrate on the collector-side of the heat exchanger the solar fraction increases monotonically at any flowrate of the tank-side. A broad maximum below the highest tank side flowrate is found for collector flowrates above 12 $l/hr\text{-}m^2$. The solar fraction is plotted vs. the ratio of average flow on the tank-side of the heat exchanger to load flow, $(\overline{M}_c/M_l)$ in Figures IV.5 and IV.6. The maximum for these curves is found to be at $\overline{M}_c/M_l$ of about 5.5.

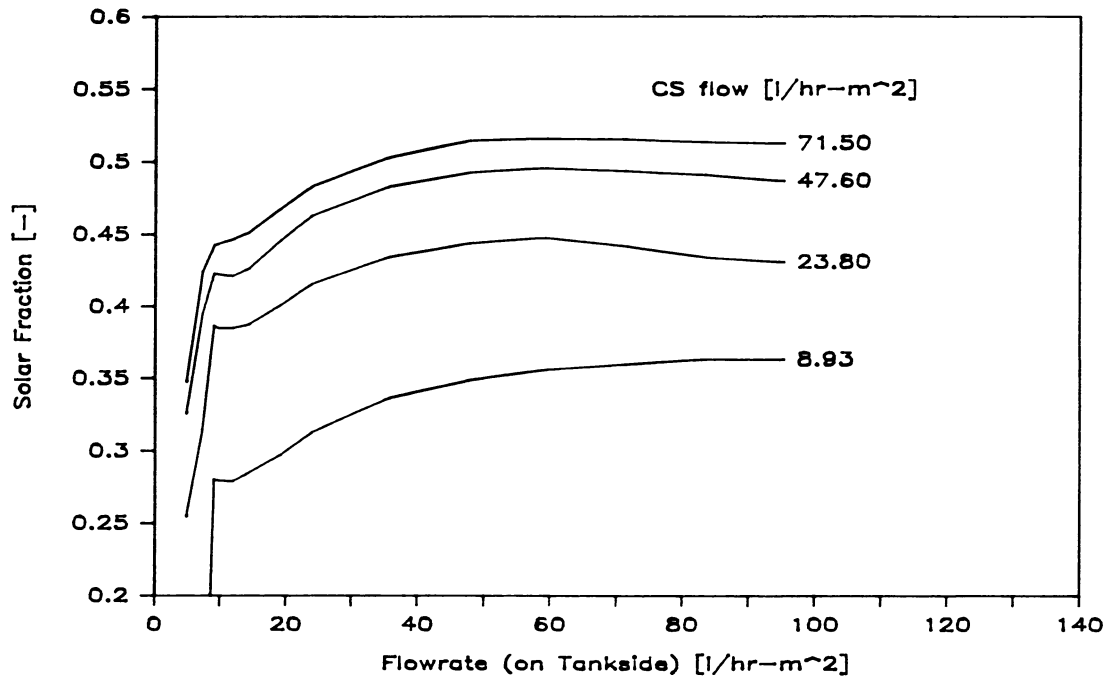

Figure IV.3. Solar fraction vs. collector flowrate on the tank side. For the single-tank base case system with heat exchanger. March in Madison. CS = flowrate on collector side.

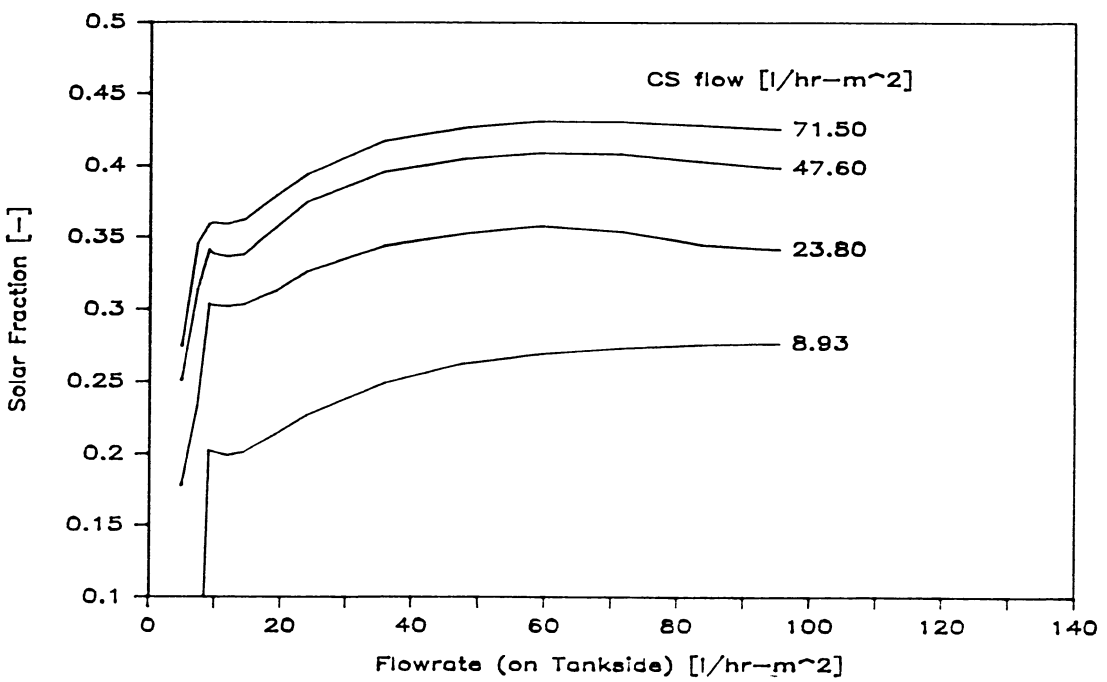

Figure IV.4. Solar fraction vs. collector flowrate on the tank side. For the double-tank base case system with heat exchanger. March in Madison. CS = flowrate on collector side.

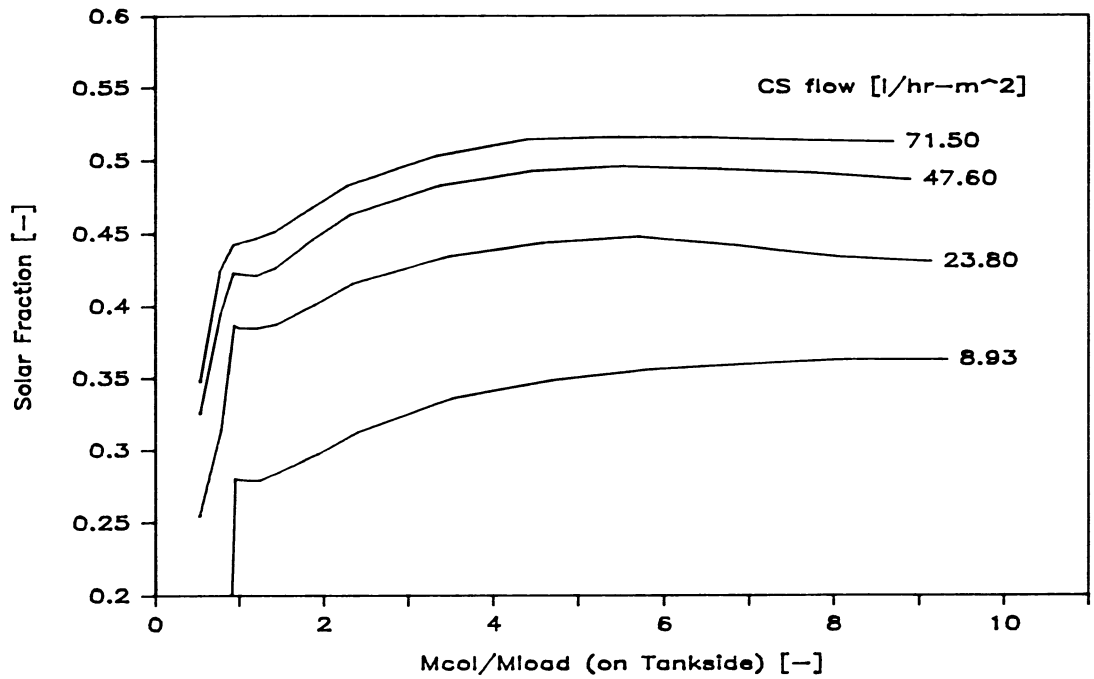

Figure IV.5. Solar fraction vs. $\overline{M}_c/M_l$ ($\overline{M}_c$ on the tank side of the heat exchanger). For the single-tank base case system with heat exchanger. March in Madison. CS = flowrate on collector side.

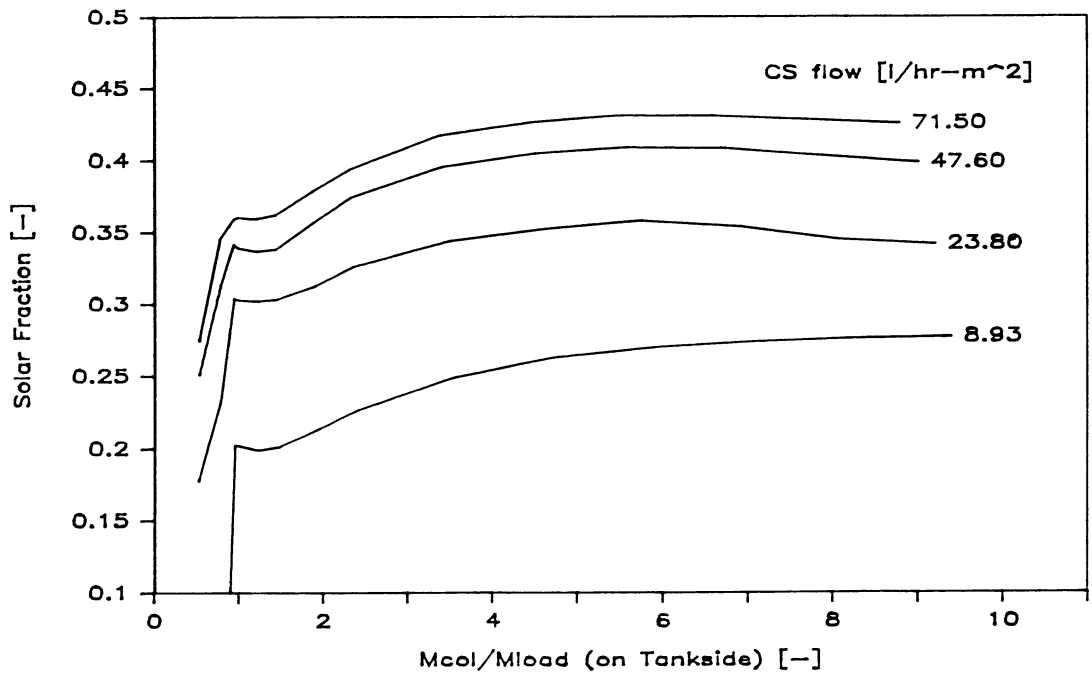

Figure IV.6. Solar fraction vs. $\overline{M}_c/M_l$ ($\overline{M}_c$ on the tank side of the heat exchanger). For the double-tank base case system with heat exchanger. March in Madison. CS = flowrate on collector side.

IV.3.2 Increased Collector Area for the Base Case System

The solar fraction for the base case system with twice the collector area is shown in Figures IV.7 and IV.8 vs. the tank-side flowrate and in Figures IV.9 and IV.10 vs. $\overline{M}_c/M_1$. Again the one and the two-tank systems show similar effects.

An upper limit for the performance seems to be reached below the highest specific collector flowrate simulated. Note that doubling the collector area results in twice the collector-side flowrate through the heat exchanger. At high specific collector flowrates the limiting capacitance rate is on the tank-side of the heat exchanger. Additionally, the UA_{HX} values of the heat exchanger do not increase rapidly enough with the collector-side flowrate to transfer the collected energy. Both effects increase the average collector inlet temperature, thereby reducing its efficiency and increasing its losses. The temperature in the collector loop could even reach boiling conditions, so that energy would have to be dumped. A larger heat exchanger and higher flowrate on the tank side could prevent this.

No maximum solar fraction was found for these limited collector flowrates. At lower collector flowrates a maximum still exists at a slightly reduced $\overline{M}_c/M_1$ of about 4.5.

IV.3.3 Effect of larger Heat Exchanger

A heat exchanger with UA_{HX} values which are n times as high as in the base case was used to simulate SDHW systems with better or larger heat exchangers. Only the highest collector flowrate of

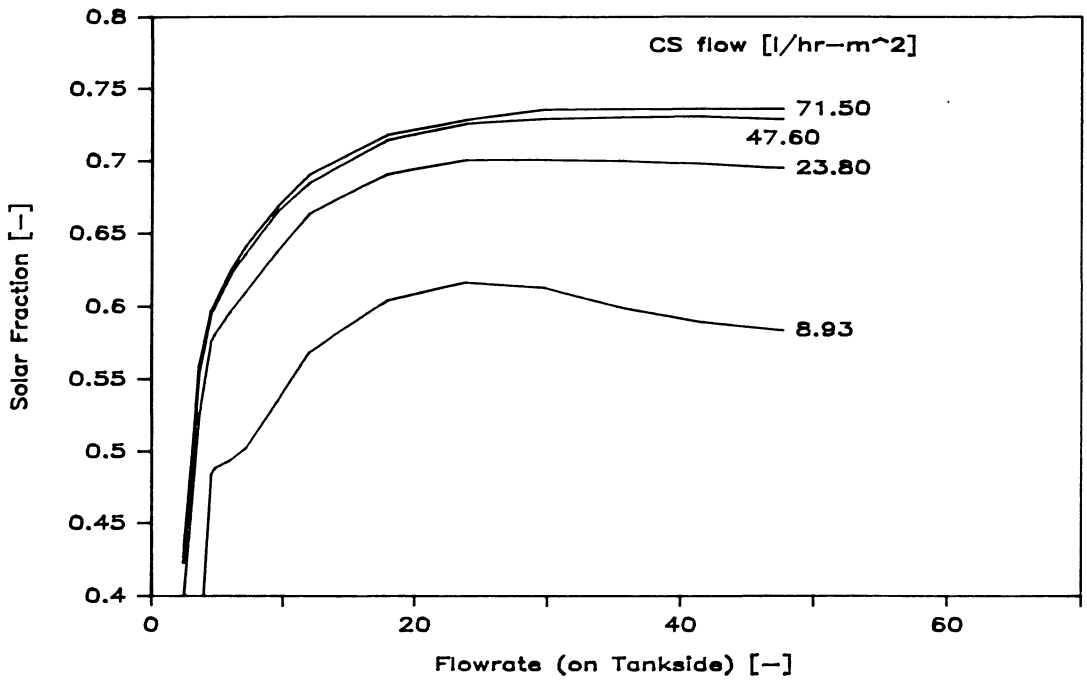

Figure IV.7. Solar fraction vs. collector flowrate on the tank side. For the single-tank base case system with heat exchanger with double the collector area. March in Madison. CS = flowrate on collector side.

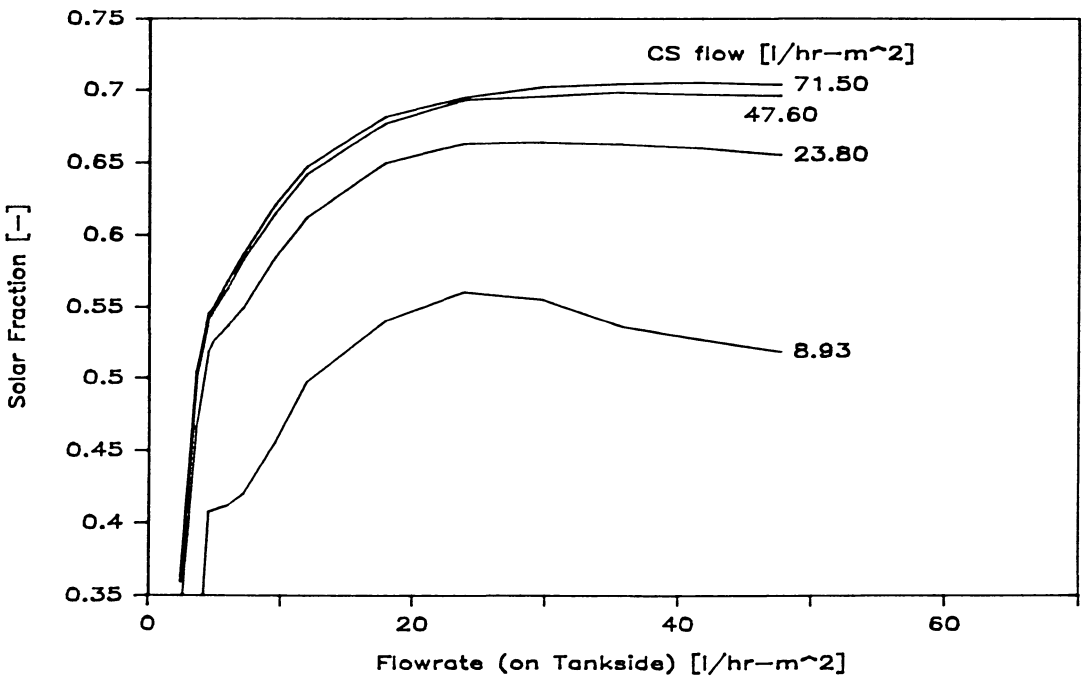

Figure IV.8. Solar fraction vs. collector flowrate on the tank side. For the double-tank base case system with heat exchanger with double the collector area. March in Madison. CS = flowrate on collector side.

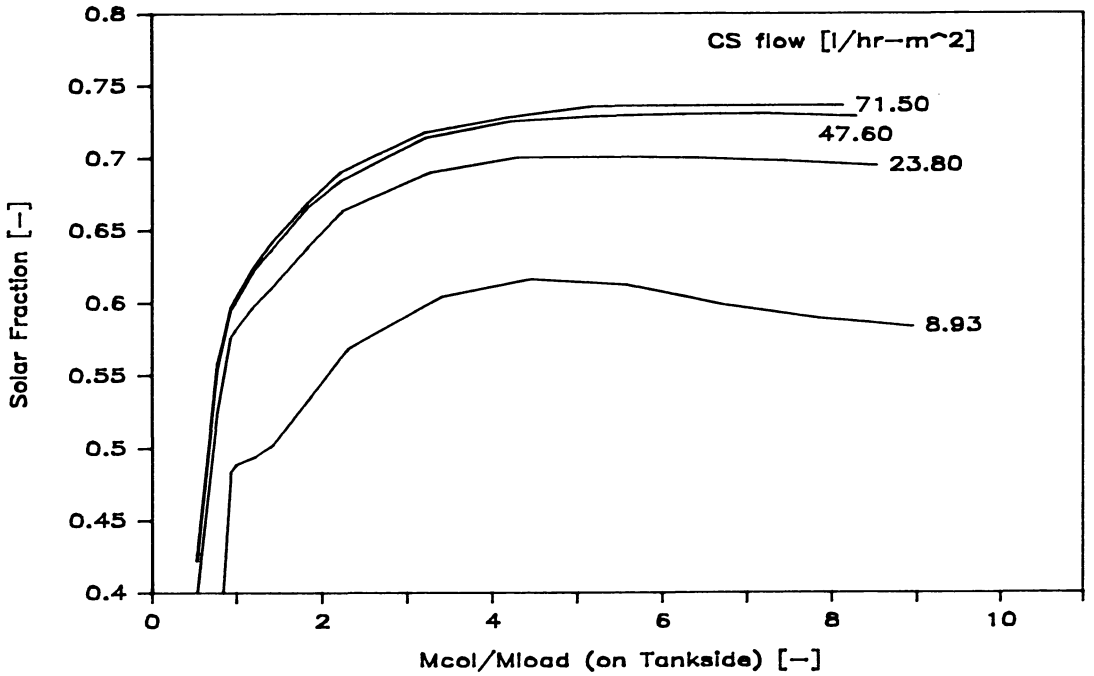

Figure IV.9. Solar fraction vs. $\overline{M}_c/M_l$ ($\overline{M}_c$ on the tank side of the heat exchanger). For the single-tank base case system with heat exchanger with double the collector area. March in Madison. CS = flowrate on collector side.

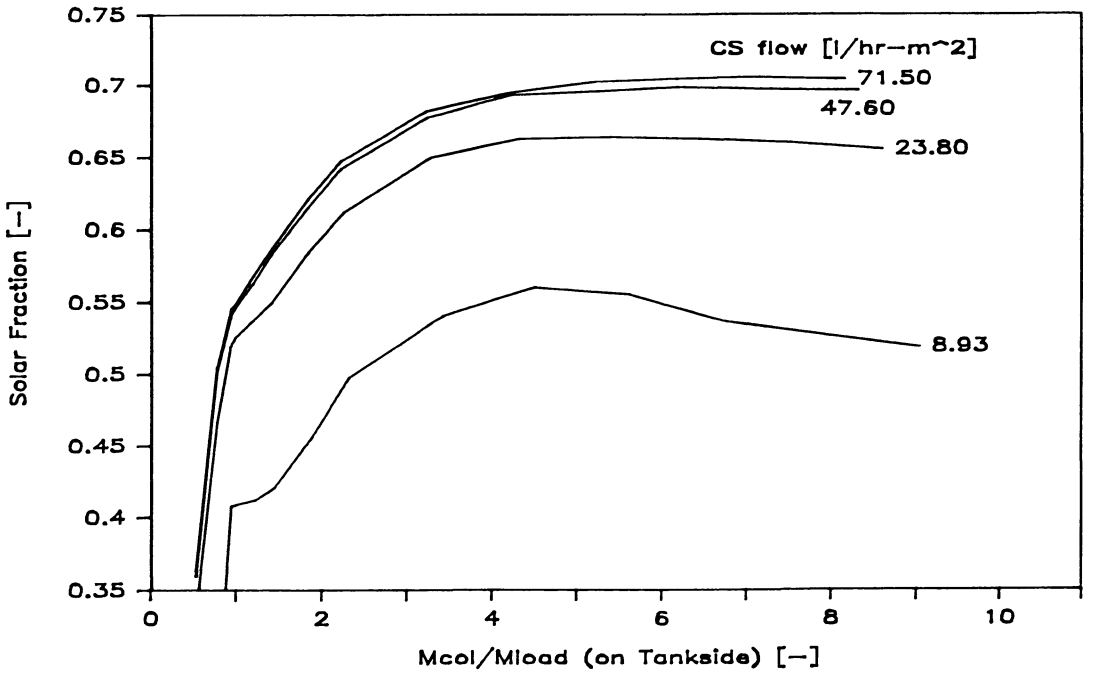

Figure IV.10. Solar fraction vs. $\overline{M}_c/M_l$ ($\overline{M}_c$ on the tank side of the heat exchanger). For the double-tank base case system with heat exchanger with double the collector area. March in Madison. CS = flowrate on collector side.

71.5 l/hr-m^2 was investigated because of the monotonical relationship between collector flowrate and system performance in all of the previous calculations. The solar fractions for single- and double-tank SDHW systems with heat exchangers of n times the transfer area are shown in Figures IV.11-IV.14. The maxima observed previously become more distinct with increasing n, while showing a tendency to lower $\overline{M}_c/M_l$. For the largest n the maximum is found at $\overline{M}_c/M_l$ of 4.25. For both systems the solar fraction is 5 percentage points better than the solar fraction of the normally operated SDHW system with n = 1.

The simulation results show no increase of solar fraction at n = 1 for reduced flowrates. With better heat exchangers, however, an improvement may be realized by reducing flowrates on the tank-side of the heat exchanger. Care must be taken that the tank-side capacitance rate does not limit the system performance. A more detailed study on the effects of HXs on SDHW systems and a verification of the simulation results by field experiments is necessary to confirm the described observations.

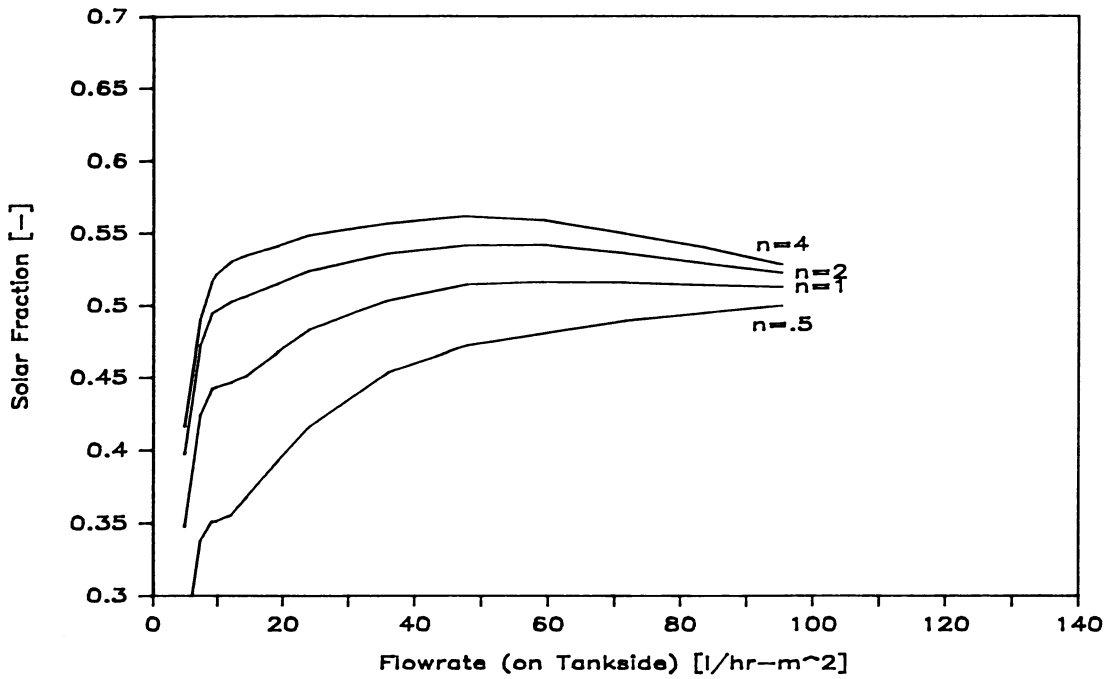

Figure IV.11. Solar fraction vs. collector flowrate on the tank side. For the single-tank system with heat exchanger at a collector side flowrate of 71.5 l/hr-m^2. March in Madison. n times the UA values of the base case.

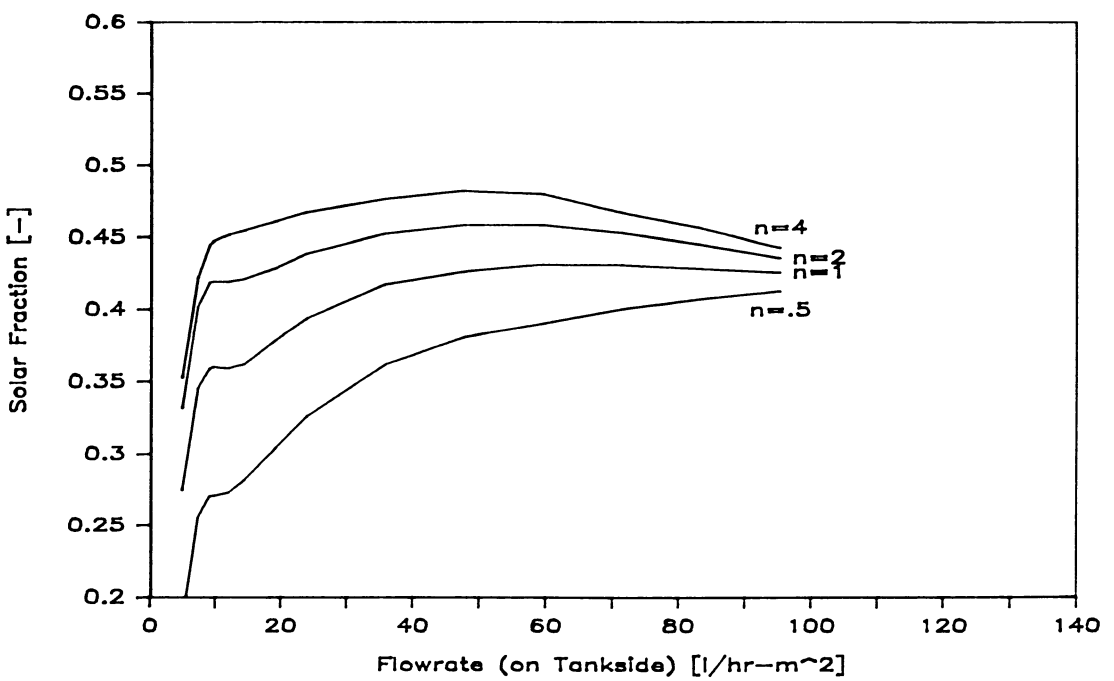

Figure IV.12. Solar fraction vs. collector flowrate on the tank side. For the double-tank system with heat exchanger at a collector side flowrate of 71.5 l/hr-m^2. March in Madison. n times the UA values of the base case.

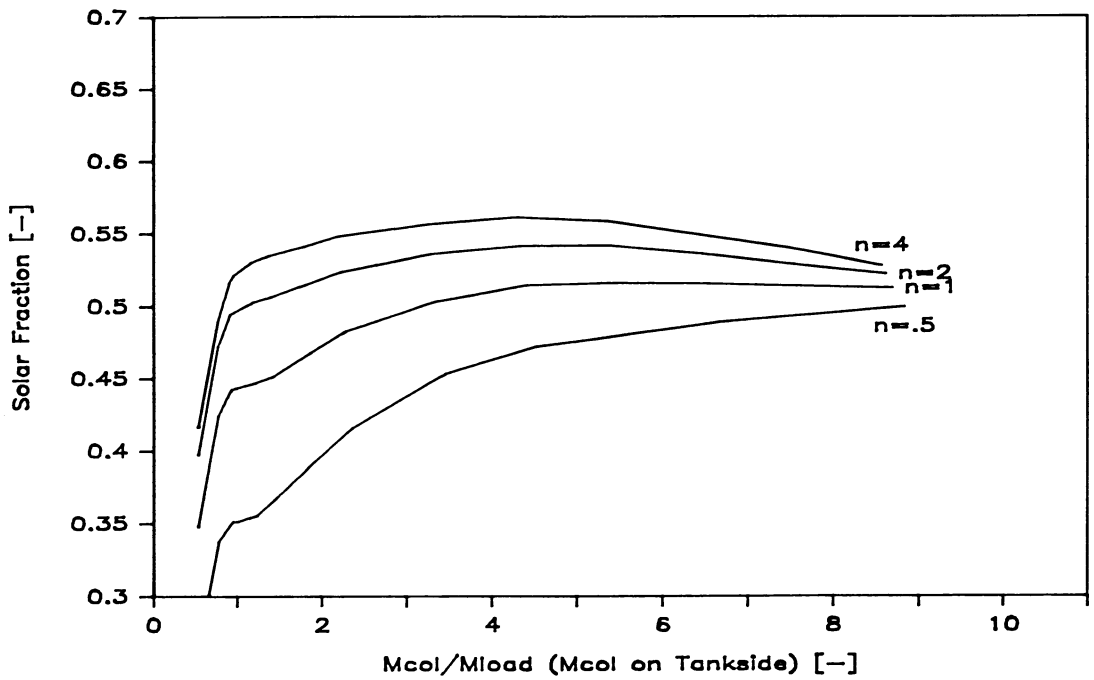

Figure IV.13. Solar fraction vs. $\overline{M}_c/M_l$ ($\overline{M}_c$ on the tank side of the heat exchanger). For the single-tank system with heat exchanger at a collector side flowrate of 71.5 l/hr-m^2. March in Madison. n times the UA values of the base case.

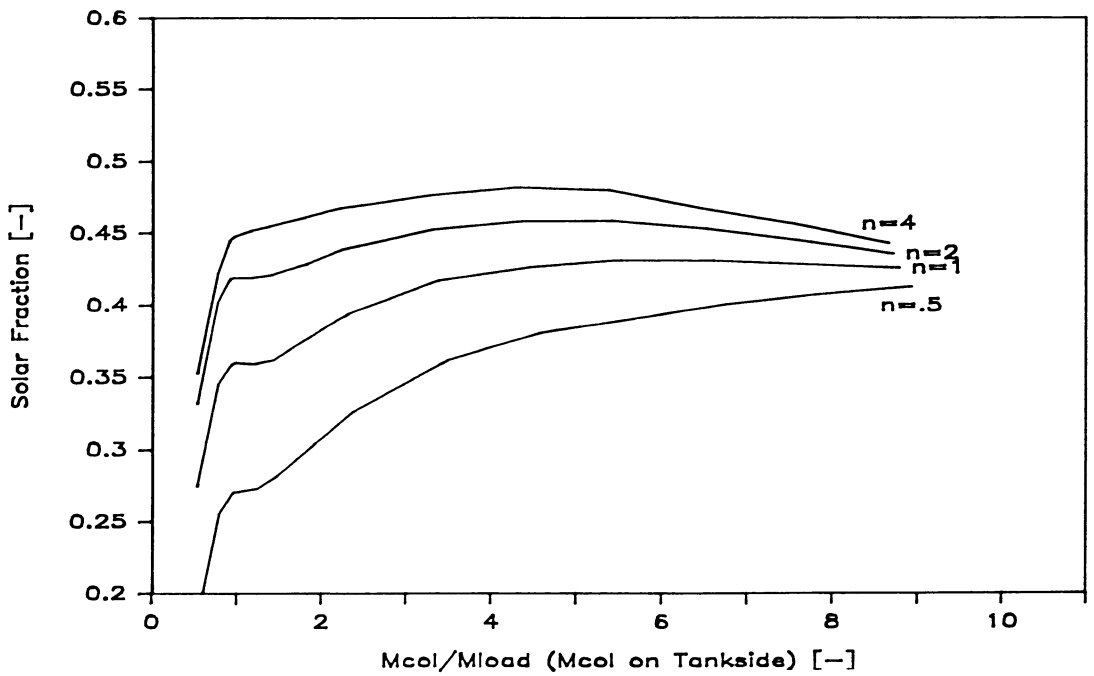

Figure IV.14. Solar fraction vs. $\overline{M}_c/M_l$ ($\overline{M}_c$ on the tank side of the heat exchanger). For the double-tank system with heat exchanger at a collector side flowrate of 71.5 l/hr-m^2. March in Madison. n times the UA values of the base case.

V. CONTROL OF SDHW SYSTEMS AT REDUCED COLLECTOR FLOWRATES

By reducing the collector flowrate, the operating conditions of an active SDHW system are significantly changed. It is of interest to determine whether the current controllers are appropriate for the low collector flowrate mode of operation and if a different control strategy would enhance the system performance even further.

V.1 Controllers in SDHW Systems

Many control strategies for SDHW systems are possible. The characteristics of on/off and proportional (P-) controllers have been thoroughly studied for high collector flowrate operating conditions [10,32,33]. In his discussion of controls Winn [32] included also integral (I-) and proportional/integral/differential (PID-) controllers. He concluded that on/off controllers are optimal if parasitic power consumption is not considered. Considering parasitics, the optimal control of the collector flowrate is a controller proportional to the collector temperature rise. Winn reports however, that the improvement over on/off control is only 5% of the annual collected energy in Ft. Collins, CO; this value increased with reduced radiation levels. The controller analysis was based on the assumption of fully mixed storage tanks implying a high collector flowrate. Other controllers did not yield further improvement.

V.2 Control Strategy in SDHW Systems

V.2.1 Task of Control Strategy in SDHW Systems

The controller is used to control the pump operating the collector loop in a SDHW system. Other objectives such as overheat protection or freeze protection are not included in this investigation, because they do not significantly affect the performance of a well-designed system (assuming proper operation). The base case controller operation is shown in Figures I.1 and I.2. Its operation is determined by a comparison of collector-header minus tank-outlet temperature and set-point temperature differences, which are user specified. For practical reasons, such as cost, reliability, maintenance requirements and simplicity the number and location of temperature sensors were retained.

The controller has to satisfy three control objectives:

1) Operate the pump only if energy collection justifies the use of pumping power.
2) Prevent cycling of pump, i.e. make stable control decisions.
3) Enhance temperature stratification in the storage tank.

The order of these objectives reflects their relative importance. Although objective three is not restricted to reduced collector flowrate operation, it cannot have significant effects at high flowrates. At high flowrates the input momentum results in well mixed storage tanks and the temperature rise is too small to enhance stratification.

V.2.2 Formulation of Control Objectives

To identify the controller logic, the objectives have to be formulated in a mathematical way. Objective one can be formulated to cease operation if the rate at which energy is collected ($\dot{Q}_u$) is less than the parasitic power consumption (P):

$$\dot{Q}_u < P \tag{V.1}$$

where

$$\dot{Q}_u = \dot{m}_c \, c_p \, (T_{Co} - T_{Ci}) \tag{V.2}$$

If losses of the pipe from the tank to the collector are neglected

$$\dot{Q}_u = \dot{m}_c \, c_p \, (T_{Co} - T_{To}) = \dot{m} c_p \, \Delta T_{measured} \tag{V.3}$$

where: $\dot{m}_c$ = actual collector flowrate

c_p = specific heat capacitance

T_{Co} = collector outlet temperature

T_{Ci} = collector inlet temperature

T_{To} = tank outlet temperature

$\Delta T_{measured}$ = temperature difference measured by controller

The pump power is

$$P = \frac{1}{\eta_p} \dot{V} \Delta p = \frac{\dot{m}_c}{\eta_p \cdot \rho} \Delta p \tag{V.4}$$

with the pressure drop for a closed circulation system as derived in

Chapter III.2

$$\Delta p = \frac{8}{\pi} \frac{f}{\rho} \frac{L}{D^5} \dot{m}_c^2 \qquad (V.5)$$

where: η_p = pump efficiency

$\dot{V}$ = volume flowrate

Δp = pressure drop of the whole system

ρ = water density

f = friction factor

L = length of the total collector flowpath

D = averaged hydraulic diameter of the collector loop

Because f is a function of flowrate - see Eqs. (III.4) and (II.5) and with α defined between 1 for laminar flow and 2 for turbulent flow the pressure drop can be written as

$$\Delta p = C_1 (\dot{m}_c)^{\alpha} \qquad (V.6)$$

With Eqs. (V.1)-(V.6) the first control law is

$$U = 0 \quad \text{for} \quad \Delta T_{measured} < \Delta T_{off}$$

$$\Delta T_{off} = \frac{C_1}{\eta_p \rho c_p} (\dot{m}_c)^{\alpha} = C (\dot{m}_c)^{\alpha} \qquad (V.7)$$

where U is the controller decision and C_1 and C are constants.

The second control law is discussed in detail in [10]. It is concluded that for

$$\Delta t > \frac{\dot{m}_c c_p}{A_c F_R U_L} \Delta T_{off} \tag{V.8}$$

no cycling occurs. The resulting control law is then

$$\begin{aligned} U &= 1 \qquad \text{for} \qquad \Delta T_{measured} > \Delta T_{on} \\ \Delta T_{on} &= \frac{\dot{m}_c c_p}{A_c F_R U_L} \Delta T_{off} \end{aligned} \tag{V.9}$$

These two control laws define the on/off hystereses controller. The on/off controller output for decisions of 0 or 1 vs. the measured temperature difference is shown in Figure V.1. ΔT_{on} cannot be chosen independently but depends on ΔT_{off} according to Eq. (V.9). Control law one only requires a minimum ΔT_{off} to prevent system operation when less energy is collected than used by the circulation pump. It allows values of ΔT_{off} to be larger than the minimum ΔT_{off}. The effects, which can be denoted to values of ΔT_{off} larger than the minimum value, are not obvious. For constant ratio of $\Delta T_{on}/\Delta T_{off}$ (according to control law two) a larger ΔT_{off} results in a reduced system operating time because it takes longer to start operation. Also a larger ΔT_{off} turns the system off earlier. On the other hand, this reduced operating time may prevent mixing of the tank at low radiation levels, i.e. a small temperature rise across the collector.

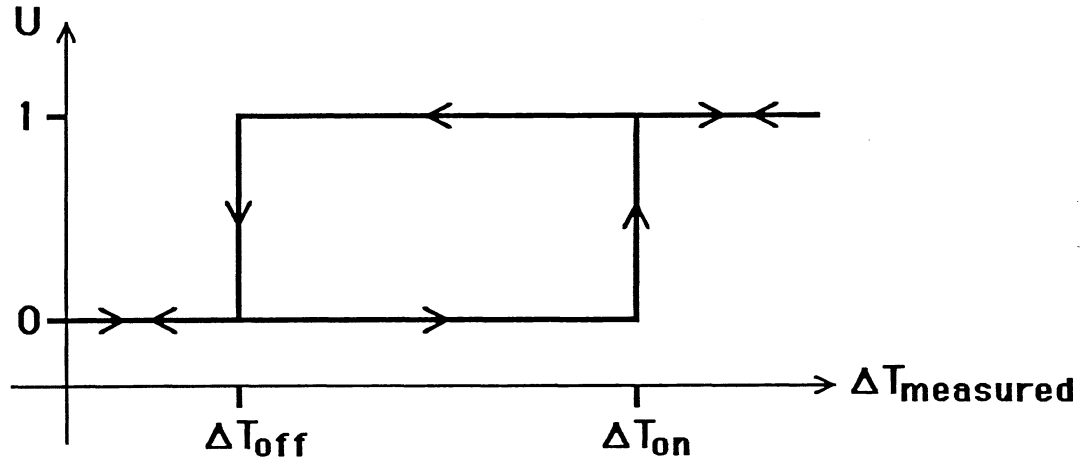

Figure V.1. On/off controller with hysteresis.

If the tank is well stratified, turn-off may be delayed because of a low tank bottom temperature; the collector efficiency will also be higher. It is not clear which of these effects is dominant. Therefore simulations of increased ΔT_{off} at low collector flowrate were conducted for the base case systems; results are included in section three of this chapter.

Stratification devices and operating strategies are discussed in [1,5,14,34]. The common conclusion is that low collector flowrates result in a momentum small enough to prevent mixing in the tank and that they supply a large enough temperature rise to stratify the tank. Objective three is therefore met by a low collector flowrate. The collector temperature rise depends on flowrate. It is of interest which temperature rise would be appropriate to reach the best system performance with a stratified tank. Provided that the tank capacitance is sufficient it is not necessary to collect energy at temperatures above the supply set temperature. Higher collector temperatures would decrease the collector efficiency and result in a larger amount energy supplied to the load for a certain amount of water draw.

Simulation results of three control strategies for variable flowrates are reported by Wuestling [1]: fixed collector outlet temperature, fixed temperature rise across the collector and flowrate proportional to radiation while satisfying a preset $\overline{M}_c/M_1$ ratio. All strategies resulted in solar fractions lower or equal to the one reached with constant collector flowrate and on/off control. The

proportional controller used by Wuestling did not conform to control law one and two.

V.2.3 Control Strategies with Variable Collector Flowrate

To satisfy control laws one and two and still restrict the collector outlet temperature, a proportional controller was combined with the on/off control strategy. The proportional controller was set to keep the collector outlet temperature at the supply set-temperature

$$\dot{m}_{c,P} = \frac{T_{Co}}{T_{set}} \dot{m}_c \qquad (V.10)$$

where: $\dot{m}_{c,P}$ = proportional collector flowrate

T_{set} = supply set-temperature

Several restrictions apply: the flowrate was constrained between 9 l/hr-m^2 and 71.5 l/hr-m^2, which are the reduced and standard flowrate, respectively, as used in experiments and previous simulations. For stable control decisions changes of the controller output were only allowed if they met the requirement

$$\left|\frac{\text{old flowrate}}{\text{new flowrate}} - 1\right| > DS \qquad (V.11)$$

DS = controller decision parameter.

The on/off controller has a higher priority than the proportional controller. It operates the pump at the low collector flowrate. Whereas the proportional control operates the system at in-

creased flowrates. The proportional control will affect the system only if the collector outlet temperature exceeds the supply set-temperature while operating at low flowrates. The control characteristic is shown in Figure V.2. Note that overheat protection is a beneficial side-effect, because the collector outlet temperature is controlled to be at the supply temperature.

The control variable for the proportional controller is the collector outlet temperature T_{Co}. To allow the collector outlet temperature to be a few degrees higher (or lower) than the load-supply set-temperature, a deviation parameter DTO (Deviation of Temperature Outlet) was subtracted from T_{Co} before computing the control decision. This means that the collector outlet temperature is controlled to stay above (or below) the load-supply set-temperature allowing to optimize the control strategy.

Wuestling [1] found an optimal system performance for a certain $\overline{M}_c/M_1$ ratio. Another strategy is therefore to increase the flowrate to meet the recommended $\overline{M}_c/M_1$ ratio. This is done using either the proportional-controller flowrate $\dot{m}_{c,P}$ or an integral-controller flowrate $\dot{m}_{c,I}$, whichever is higher. $\dot{m}_{c,I}$ was calculated as

$$\dot{m}_{c,I} = \frac{\text{requested } \overline{M}_c/M_1}{\text{actual } \overline{M}_c/M_1}\,\dot{m}_c = \left[\frac{(\overline{M}_c/M_1)}{(\int_0^t \dot{m}_c\,dt)/((TCT - A)\,M_1/TCT)}\right]\dot{m}_c \qquad (V.12)$$

where: TCT = total daily collection time (controller parameter)

t = actual time

M_1 = total daily load draw (controller parameter)

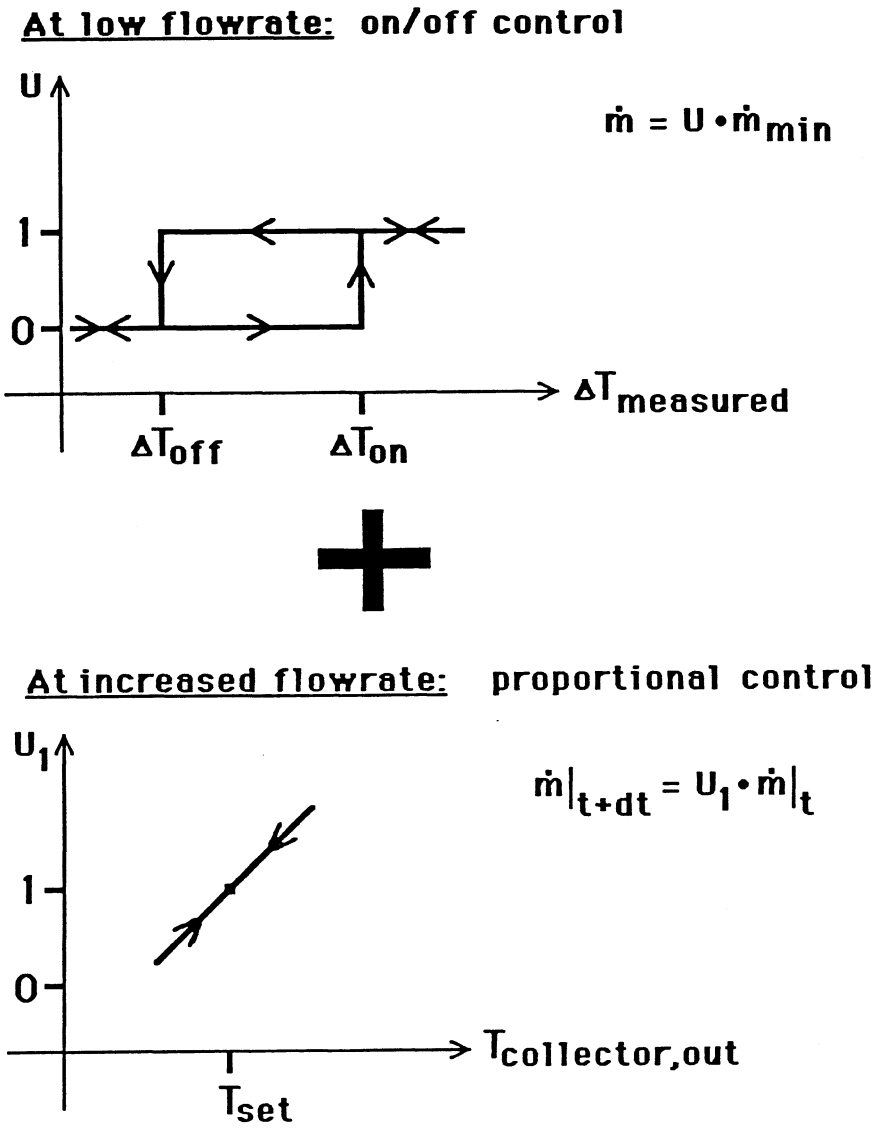

Figure V.2. Proportional controller characteristic. Used as indicated.

$(\overline{M}_c/M_1)$ = requested $\overline{M}_c/M_1$ ratio (controller parameter)

The coefficient for the flowrate can be interpreted as the ratio of requested $\overline{M}_c/M_1$ over the actual $\overline{M}_c/M_1$. Two drawbacks of this control strategy should be noted:

1) TCT and M_1 are unknown values depending on future weather conditions and individual water usage.
2) $(\overline{M}_c/M_1)$is a monthly average value. Even if $(\overline{M}_c/M_1)$ would be adjusted for each month, the controller is based on a daily cycle so that only values for each day would be appropriate.

Results of system performance with this control strategy are included in section three.

V.3 Effects of Controllers on SDHW Systems

All simulations were done using the base case systems described in Chapter II for March in Madison. The only difference between the simulations were the controllers used. In the discussion below, base case refers to a system with on/off control and set points as chosen by Fanney [8] (ΔT_{on} = 11.1°C; ΔT_{off} = 2.8°C).

V.3.1 SDHW Systems with On/Off Differential Controller

The base case on/off controller was used in NBS experiments regardless of the flowrate. The previous discussion suggested that a change in flowrate requires a concomitant change of the controller set-temperatures to achieve a good performance. The system description did not allow an analytical determination of ΔT_{off}. ΔT_{off} = 2.8°C is a typical value for high collector flowrates [33]. Therefore it was assumed that control law one is satisfied for ΔT_{off} =

2.8°C at a collector flowrate of 71.5 l/hr-m^2. For a low flowrate of 9 l/hr-m^2 the set-temperature difference ΔT_{off} is then determined by using Eq. (V.7) to calculate the ratio

$$\frac{\Delta T_{off}|_{LFR}}{\Delta T_{off}|_{HFR}} = \frac{C \cdot (\dot{m}_c)^{\alpha}|_{LFR}}{C \cdot (\dot{m}_c)^{\alpha}|_{HFR}}$$

To estimate this ratio α and C were assumed to be independent of flowrate so that

$$\frac{\Delta T_{off}|_{LFR}}{\Delta T_{off}|_{HFR}} = \left(\frac{\dot{m}_{c,LFR}}{\dot{m}_{c,HFR}}\right)^{\alpha}$$

with the values for high and low collector flowrate this ratio is

$$\left(\frac{\dot{m}_{c,LFR}}{\dot{m}_{c,HFR}}\right)^{\alpha} = \begin{cases} 0.125 & \text{for } \alpha = 1 \\ 0.016 & \text{for } \alpha = 2 \end{cases}$$

Independent of α the value for ΔT_{off} at low flowrate is significantly lower than one degree. Sensors of commercial quality have an accuracy which would allow very low temperature differences to be measured. However, sensors with an accuracy of one degree or more are both reliable and cost effective [18]. Therefore ΔT_{off} for the low collector flowrate simulations was set at one degree.

Control law two with parameters from Table II.3 results in ratios for

$$\frac{\Delta T_{on}}{\Delta T_{off}} = \begin{cases} 16.2 & \text{for high flowrate} \\ 2.0 & \text{for low flowrate} \end{cases}$$

With the assumption that ΔT_{off} of 2.8°C is correct at high collector flowrate Table V.3 shows the on/off controller settings resulting from control laws one and two.

The effect of different ΔT_{on} set-points for the on/off controller is shown in Figure V.4. Simulations were done for low and high collector flowrates and single and double tank systems. A range of ΔT_{on} around the calculated settings and the base case, i.e. the NBS experiment set-points, are compared. It should be noted that the base case systems perform about 4% better than the ones with ΔT_{on} as calculated at high collector flowrate. The low collector flowrate systems do not show significant changes for any of the controller settings. The base case, however, has the lowest solar fraction. Increasing ΔT_{on} above the values of Table V.3 did not show any effect for all cases investigated.

The number of cycles (switch from on to off and back) for the simulations with high collector flowrate vs the ratio of $\Delta T_{on}/\Delta T_{off}$ is plotted in Figure V.5. Single and double tank systems show significant cycling for ratios of $\Delta T_{on}/\Delta T_{off}$ lower than 14. The base case experienced well over 1500 cycles during the month. For the low collector flowrate cycling does not exceed 250 even for $\Delta T_{on}/\Delta T_{off}$ of one as shown in Figure V.6. The better system performance of the base case systems results in a large number of cycles. As explained

	high flowrate 71.5 l/hr-m²	low flowrate 9 l/hr-m²
ΔT_{off}	2.8 °C	1 °C
ΔT_{on}	45 °C	2 °C

Table V.3. On/off controller temperature-difference set-points.

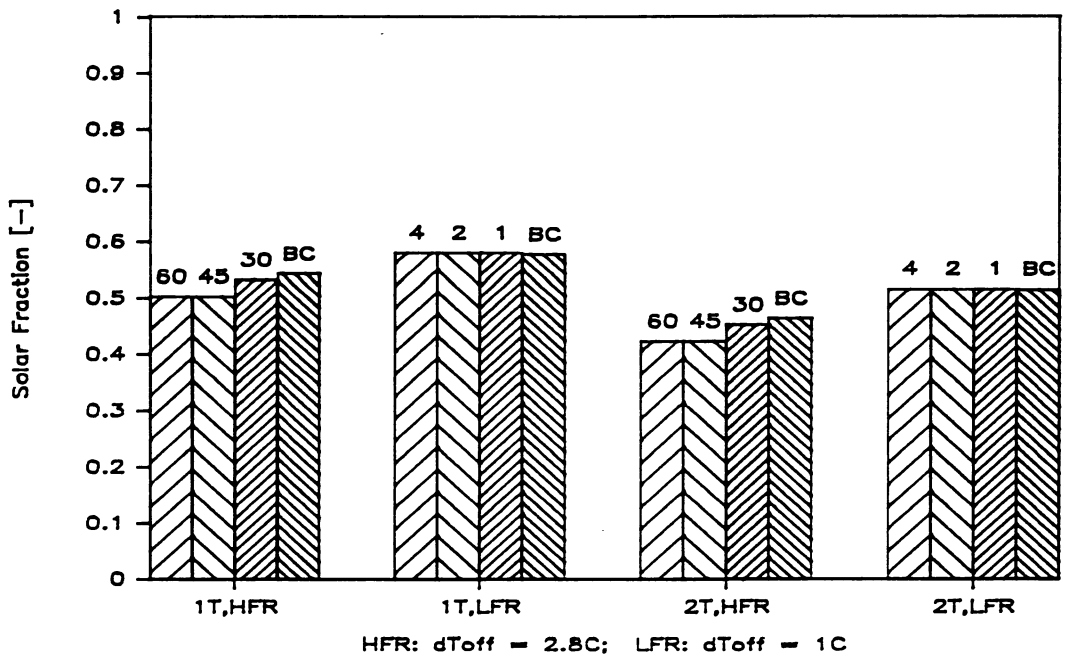

Figure V.4. On/off controller set-point comparison. For single (1T) and double (2T) tank system at high (HFR) and loaw (LFR) flowrate. $\Delta T_{off,HFR} = 2.8°C$, $\Delta T_{off,LFR} = 1°C$, ΔT_{on} as labled, BC = base case.

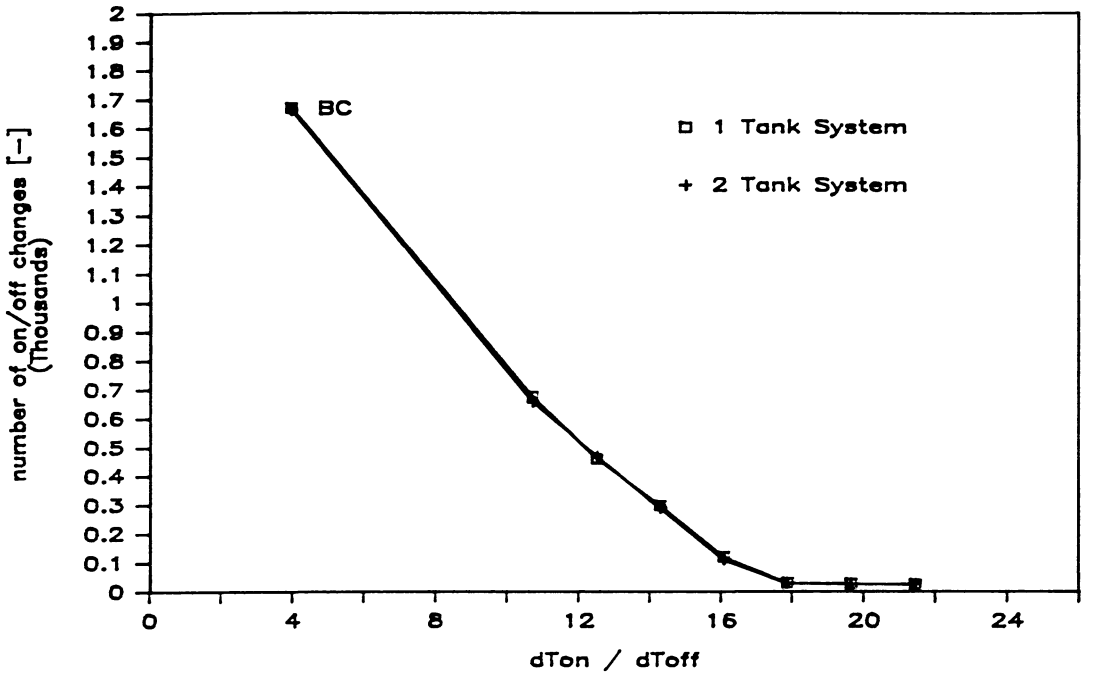

Figure V.5. On/off controller cycling vs. $\Delta T_{on}/\Delta T_{off}$. For a flow-rate of 71.5 l/hr-m^2, ΔT_{off} = 2.8°C, BC = base case.

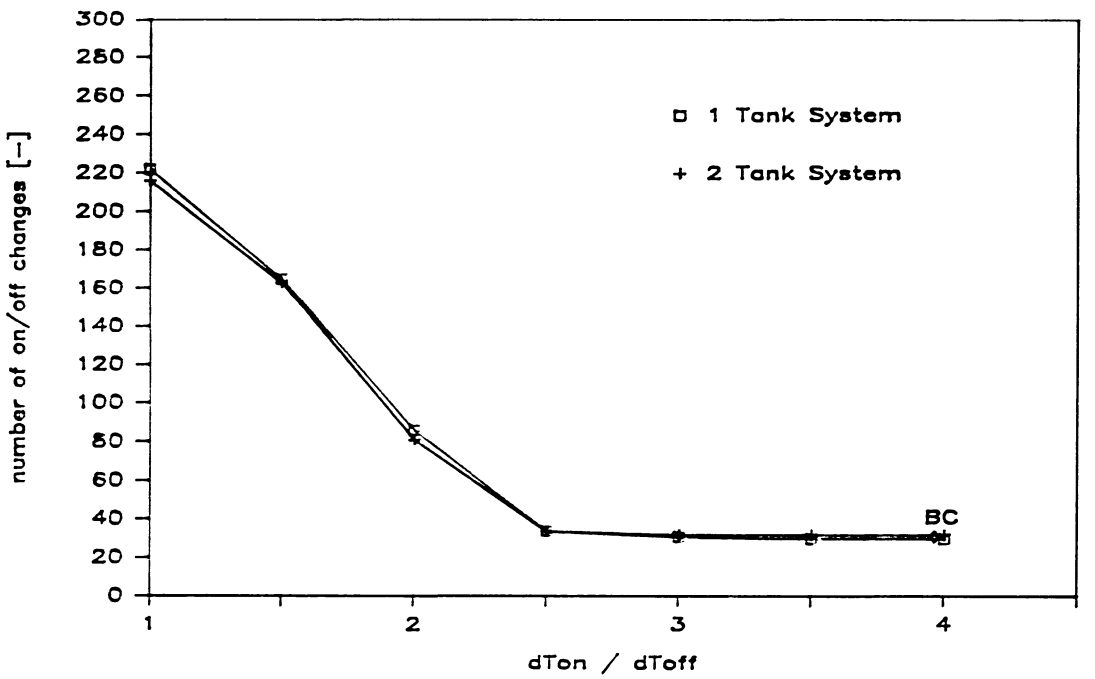

Figure V.6. On/off controller cycling vs. $\Delta T_{on}/\Delta T_{off}$. For a flow-rate of 9 l/hr-m^2, ΔT_{off} = 1°C, for base case (BC): ΔT_{off} = 2.8°C.

in Chapter II the collector was simulated without capacitance. In real collectors the number of cycles is lower because of capacitance, delay times in the piping and reaction times of sensor and controller. The experimental data, however, show for most operating hours an pump operation time of less than 60 minutes at the high collector flowrate indicating at least one cycle for that hour.

To investigate the effect of ΔT_{off} larger than calculated above, a number of simulations for single and double tank systems at low collector flowrate were conducted. $\Delta T_{on}/\Delta T_{off}$ was set to the calculated ratio of two and an increased ratio of four. The solar fraction is plotted in Figure V.7. It decreases with increasing ΔT_{off} for both systems. An increasing ΔT_{off} means that the temperature rise across the collector is higher at the time when the system is turned on or shut down. This results in less pump operation time reducing the system performance.

However, the slope of the curves in Figure V.7 is very small at a ΔT_{off} of about one. The tank model simulates stratification in an ideal manner by always putting water into the node closest in temperature. Mixing occurs even at low flowrates for a real tank [5,14]. Although no optimum was found it may exist if mixing is included at a low collector flowrate for a slightly increased value of ΔT_{off}. This increase would shut the system down when the energy gain is to small to outweigh the disadvantage of mixing while still being high enough to justify pump operation.

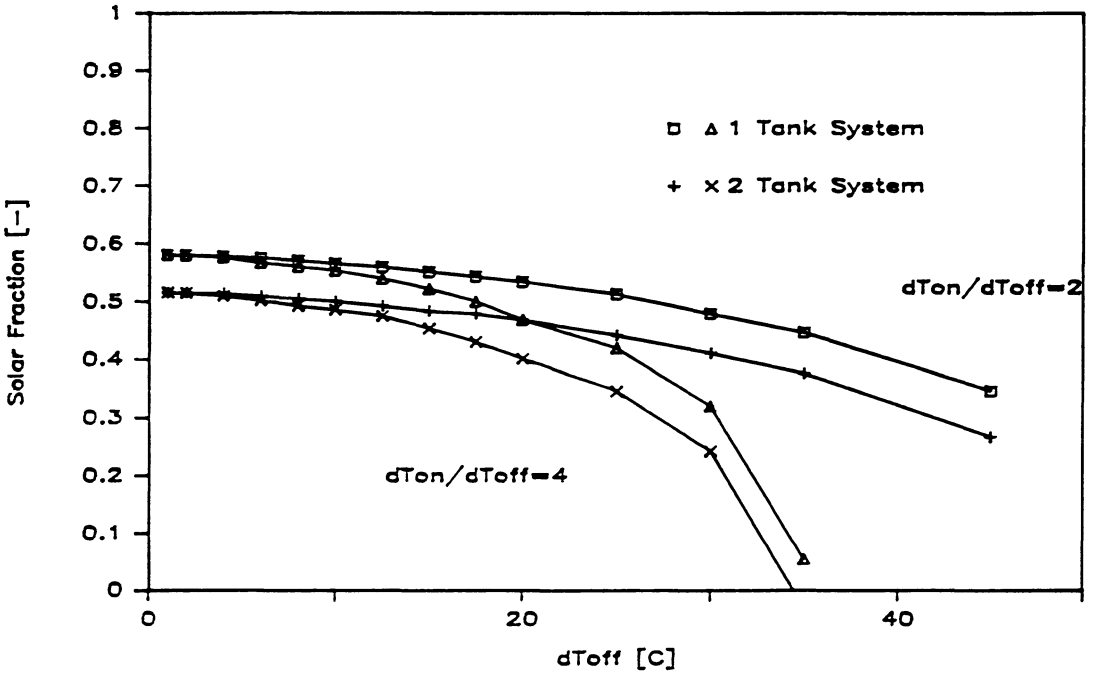

Figure V.7. Solar fraction vs. ΔT_{off}. At a flowrate of 9 l/hr-m^2.

V.3.2 Alternative Control Strategies

Simulations using a proportional and a proportional/integral controller were conducted for single and double tank systems with an on/off controller. The on/off controller has the set-points previously calculated (ΔT_{on} = 2°C; ΔT_{off} = 1°C) at a flowrate of 9 l/hr-m^2. Listings of the controller subroutines are in Appendix E.

Systems using the proportional controller were simulated for a variety of collector outlet temperature deviations (DTO) as described in Section V.2. With an upper flowrate constraint of 71.5 l/hr-m^2 the solar fractions for three control decision parameters (DS) are in Figure V.8 (single tank) and V.9 (double tank). The optimum solar fractions of 59.5% and 52% for single and double tank system, respectively, occurred at DTO = 0°C. This is an improvement over the on/off control strategy of 2% and 0.5% for the single and double tank system, respectively. The optimum was not very sensitive to DS. At DS = 0 the system became unstable and simulations were terminated. Therefore a decision parameter of 0.1 was used to ensure good numerical stability in further simulations. In Figure V.10 the sensitivity of the system performance to the upper flowrate constraint is shown for DTO of 0°C and 5°C. It is found to be negligible for flowrates as low as twice the low collector flowrate.

The proportional controller yielded an improvement of 2-0.5 percent points of the solar fraction compared to on/off controlled low flowrate systems. The controller worked best when the collector

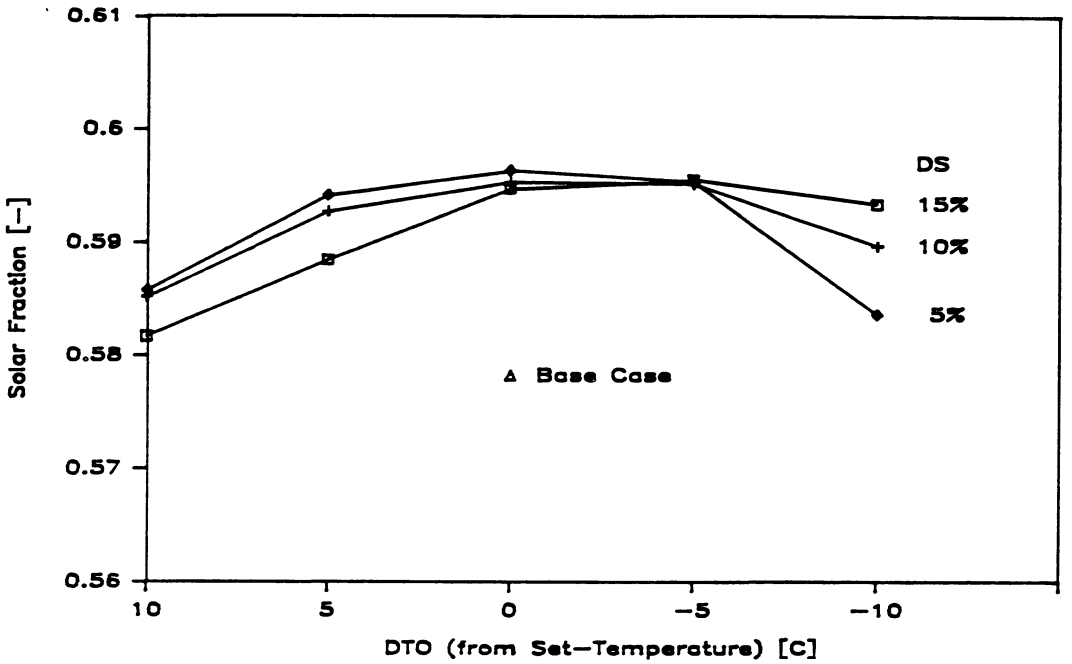

Figure V.8. Solar fraction vs. collector outlet-temperature deviation DTO. For a single tank system at a minimum flow-rate of 9 l/hr-m^2. DS = control decision parameter.

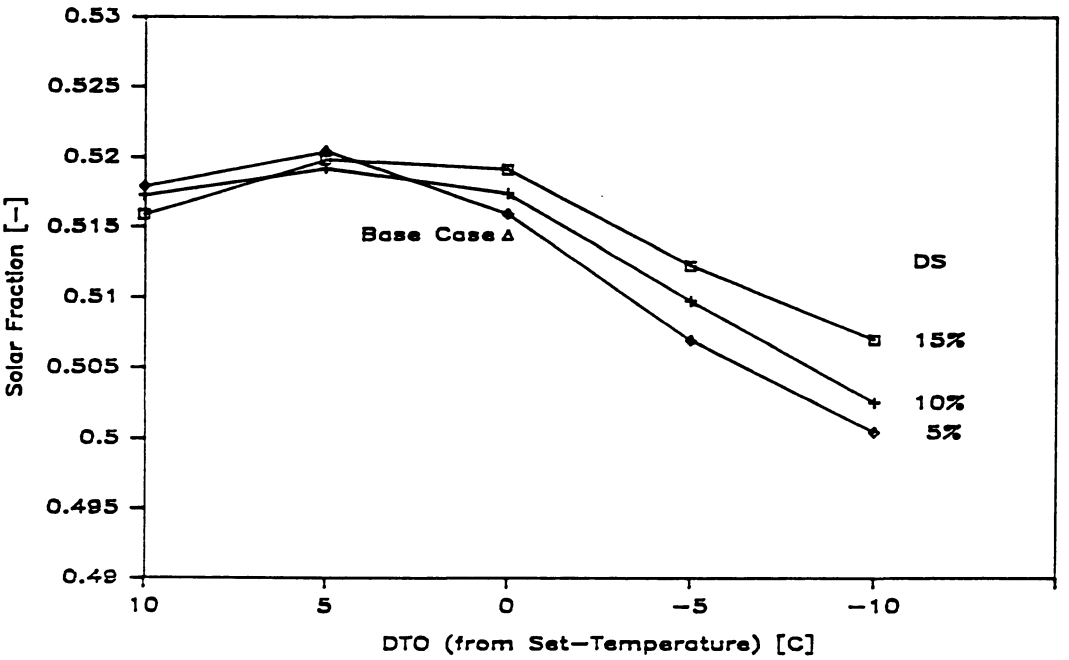

Figure V.9. Solar fraction vs. collector outlet-temperature deviation DTO. For a double tank system at a minimum flow-rate of 9 l/hr-m^2. DS = control decision parameter.

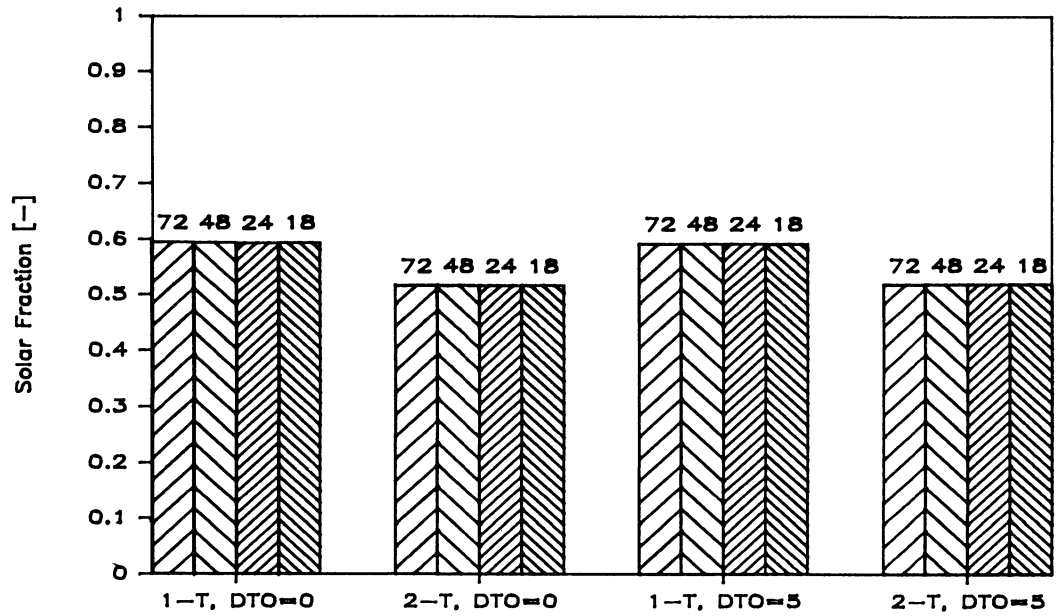

Figure V.10. Effect of maximum flowrate for proportional control. Maximum flowrate as labled in [l/hr-m^2], minimum flowrate 9 l/hr-m^2.

flowrate was chosen so that the collector outlet temperature and the load supply temperature were the same.

Investigations of the proportional/integral controller were done for $(\overline{M}_c/M_l)$ ratios from 1 to 1.5 over a range of total-collection-times (TCT). The range of TCT was chosen around the average operating time of the base case low flowrate systems. The setting of the proportional controller was DTO = 0°C and DS = 0.1 at a maximum flowrate of 71.5 l/hr-m^2. In Figure V.11 the solar fraction of single and double tank simulations are plotted. The solar fraction stays basically constant for all $(\overline{M}_c/M_l)$ ratios and the range of TCT. The explanation is that the integral controller will only increase the flowrate to reach the $(\overline{M}_c/M_l)$ ratio but cannot decrease the proportional controller output. In other, words as long as the proportional control results in a flowrate exceeding the requested $(\overline{M}_c/M_l)$ ratio the integral control decision is ignored. The values tested for $(\overline{M}_c/M_l)$ were derived from simulations with the on/off controller at the low flowrate. Because the proportional controller already raises the flowrate, the requested $(\overline{M}_c/M_l)$ ratio is satisfied earlier and the effect of the integral controller further reduced.

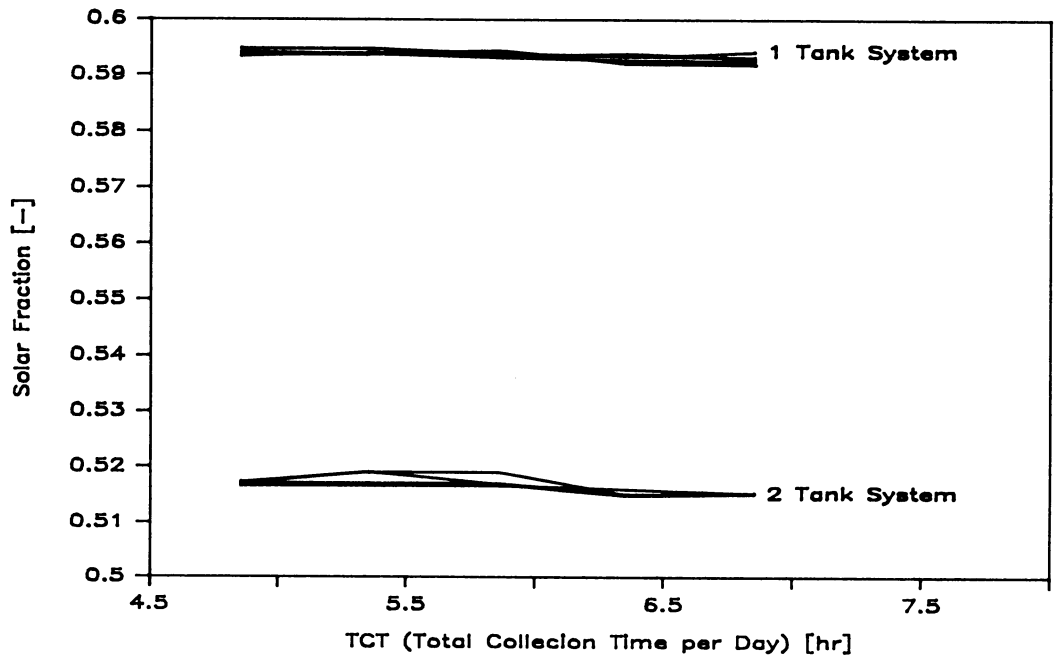

Figure V.11. Solar fraction vs. TCT parameter of proportional/integral controller. Higher values are for single, lower for double tank system. Each range containing 5 curves for $(\overline{M}_c/M_1)$ of 1, 1.1, 1.2, 1.3, 1.5.

VI. CONCLUSIONS AND RECOMMENDATIONS

VI.1 Conclusions

Three advantages of the low collector flowrate operating strategy can be concluded from the previous discussion:

1) The low flowrate strategy is applicable to SDHW systems without major system adjustments.
2) Standard flat-plate collectors do not need design changes to obtain a system performance improvement by reducing the flowrate.
3) The widely-used on/off controller is appropriate for use in a reduced collector flowrate SDHW system.

Comparisons of TRNSYS simulations with side-by-side experiments of low and high collector flowrate SDHW systems showed that simulation results agree with experimental data. Although the parameters of the SDHW experimental systems have been used as base case systems, simulation results reflect the general behavior for a variety of SDHW systems. Furthermore simulations with various weather data resulted in improved system performance for essentially different climates. These facts as well as other research publications confirm that SDHW systems yield improved performance at reduced collector flowrate. The optimal flowrate was found to be approximately 10 l/hr-m^2 for the base case system with a ratio of daily load to tank-volume of 1 and collector area of 1.1 m^2 per 75 l tank volume.

An investigation of the dependence of the collector heat removal factor F_R on flowrate distribution was conducted. The results of

calculations of flowrate distributions showed that even at low flowrates highly uneven distributions occur. Reports of experimenters that a reduced collector flowrate produces a higher degree of uneven distribution than at higher flowrates were confirmed for nonidentical risers. For identical risers the distributions were found to be more uniform at reduced collector flowrate than at high flowrate. The effects of uneven distributions on the collector heat removal factor F_R were found to be not significant. This indicates that the standard flat-plate collector design with manifold and risers is appropriate for a low collector flowrate operating strategy.

The on/off controller temperature-difference set-points employed in NBS experiments and simulations were compared with simulations for a variety of set-points. It was found that at a high flowrate, the simulations showed extensive cycling with the base case settings. Improved controller stability resulted in lower solar fractions at high collector flowrates. The controller setting for the low flowrate was also adjusted but did not result in improved system performance. However, a performance improvement was obtained with a combination of proportional and on/off control. The increase of solar fraction was 2 and 0.5 percentage points for single and double tank system, respectively. Combining integral with proportional and on/off control did not yield a further improvement.

The investigation of SDHW systems with heat exchangers resulted in a reduction of the solar fraction for operating conditions of reduced flowrate on either side of the heat exchanger. Parameter

studies, however, showed a flat maximum below the high tank-side flowrate of a heat exchanger with improved heat transfer. The penalty of a reduced heat transfer coefficient for lower flowrates generally outweighed the advantages of a well-stratified tank for SDHW systems.

VI.2 Recommendations

The comparison between single and double tank SDHW systems at high and low collector flowrates revealed a discrepancy in the amount of predicted improvement. The single tank system did not improve its system performance as much as the double tank system did. The total amount of predicted performance improvement for either system was smaller than predictions of flowrate-related improvements in other reports. This is due to the use of the same tank model at all collector flowrates investigated. The model does not account for internal mixing. Predictions at the high flowrate could have been done with a fully mixed tank model. This would have reduced the solar fraction at high flowrate and thereby increased the predicted performance improvement for low collector flowrate. This was not done for the sake of comparable simulations. To account for mixing, a tank model with flowrate-dependent dynamic mixing would be useful. Dynamic mixing would also show whether auxiliary heated and solar preheated water is mixed in the single tank system at a high flowrate. This would explain why simulations for the single tank system did not show a larger performance improvement than the double tank system.

For flat plate collectors, no design restrictions for low flowrate operation are necessary. Installed systems should yield an improved performance with a reduced collector flowrate. For new systems, smaller pipes and pumps are appropriate. To reduce the possible effects of flowrate mal-distribution the collectors can be installed in series or single-flow-path collectors such as serpentine collectors may be used.

SDHW systems which include a heat exchanger generally show no improvement at reduced flowrates. A validation of simulation results by experiments as well as an investigation of whether a performance maximum at lower flowrates does exist for improved heat exchangers is recommended, since many SDHW systems use this method of freeze protection.

Low collector flowrate SDHW systems can be further improved by using the appropriate controller. On/off controllers are sufficient and stable if the set temperature-differences are chosen in accordance to the control objectives. An improvement in solar fraction was realized by adding a variable speed pump and a proportional controller to the simulated systems. The decision on whether or not to include a proportional controller and a variable speed pump will depend on system size, as well as other variables such as maintenance and installment costs, and component availability. Therefore the most efficient controller varies for different systems. However, the on/off controller will suit most SDHW systems.

APPENDIX A: Listings of Sample TRNSYS Simulation Decks

This Appendix contains listings of two of the TRNSYS decks used for this research. Deck one is the base case simulation of the single-tank system for March in Madison. The double tank system contains only an additional storage tank and a modified output summary. This deck was used for the comparisons of experiments with simulations. For monthly and annual simulations as well as for the various load draw schedules, minor changes had to be made but the deck structure was conserved.

In the second deck the two-tank system with heat exchanger is listed. The heat exchanger subroutine (UNIT 5) contains the algorithm for finding UA values as a function of temperature and flowrate. That is the reason that in the constant card UA was supplied as zero.

```
NOLIST
*****************************************************
*                    TRANSYS DECK                   *
*                  BASE CASE SYSTEM                 *
*       SIMULATION OF NBS-EXPERIMENTS WITH TWO       *
*                SIDE-BY-SIDE SYSTEMS               *
*         LOW FLOWRATE (SYSTEM B: 1/8*1.32 gal/min) *
*              MULTINODETANK AS PREHEATTANK         *
*                    1 TANK SYSTEM                  *
*     ON/OFF CONTROLLER  DT-ON=11.1  DT-OFF=2.8     *
*****************************************************
CONSTANS 31
TSTART = 1416 , NOOFDAYSTOSIMULATE = 31
TEND = NOO * 24 + TST-1 , TSIM = TEN - TST
STEP = 1. / 60. , DAYSTART = 60
FRTANTEST = .763 , FRULTEST = 18.5
TESTFLOW = 35.50 , AC= 4.2
B0 = 0.1 , CP = 4.185
ROWATER = 1000 , FLW = 37.5
TUDEADBAND = 11.1 , TLDEADBAND = 2.8
PVOLUME = 0.275 , PHEIGHT = 1.5
PUA = 10.0 , PTEMPERATURINITIAL = 40.
PSURFACE = 2.64 , PUT = PUA / PSU
AQFLOWMAX = 12600.
ATSET = 60. , ATDEADBAND = 5.
LATIDUDE = 43.0 , SOLARCONSTANT = 4871.
TOTALLOADFLOWPERDAY = 260.0
ROGROUND = 0.2 , AZIMUTHANGEL = 0.0
BETHA = LATIDUDE
SIMULATION TST TEN STE
TOL -.01 -.01
LIMITS 50 10 50
WIDTH 132
*
UNIT 9 TYPE 9 DATA READER (FORMATTED)
PAR 10
2 1 -1 1 0 -2 1 0 10 1
(T25,F4.0,T30,F4.1)
*
UNIT 16 TYPE 16 SOLAR RADIATION PROCESSOR
PAR 7
3 1 DAY LAT SOL 0.0 -1
INPUTS 6
9,1 9,19 9,20 0,0 0,0 0,0
0.0 0.0  1.0  ROG BET AZI
*
UNIT 1 TYPE 1 COLLECTOR
PAR 12
1 1 AC CP 1 TES FRTA FRUL 0 CP 1 B0
```

```
INPUTS 10
38,1 3,2 0,0 9,2 16,6 16,4 16,5 0,0 16,9 0,0
25. 0.0 0.0 20. 0.0 0.0 0.0 ROG 0.0 BET
*
UNIT 13 TYPE 13 PRESSURE RELIFE VALVE
PAR 2
100. CP
INPUTS 3
1,1 1,2 1,1
25. 0.0 25.
*
UNIT 38 TYPE 4 MULTINODE PRHEATTANK
PAR 13
2 PVO CP ROW PUT -1.5 AQF 2 1 ATS ATD 0 60.
INPUTS 6
13,1 13,2 0,0 15,1 0,0 0,0
30. 0.0 20. 0.0 21. 1.0
DERIVATIVES 10
PTE PTE PTE PTE PTE PTE PTE PTE PTE PTE
*
UNIT 2 TYPE 2 PUMP-CONTRTOLER
PAR 3
3 TUD TLD
INPUTS 3
1,1 38,1 2,1
30. PTE 0
*
UNIT 5 TYPE 15 CHECKING FOR OVERHEAT
* 1 FOR CONTROLLER ON AND TOP TANK TEMP
* LESS THAN 100 DEG C
* IN ALL OTHER CASES 0 (NULL)
PAR 7
-1 100. 0 9 0 1 -4
INPUTS 2
38,3 2,1
0.0 0.0
*
UNIT 3 TYPE 3 PUMP
PAR 1
FLW
INPUTS 3
38,1 38,2 5,1
PTE 0.0 0
*
UNIT 14 TYPE 14 LOADFRACTION RAND PROFILE
PAR 82
0,0 5,0 5,.125 6,.125 6,.391 7,.391 7,.625
8,.625 8,.703 9,.703 9,.549 10,.549
10,.391 11,.391 11,.297 12,.297 12,.422
```

```
13,.422 13,.242 14,.242 14,.203 15,.203
15,.156 16,.156 16,.297 17,.297 17,.549
18,.549 18,1.0 19,1.0 19,.786 20,.786
20,.549 21,.549 21,.422
22,.422 22,.391 23,.391 23,.156 24,.156 24,0.0
*
UNIT 15 TYPE 15 RAND LOAD-SYNTHY
PAR 8
-1 TOT -1 8.254 2 0 1 -4
INPUTS 1
14,1
0.0
*
UNIT 28 TYPE 28 SIMSUM FOR SIMULATIONS
PAR 56
* FIRST SETTINGS
TSI TST TEN 15 2 2
*CALCULATION OF ALL ENERGIES
*IS IN kWh AND TIMES IN min
*stored energy input and conversion
0 -1 3600 2
*Q auxiliary
0 -1 3600 2 -4
*PUMP RUNNING TIME
0 -1   60 1 -4
*Q in tank from collector
0 -1 3600 2 -4
*Q losses from all tanks
0 -1 3600 2 -4
*Q delivered to load
0 -1 3600 2 -4
*Q stored PREHEAT TANK output
-4
*FLOWRATI
-14 -1 FLW 1 -1 TOT -1 NOO 1 2 -4
*SF
-17 -13 4 -17 -1 1 12 2 -4
INPUTS 6
38,7 38,8 5,1 1,3 38,5 38,6
LABELS 8
Qhe PRT Qsol Qloss Qload QstorP Florat SF
*
END
```

```
NOLIST
*****************************************************
*                    TRANSYS DECK                   *
*                  BASE CASE SYSTEM                 *
*       SIMULATION OF NBS-EXPERIMENTS WITH TWO      *
*                SIDE-BY-SIDE SYSTEMS               *
*                 WITH A HEAT EXCHANGER,            *
*       UA-HX VALUE DEPENDENT ON REYNOLDS NUMBERS   *
*         (RE NUMBERS ARE CALCULATED IN THE ROUTINE *
*         OF THE HX AND UA IS LOOKED UP IN A TABLE) *
*        HIGH FLOWRATE (SYSTEM A: 1*1.32 gal/min)   *
*              MULTINODETANK AS PREHEATTANK         *
*                    2 TANK SYSTEM                  *
*    ON/OFF CONTROLLER  DT-ON=11.1  DT-OFF=2.8      *
*****************************************************
CONSTANS 42
TSTART = 1416 , NOOFDAYSTOSIMULATE = 31.
TEND = NOO * 24 + TST-1 , TSIM = TEN - TST
STEP = 1. / 60. , DAYSTART = 60
FRTANTEST = .763 , FRULTEST = 18.5
TESTFLOW = 35.50 , AC= 4.2
BO = 0.1 , CPW = 4.185
ROWATER = 1000. , CPGLYCOL = 3.52
UAHX = 0.0 , FLWATER = 300.0
FLGLYCOLWATER = 300.0 , TUDEADBAND = 11.1
TLDEADBAND = 2.8 , PVOLUME = 0.275
PHEIGHT = 1.5 , PUA = 10.0
PTEMPERATURINITIAL = 40. , PSURFACE = 2.64
PUT = PUA / PSU , AVOLUME = 0.135
AHEIGHT = 1.4 , AUA = 7.02
ATEMPRATURINITIAL = 60. , AOFLOWMAX = 12600.
ATSET = 60. , ATDEADBAND = 5.
AUXILARYTANKSURFACE = 1.74 , AUT = AUA / AUX
A1NODE = 9 / 10 * AHE , A2NODE = 1 / 10 * AHE
LATIDUDE = 43.0 , SOLARCONSTANT = 4871.
TOTALLOADFLOWPERDAY = 260.0 , ROGROUND = 0.2
AZIMUTHANGEL = 0.0 , BETHA = LATIDUDE
SIMULATION TST TEN STE
TOL -.01 -.01
LIMITS 50 20 47
WIDTH 132
*
UNIT 9 TYPE 9 DATA READER (FORMATTED)
PAR 10
2 1 -1 1 0 -2 1 0 10 1
(T25,F4.0,T30,F4.1)
*
UNIT 16 TYPE 16 SOLAR RADIATION PROCESSOR
PAR 7
```

```
3 1 DAY LAT SOL 0.0 -1
INPUTS 6
9,1 9,19 9,20 0,0 0,0 0,0
0.0 0.0  1.0  ROG BET AZI
*
UNIT 1 TYPE 1 COLLECTOR
PAR 12
1 1 AC CPG 1 TES FRTA FRUL 0 CPG 1 B0
INPUTS 10
-50,1 32,2 0,0 9,2 16,6 16,4 16,5 0,0 16,9 0,0
25.  0.0  0.0 20. 0.0  0.0  0.0  ROG 0.0  BET
*
UNIT 13 TYPE 13 PRESSURE RELIFE VALVE
PAR 2
105. CPG
INPUTS 3
1,1 1,2 1,1
25. 0.0 25.
*
UNIT 32 TYPE 3 PUMP COLLECTOR SIDE OF HX LOOP
PAR 1
FLH
INPUTS 3
-50,1 -50,2 5,1
PTE  0.0  0.0
*
UNIT 50 TYPE 5 HEAT EXCHANGER HX
PAR 4
2 UAH CPG CPW
INPUTS 4
13,1 13,2 38,1 31,2
PTE  0.0  PTE  0.0
*
UNIT 38 TYPE 4 MULTINODE PRHEATTANK
PAR 6
2 PV0 CPW ROW PUT -1.5
INPUTS 6
-50,3 -50,4 0,0 15,1 0,0 0,0
30.  0.0  20. 0.0  21. 0.0
DERIVATIVES 10
PTE PTE PTE PTE PTE PTE PTE PTE PTE PTE
*
UNIT 4 TYPE 4 2-NODE AUXILARY TANK
PAR 14
1 AV0 CPW ROW AUT A1N A2N A0F 1 1 ATS ATD 0 60.
DERIVATIVES 2
60 55
INPUTS 6
0,0 0,0 38,3 38,4 0,0  0,0
```

```
0.0 0.0 PTE  0.0  21.0 1.0
*
UNIT 2 TYPE 2 PUMP-CONTRTOLLER FOR BOTH PUMPS
PAR 3
3 TUD TLD
INPUTS 3
1,1 38,1 2,1
30. PTE 0
*
UNIT 5 TYPE 15 CHECKING FOR OVERHEATPREVENTION
*OUTPUT1; 1 FOR CONTROLLER ON AND TOP TANK TEMP
*         LESS THAN 100 DEG C
*         IN ALL OTHER CASES 0 (NULL)
PAR 7
-1 100. 0 9 0 1 -4
INPUTS 2
38,3 2,1
0.0 0.0
*
UNIT 31 TYPE 3 PUMP
PAR 1
FLW
INPUTS 3
38,1 38,2 5,1
PTE 0.0 0
*
UNIT 14 TYPE 14 LOADFRACTION RAND PROFILE
PAR 82
0,0 5,0 5,.125 6,.125 6,.391 7,.391
7,.625 8,.625 8,.703 9,.703 9,.549 10,.549
10,.391 11,.391 11,.297 12,.297 12,.422
13,.422 13,.242 14,.242 14,.203 15,.203
15,.156 16,.156 16,.297 17,.297 17,.549
18,.549 18,1.0 19,1.0 19,.786 20,.786
20,.549 21,.549 21,.422 22,.422 22,.391
23,.391 23,.156 24,.156 24,0.0
*
UNIT 15 TYPE 15 RANDLOAD-SYNTHY
PAR 8
-1 TOT -1 8.254 2 0 1 -4
INPUTS 1
14,1
0.0
*
UNIT 27 TYPE 15 AUXILIARY CALCULATOR
PAR 12
*ADD LOAD OF PRE AND AUX TANK
0 0 3 -4
*ADD LOSSES FROM PRE AND AUX TANK
```

```
0 0 3 -4
*ADD DIFFERENCE IN STORED ENERGY SINCE
*SIM START FROM PRE AND AUX TANK
0 0 3 -4
INPUTS 6
38,6 4,6 38,5 4,5 38,7 4,7
0.0 0.0 0.0 0.0 0.0 0.0
*
UNIT 28 TYPE 28 SIMSUM FOR NBS EXPERIMENT SIMULATIONS
PAR 55
* FIRST SETTINGS
TSI TST TEN 15 2 1
*CALCULATION OF ALL ENERGIES IS IN kWh AND TIMES IN min
*Q STORED INPUT
0 -1 3600 2
*Q COLLECTED BY COLLECTOR
0 -1 3600 2 -4
*Q HEAT EXCHANGER HX
0 -1 3600 2 -4
*Q in tank from HX
0 -1 3600 2 -4
*Q delivered to load
0 -1 3600 2 -4
*Q losses from all tanks
0 -1 3600 2 -4
*Q auxiliary
0 -1 3600 2 -4
*Q stored OUTPUT
-4
*PUMP RUNNING TIME
0 -1 60 1 -4
*SF (Qload-Qheater)/Qload
-15 -17 4 -15 -1 1 12 2 -4
INPUTS 8
27,3 1,3 50,5 38,9 27,1 27,2 4,8 5,1
LABELS 9
Qcoll Q-HX Qtank Qload Qloss Qheat Qstor PRT SF
*
UNIT 25 TYPE 25 PRINTER
PAR 4
.5 1685 1699 15
INPUTS 6
31,2  32,2  50,6 50,7   50,8   50,9
FLW-W FLW-G EFF  RE-WAT RE-GLY UA-HX
*
END
```

APPENDIX B: Explanation of Simulation Time Step and Reason for Use of a Multi-Node Tank

B.1 Time Step

Simulations of solar energy collection systems have usually a time step between 1/2 and 1/4 of the intervals at which weather data are available. Most weather and radiation data are available as hourly averages, so that for simulation time steps of less than one hour the data are either interpolated as in TRNSYS or assumed to be constant.

Time steps on the order of 1/2 or 1/4 hour are significantly longer than collector time constants, which are on the order of minutes (high flowrates) or tens of minutes (low flowrates). Because of the small thermal mass of a collector, the loss of dynamics in simulations of solar collectors does not significantly affect long term simulation results. Dynamic effects during heat-up and cool-down of real collectors are only significant in the morning and the evening at low incident radiation or during unsteady weather conditions. Although the Hottel - Whillier equation (Eq. II.1) does not include short term collector dynamics it has proven to be very useful. Pipes can be included in the collector efficiency function, but their delay times are neglected [10]. For typical SDHW systems, the only component with significant dynamic behavior is the storage tank. Therefore the storage tank dynamics determine the simulation time step.

To show the effects of an incorrect time steps the base case systems were simulated for March in Madison with flowrates of 71.5 $l/hr\text{-}m^2$ (HFR) and 9 $l/he\text{-}m^2$ (LFR) for various simulation time steps. The results are plotted as solar fraction vs simulation time step in Figures B.1 and B.2. Figure B.1 contains simulations of the base case and B.2 shows the base case with a loss-free solar tank. The curves for the high flowrate in the single- and double-tank system show a steady increase in solar fraction. An incorrect time step would influence the predicted improvement significantly. On an extended scale, the curves level off and remain approximately constant for steps lower than one minute. The slightly uneven shape of the curves results from the numerical tolerance of absolute 0.01 for inputs to system components at any time.

A justification for the choice of a time step smaller than the tank time constant is expressed in Figure B.3. The reasoning is: If the step is significantly larger than the tank time constant the entering mass is more than the node contents. Therefore the temperature of the node at $t + \Delta t$ is about the same as that of the entering fluid. For a time step approximately equal to the node time constant the temperature would be about the average temperature between entering water and contents. In order to show smooth transient behavior the time step at which the temperature is calculated has to be significantly smaller than the node time constant.

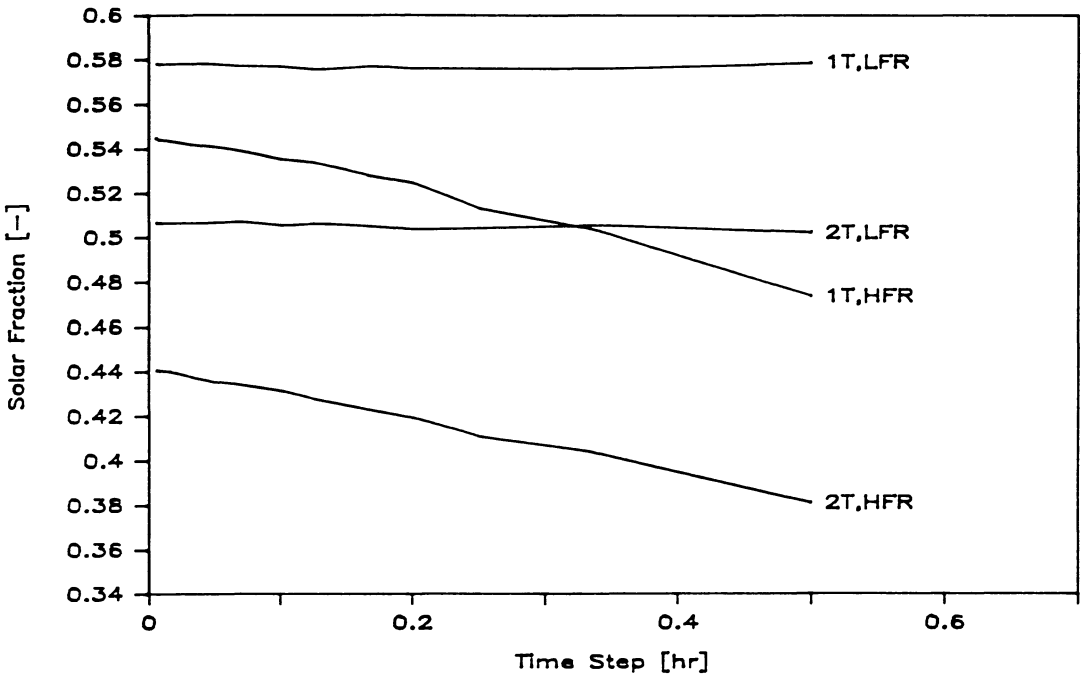

Figure B.1. Solar fraction vs. simulation time step for base case systems. 1T - single tank, 2T - double tank system. At flowrates of 71.5 l/hr-m^2 (HFR) and 9 l/hr-m^2 (LFR).

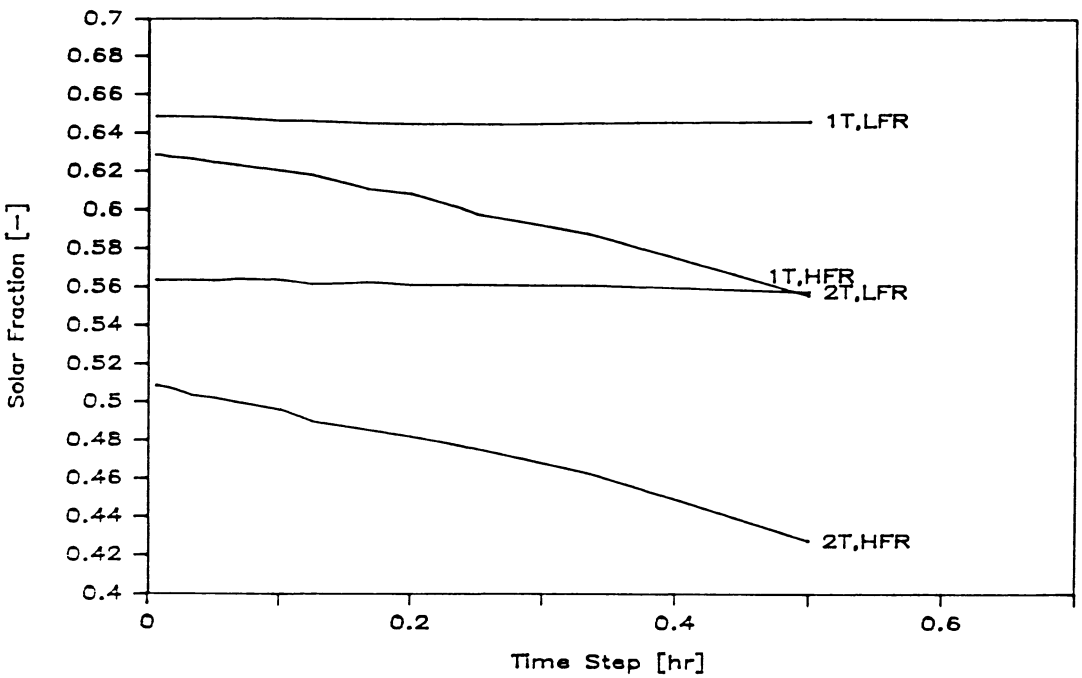

Figure B.2. Solar fraction vs. simulation time step without tank losses. Base case systems with loss free tanks. 1T - single tank, 2T - double tank system. At flowrates of 71.5 l/hr-m^2 (HFR) and 9 l/hr-m^2 (LFR).

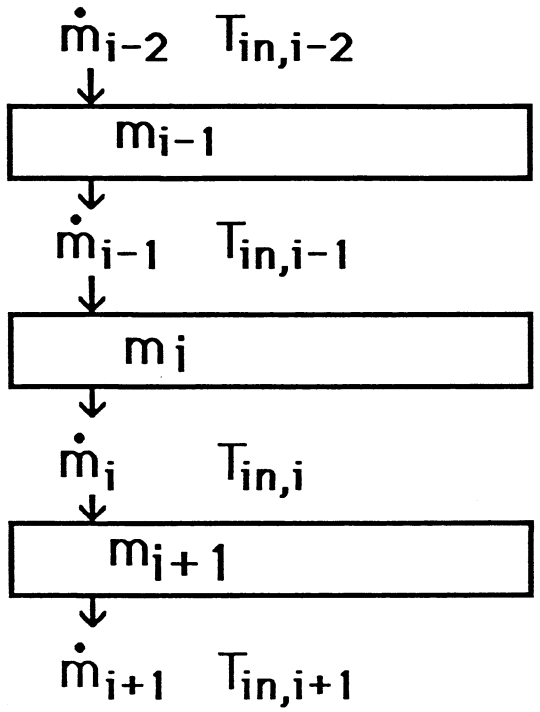

$$m_i = \text{constant} \Longrightarrow \dot{m}_{i-1} - \dot{m}_i = 0$$

$$t_{tank} = m_i / \dot{m}_i$$

$$\Delta t \gg t_{tank} \Longrightarrow \dot{m}_i \cdot \Delta t \gg m_i \Longrightarrow T_i\big|_{t+\Delta t} \approx T_{in}$$

$$\Delta t \approx t_{tank} \Longrightarrow \dot{m}_i \cdot \Delta t \approx m_i \Longrightarrow T_i\big|_{t+\Delta t} \approx (T_i + T_{in})/2$$

$$\Delta t \ll t_{tank} \Longrightarrow \dot{m}_i \cdot \Delta t \ll m_i \Longrightarrow T_i\big|_{t+\Delta t} \approx T_i + \int_{\Delta t} dT$$

Figure B.3. Simulation time step for a system with multinode tank.

B.2 Multi-node vs. Plug-flow Model

The plug-flow model in the TRNSYS library is an algebraic book-keeping routine which analyzes entering and exiting streams and shifts the temperature and volume profile accordingly. A description is shown in Figure B.4 and a detailed explanation is included in the TRNSYS manual [9].

Despite the fact that Wuestling [1] reported good agreement between the plug-flow and multi-node models and that the plug-flow model needs considerably less computer time, three factors -- described in the following paragraphs -- were reason enough to use the multi-node model. Wuestling did not state the time step used in the simulation comparisons of plug-flow and multi-node model but the simulation deck listings include a time step of 15 minutes, which does not substantiate his results.

A) The simulation of the plug-flow model is dependent on the flowrate through it. In one time step at a low flowrate the volume of entering water is smaller than for a high flowrate so that the smallest possible node size is proportional to the flowrate. The possible number of nodes in a tank is the ratio of total tank volume to the smallest possible node volume. Therefore the number of nodes possible for the plug-flow tank model depends on the flowrate and system simulations including the plug-flow model differ according to the flowrate. This restricts comparisons of systems with different flowrates.

Three numerical limitations on the plug-flow model should be noted:

1) a predefined "significant" temperature difference between the temperature of the entering water and existing nodes must be exceeded.
2) a new node must have a volume of more than a "significant" fraction of the tank volume in order to be generated.
3) the total number of nodes allowed in the tank is also predefined. This causes another dependence of the simulation on flowrate, which is independent of the numeric values chosen for the temperature difference and of the maximum number of nodes.

B) A change in radiation level results in a smaller temperature change of the collector return water for high flowrates than for low flowrates. If temperatures are similar between entering water and tank contents no new node is generated but the water mixed into an existing node. On the other hand, for the same simulation time step lower flowrates approach the minimum node size faster than higher flowrates. This makes the simulated tank dependent on flowrate and time step.

C) The simulation time step of one minute results in a high number of bookkeeping operations, which increases the total number of generated nodes. If the limit for the maximum number of nodes is exceeded the routine combines nodes thereby reducing the temperature stratification. This occurs sooner for lower flowrates, so that the way the tank is simulated again depends on the flowrate.

To simulate a tank independent of flowrate the plug-flow model is not sufficient. The multi-node tank model on the other hand simulates a tank identically at low and high flowrates. Therefore it was used for this research.

The multi-node tank model does not account for internal mixing. Flowrate-dependent internal mixing would reduce the stratification at higher flowrates. This makes the multi-node tank model a conservative assumption for comparisons of SDHW systems at various collector flowrates. The plug-flow model may or may not be a conservative assumption, which justifies its rejection for comparisons.

A ten node multi-node tank model was chosen for all simulations. The number of nodes is relevant for the achievable stratification. To calculate the appropriate simulation time step in Chapter II it was necessary to know the number of nodes. The relationship between the time constant and the number of nodes was implicitly given in Eq. (II.24) as

$$t_n = \frac{V_n}{\dot{V}} = \frac{V_t/n}{\dot{V}}$$

Therefore

$$t_n \propto \frac{1}{n}$$

where: t_n = node time constant

V_n = node volume

V_t = tank volume

$\dot{V}$ = Volume flowrate

n = number of nodes

An increase in the number of nodes has to be taken into account for the simulation time step. For example, twice the number of nodes would result in half of the simulation time step, i.e. twice the computer time. A small number of nodes reduces therefore the necessary computer time.

Another factor which has to be taken into account is the accuracy of the simulation results (within the requirements of the problem under discussion). The relationship between the number of nodes in the tank and the solar fraction for the single tank SDHW system is shown in Figure B.4 and B.5. Differences between the solar fraction of simulations using 5 and 10 node tank models are quite large. The difference between simulations using 10 and 20 node tank models are only 3% and the curves are virtually parallel. Also, the optimum solar fractions occur at the same collector flowrate and $\overline{M}_c/M_1$.

It can be inferred that the results of SDHW system performance comparisons do not depend on whether 10 or 20 nodes are used. Comparisons between different control and operating strategies have been a main concern of this study. The good agreement of experimental data with simulation results using a 10 node tank model and the relation between the number of nodes and the computer time determined in the choice of a 10 node tank model for TRNSYS simulations.

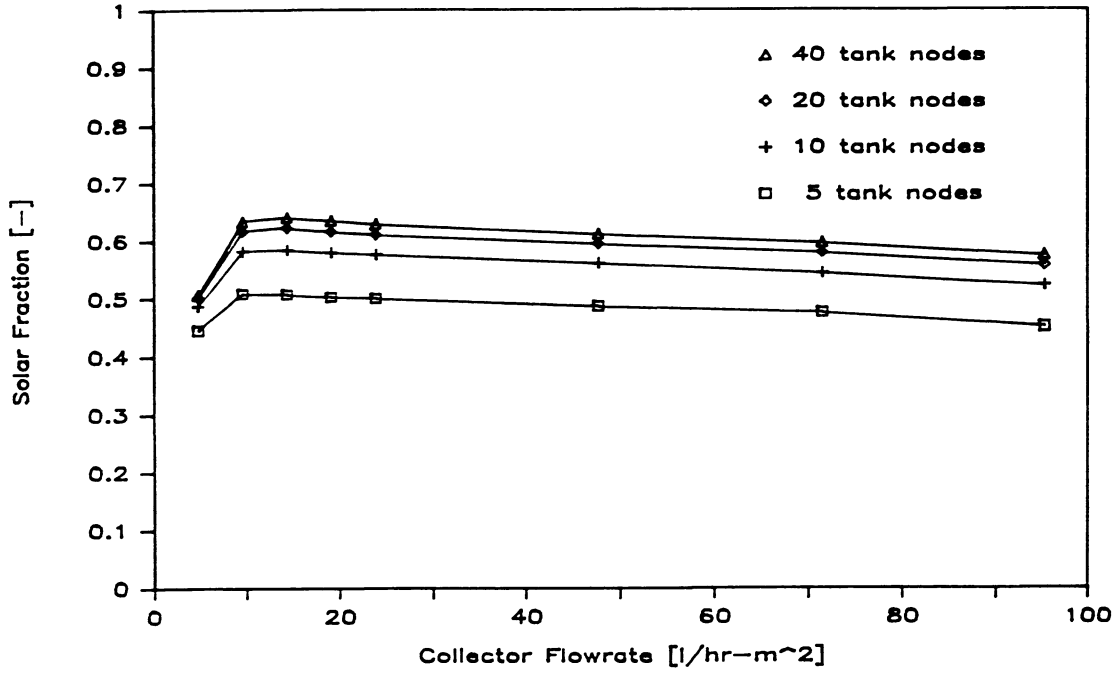

Figure B.4. Solar fraction vs. flowrate for different numbers of nodes in the multinode tank model. For the single tank base case system.

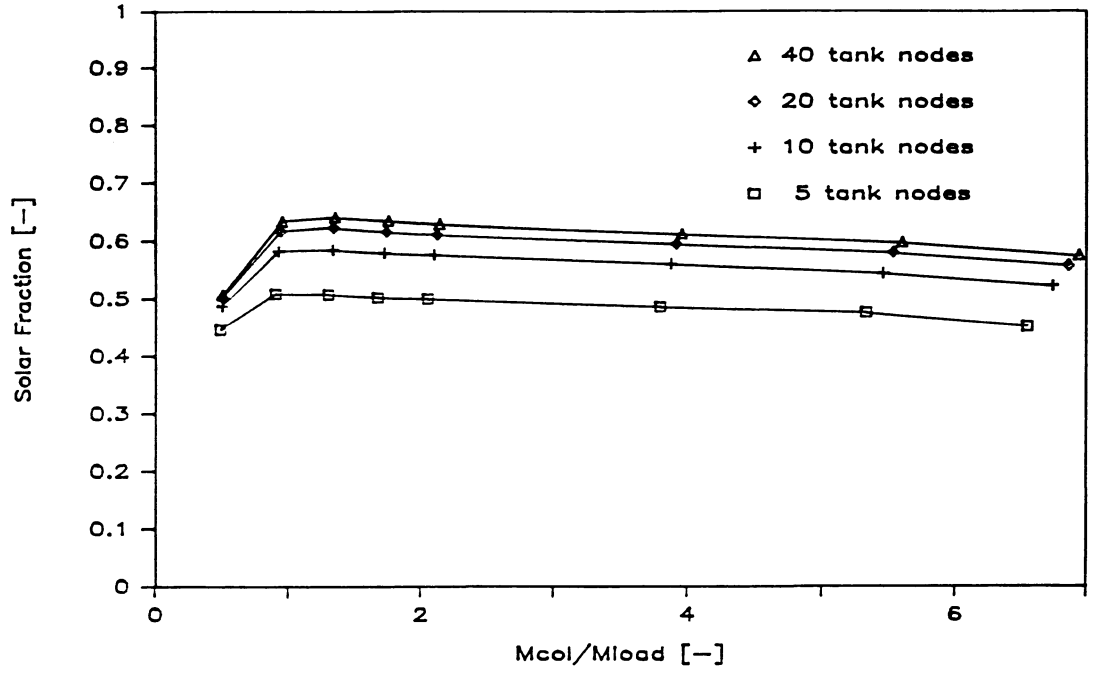

Figure B.5. Solar fraction vs. $\overline{M}_c/M_l$ for different numbers of nodes in the multinode tank model. For the single tank base case system.

APPENDIX C: Data Output as Supplied by NBS

Data outputs were the base for both nine day comparisons between TRNSYS simulations and NBS experiments. This is the output of one hour of data for the single tank system and the double tank system.

NBS data output for the double tank SDHW system.
Summary for the time 12 - 13 pm on Aug. 20. 1984

```
******** HOURLY DATA ********

AUGUST  20 , 1984
TIME 13:01:40

H HORZ (W/m^2)          1017.2
H TILT (W/m^2)          1102.1
Ta OUTDOOR (deg C)      22.117
Ta INDOOR (deg C)       21.045
WIND SPEED (MPH)        7.1175
WIND SPEED (m/s)        3.1815
WIND DIRECTION (deg)    14.024

PREHEAT TANK TEMPERTURES DEG C
HEIGHT     SYSTEM A     SYSTEM B
6           51.962       28.213
12          51.775       33.398
18          51.658       39.37
24          51.542       46.55
30          51.822       54.009
36          51.402       59.534
42          51.332       60.131
48          51.308       60.2
54          51.285       60.131
AVE TANK    51.566       49.059

   AUX TANK TEMPERATURES DEG C
6           52.684       54.938
12          62.267       62.425
18          62.63        62.973
14          62.653       62.699
30          62.653       62.768
36          62.608       62.539
42          62.585       62.653

AVE TANK    61.157       61.57

T IN LOAD   19.847       19.35
TOT 80 GAL  49.555       58.452
TOT 40 GAL  61.44        62.241
ΔT AUX      11.499       3.45
ΔT PRE      29.137       36.405
T IN COLL   35.324       25.92
T OT COLL   58.544       92.151
ΔT COLL     22.957       55.895
T IN TANK   57.76        74.471
T OT TANK   27.239       20.835
ΔT TANK     28.704       53.494

FR CL(l/s)  .083597      .01042

Q CL IC(kW)      4.6156

Q CL(kW)    7.9738       2.4281
Q TNK(kW)   9.9926       2.7256
Q H EL(kW)  0            0

QL 80GAL(kW)
            .072487      .073593
QL 40GAL(kW)
            .077376      .079632
HE STATUS OFF            OFF
FRZ STAT  OFF            OFF
PMP STAT  ON             ON

**********************************
********** Q LOAD ***********

NO. OF SCANS 2
SOL DEL SYS A .46833 kWh
AVE.ΔT PREHEAT 30.079
AVE.D  9983
AVE Cp PREHEAT 4.1782
AVE ΔT LOAD 41.4495
AVE Cp LOAD 4.17875
TOTAL LOAD SYS A .64546 kHw

SOL DEL SYS B  .60005 kWh
AVE.ΔT PREHEAT 38.533
AVE.D .99835
AVE Cp PREHEAT 4.1786
AVE ΔT LOAD 41.526
AVE Cp LOAD 4.1788
TOT LOAD SYS B  .64669 kWh
**********************************

*********** SUMS ***********

ΣQ CL(kWh) 2.3613        2.5533
ΣQ TK(kWh) 2.2539        2.3377
ΣQ HE(kWh) 0             0

ΣL80(kWh)   .077468      .078768
ΣL40(kWh)   .074889      .078483
PM ON(min) 54            60
AV FR(l/s)  .084207      .010372
WM COUNTER 49            66

**********************************


*********MORE SUMS***********

SOL DLkWh  1.5097        1.7724
TQ LD(kWh) 2.47334       2.46074
AVG WIND SP(mph)         4.3467
AVG WIND SP(m/s)         1.943
AVG Tamb out(C)          22.9
AVG Ti CL(C)    50.767   25.985
AVG Gt(W/sq m)           946.07
I tilt(MJ/sq m)          3.4054
**********************************
```

NBS data output for the single tank SDHW system.
Summary for the time 12 - 13 pm on Sep. 22. 1984

```
******** HOURLY DATA *********

SEPTEMBER  22 , 1983
TIME 13:01 30

H HORZ (W/m^2)          720.44
H TILT (W/m^2)          918.3
Ta OUTDOOR (deg C)      25.455
Ta INDOOR (deg C)       23.997
WIND SPEED (MPH)        3.2817
WIND SPEED (m/s)        1.4669
WIND DIRECTION (deg)    175.41

 T TANK TEMPERTURES IN DEG C
HEIGHT    SYSTEM A      SYSTEM B
6           49.297        22.117
12          48.993        25.724
18          49.016        31.732
24          48.922        39.131
30          49.133        52.148
36          48.876        59.695
42          49.04         60.43
48          58.797        60.614
54          59.534        60 683
AVE TANK    51.29         45.808

T IN LOAD   20.662        19.526
T OT LOAD   58.037        59.004
ΔT LOAD     36.789        36.875
T IN COLL   34.747        23.961
T OT COLL   54.922        85.195
ΔT COLL     20.01         61.171
T IN TANK   54.567        78.268
T OT TANK   27.092        20.539
ΔT TANK     24.653        57.485

FR CL(l/s)  .084329       .010954

Q CL IC(kW)       3.8458

Q CL(kW)    7.0116        2.795
Q TNK(kW)   8.657         2.6276
Q H EL(kW)  0             0
QL TNK(kW)  .064821       .057297

HE STATUS   OFF           OFF
FRZ STAT    OFF           OFF
PMP STAT    ON            ON
```

```
*****************************
********** Q LOAD ***********

NO. OF SCANS 2
TOTAL  LOAD SYS A .58836 kWh
AVE.ΔT 37.791
AVE.D .9981     AVE.Cp.4.1787
TOTAL LOAD SYS B  60298 kWh
AVE.ΔT 38.721
AVE.D .99835    AVE.Cp 4.1786

*****************************

*********** SUMS ************

ΣQ CL(kWh) 2.2732       2.8798
ΣQ TK(kWh) 2.2198       2.6723
ΣQ HE(kWh) 0            0

ΣL TK(kWh) .068113      .061514
PM ON(min) 56           60
AV FR(l/s) .085139      .011086
WM COUNTERS
           50           49

*****************************



*********MORE SUMS***********

TL TK(kWh) .19435       .18496
TQ LD(kWh) 2.3216       2.2109
AVG WIND SP(mph)        5.6843
AVG WIND SP(m/s)        2.5408
AVG Tamb out(C)         25.72
AVG Ti CL(C)   48.497   24.265
AVG Gt(W/sq m)          928.67
I tilt(MJ/sq m)         3.3427
*****************************
```

APPENDIX D: Listing of Pressure Drop and Flowrate Distribution Routines

This listing contains the routines to calculate the pressure drop and flowrate distribution in a collector or an array of parallel collectors. For these calculations it was assumed that the collectors have the design shown in Figure III.1. Other assumptions and explanations are described in the routines.

```
C*******************************************************
C
C     Main Driving Routine For Pressure Drop Calculation
C
      DIMENSION C(0:10),CD(0:10),M(0:2,0:50),
     1P(0:1,0:50)
      REAL M
C request and read the LFN for all output
      WRITE(3,'(" GIVE LFN FOR OUPUT FILE,
13=screen")')
      READ(3,*)LFN
C read the collector parameters
      CALL READIN(C,CD)
C set total number of risers
      NR=INT(C(7)+.1)
C call the collector callculation routine
C M contains the flow distribution
C P contains the pressure distribution
      CALL COLL(C,CD,M,P)
C generate output
      DO 2 I=1,NR
C calculate the equivalent average flow
      AVERFLOW=REAL(NR)*M(1,I)
C numeric output
      WRITE(LFN,*)'FLOW IN RISER',I,'IS',M(1,I)
     1,'==>AVERFLOW',AVERFLOW
    2 CONTINUE
C graphic output
      CALL OUT(M,NR,LFN)
C average flowrate deviation output
      DV=0.0
      DO 3 I=1,NR
    3 DV=DV+ABS(M(1,I)-C(0)/C(7))/C(0)*100.0
      WRITE(LFN,*)'RELATIVE AVERAGE DEVIATION OVER
     1COLLECTOR:',DV
      STOP
      END
C*******************************************************
```

```
C*****************************************************
C     READIN SUBROUTINE
C
C     this represents the input routine for the
C     pressure drop calculation
C     all units are in SI units, meter, seconds,
C     kilogramm, temperatur is always in degC ! !
C
      SUBROUTINE READIN(C,CD)
      DIMENSION C(0:10),CD(0:10)
      WRITE(3,'(" GIVE LFN FOR INPUT OF COLLECTOR DATA,
     13=screen")')
  100 READ(3,*)XIC
      IC=INT(XIC+.1)
      IF (IC.LE.10.AND.IC.NE.3) THEN
         WRITE(3,'(" LFN NOT ACCEPTABLE TRY AGAIN")')
         J=J+1
         IF(J.GT.3) STOP
         GOTO 100
         J=0
      ENDIF
C
C     the collector data cards do not have to be
C     formatted
C
C     the collector data card has to contain the
C        following information:
C     0. total mass flow through collector [kg/sec]
C     1. width of header          [m]
C     2. length of risers         [m]
C     3. length of external connectors    [m]
C     4. diameter of headers      [m]
C     5. diameter of risers       [m]
C     6. elbow flag (0=no elbows,1=two elbows)  [-]
C     7. number of risers         [-]
C     8. mean assumed collector temperatur   [degC]
C     9. total number of disturbed risers, 0 or >10=no
C        disturbance, valid between 1 and 10 for
C        disturbance
C
C     typicly: .03 .8 1.7 .1 .03 .01 0 6 80 2
C
C     second data card contains the disturbances
C     0. effective length for disturbed riser(s)
C     1. riser number of first disturbed riser
C     2. riser number of second disturbed riser
C     3. riser number of third disturbed riser
C     4. riser number of 4th disturbed riser
C     5. riser number of 5th disturbed riser
```

```
C      6. riser number of 6th disturbed riser
C      7. riser number of 7th disturbed riser
C      8. riser number of 8th disturbed riser
C      9. riser number of 9th disturbed riser
C      10. riser number of 19th disturbed riser
C
C      typicly: 3.4 2 4
C
       READ(IC,*)C(0),C(1),C(2),C(3),C(4),C(5),
      1C(6),C(7),C(8),C(9)
       GOTO (101,102,103,104,105,106,107,108,
      1109,110) INT(C(9)+.1)
       GOTO 111
  101  READ(ICD,*)CD(0),CD(1)
       GOTO 111
  102  READ(ICD,*)CD(0),CD(1),CD(2)
       GOTO 111
  103  READ(ICD,*)CD(0),CD(1),CD(2),CD(3)
       GOTO 111
  104  READ(ICD,*)CD(0),CD(1),CD(2),CD(3),CD(4)
       GOTO 111
  105  READ(ICD,*)CD(0),CD(1),CD(2),CD(3),CD(4),CD(5)
       GOTO 111
  106  READ(ICD,*)CD(0),CD(1),CD(2),CD(3),CD(4),CD(5)
     1,CD(6)
       GOTO 111
  107  READ(ICD,*)CD(0),CD(1),CD(2),CD(3),CD(4),CD(5)
     1,CD(6),CD(7)
       GOTO 111
  108  READ(ICD,*)CD(0),CD(1),CD(2),CD(3),CD(4),CD(5)
     1,CD(6),CD(7),CD(8)
       GOTO 111
  109  READ(ICD,*)CD(0),CD(1),CD(2),CD(3),CD(4),CD(5)
     1,CD(6),CD(7),CD(8),CD(9)
       GOTO 111
  110  READ(ICD,*)CD(0),CD(1),CD(2),CD(3),CD(4),CD(5)
     1,CD(6),CD(7),CD(8),CD(9),CD(10)
  111  RETURN
       STOP
       END
C*******************************************************
```

```
C*****************************************************
C     PRESSURE DROP OF SINGLE COLLECTOR SUBROUTINE
C
C     this represents the routine for the pressure drop
C     calculation of a single collector
C     assumptions:
C     isothermal
C     the two elbows have R/D=4
C     all piping is smouth
C     input is array C(i), it specifies the collector
C     design
C     all units are in SI units, meter, seconds,
C     kilogramm, temperatur is always in degC ! !
C
C     P and M are the return variables
C
C     PD is the total collector pressure drop
C     (incl.elbow and connectors)
C     and returned under P(0,0)
C
      SUBROUTINE COLL(C,CD,M,P)
      DIMENSION C(0:10),CD(0:10),M(0:2,0:50),
     1P(0:1,0:50)
      REAL M,LAMDA,NUE
      P(0,0)=0.
      M(0,0)=C(0)
      NR=INT(C(7)+.1)
      J=0
      PGO=P(0,0)-.01*C(2)*.81*(C(0)/2.)**2/
     1((C(5)**5)*RO(C(8)))*SIGN(1.,C(0))
      P(1,0)=PGO
      CALL COLL1(C,CD,M,P)
      DMO=M(0,0)-M(2,NR)
      P(1,0)=PGO*(4./(C(7)*C(7)))
      DO
      CALL COLL1(C,CD,M,P)
      DMN=M(0,0)-M(2,NR)
      EXIT DO IF(ABS(DMN/M(0,0)).LE.1.E-4)
      BV=(DMN-DMO)/(P(1,0)-PGO)
      AV=DMN-BV*P(1,0)
      DMO=DMN
      PGO=P(1,0)
      P(1,0)=-AV/BV
      J=J+1
      UNTIL(J.GT.200)
      PD=P(1,NR)-P(0,0)
      RE=1.27*ABS(M(0,0))/(C(4)*NUE(C(8))*RO(C(8)))
      PD=PD-(.81*LAMDA(RE)*M(0,0)*M(0,0)/
     1(RO(C(8))*(C(4)**5))*(2.*C(3)+
```

```
     2C(1)/C(7))-.178*M(0,0)*M(0,0)*C(6)/(RO(C(8))*
     3(C(4)**4)))*SIGN(1.,M(0,0))
      P(0,0)=-PD
 1000 RETURN
      STOP
      END
C*******************************************************



C*******************************************************
C   MASSFLOW THROUG A COLLECTOR WITH GIVEN 1ST RISER PD
C
C     this represents the routine for the massflow
C     calculation in an collector
C     assumptions:
C     isothermal
C     all units are in SI units, meter, seconds,
C     kilogramm, temperatur is always in degC ! !
C
C     M flow thru the collector
C
      SUBROUTINE COLL1(C,CD,M,P)
      DIMENSION C(0:10),CD(0:10),M(0:2,0:50),
     1P(0:1,0:50)
      REAL M,MG,LAMDA,NUE
      NR=INT(C(7)+.1)
      DO 100 I=1,NR
      CALL PIPE((C(1)/C(7)),C(4),M(0,I-1),C(8),PD)
      P(0,I)=P(0,I-1)+PD
      CALL PIPE((C(1)/C(7)),C(4),M(2,I-1),C(8),PD)
      P(1,I)=P(1,I-1)+PD
      DP=P(1,I)-P(0,I)
      M(1,I)=SQRT(ABS(DP)*(C(5)**5)*RO(C(8))*
     11.235/C(2))*(-SIGN(1.,DP))
      J=0
      DO
      J=J+1
      MG=M(1,I)
      RE=1.27*ABS(MG)/(C(5)*NUE(C(8))*RO(C(8)))
      M(1,I)=SQRT(ABS(DP)*(C(5)**5)*RO(C(8))*
     11.2337/(C(2)*LAMDA(RE)))
     2*(-SIGN(1.,DP))
      DO 110 K=1,10
      IF(I-INT(CD(K)+.1))110,120,110
  120 M(1,I)=SQRT(ABS(DP)*(C(5)**5)*RO(C(8))*
     11.2337/(CD(0)*LAMDA(RE)))
     2*(-SIGN(1.,DP))
```

```
  110 CONTINUE
      EXIT DO IF(ABS((MG-M(1,I))/M(1,I)).LE.1.E-4)
      UNTIL(J.GT.200)
      M(0,I)=M(0,I-1)-M(1,I)
      M(2,I)=M(2,I-1)+M(1,I)
  100 CONTINUE
      RETURN
      STOP
      END
C*************************************************************



C*************************************************************
C     SUBROUTINE FOR PIPE PD
C
C     this represents the routine for the PD in a pipe
C     assumptions:
C     isothermal
C     all units are in SI units, meter, seconds,
C     kilogramm, temperatur is always in degC ! !
C
C     L=length of pipe
C     D=diameter of pipe
C     F=flow through pipe
C     T=mean assumed temperatur
C
C     PD as output
C
      SUBROUTINE PIPE(L,D,F,T,PD)
      REAL L,LAMDA,NUE
      RE=1.27*ABS(F)/(D*NUE(T)*RO(T))
      PD=-LAMDA(RE)*L/D*.81*F*F/(RO(T)*(D**4))
     1*SIGN(1.,F)
      RETURN
      STOP
      END
C*************************************************************
```

```
C*****************************************************
C     OUTPUT OF MASSFLOW DISTRIBUTION OVER THE COLLECTOR
C     SUBROUTINE
C
C      this represents the routine for the output of the
C      massflow distribution in an array of collectors
C      input is a array M which contains the flowrate
C      in each riser, the total flow through the
C      array (Mcol) and the number of risers
C      (Np=risers in parallel)
C
C      all units are in SI units, meter, seconds,
C      kilogramm, temperatur is always in degC ! !
C
       SUBROUTINE OUT(M,NP,LFN)
       DIMENSION M(0:2,0:50)
       REAL M
       CHARACTER A1*70,A2*6,A3*8,A4*8
       A1='*    ****************************************
      1***********    *'
       A2='*    *'
       A3='*  --*--'
       A4='--*--  *'
       DO 100 I=1,NP
       WRITE(LFN,1000) A2,A2,A2,A2,A3,M(0,I-1),M(2,I-1)
      1,A4,A2,A2,A2,A2,A1,M(1,I),A1
  100  CONTINUE
       WRITE(LFN,1100) A2,A2,A2,A2,A3,M(0,NP),M(2,NP),
      1A4,A2,A2,A2,A2
       DO 110 I=0,NP
       WRITE(LFN,*)M(1,I)
  110  CONTINUE
 1000  FORMAT(A6,58X,A6,/,A6,58X,A6,/,A8,E12.4,30X,
      1E12.4,A8,/,A6,58X,A6
      2,/,A6,58X,A6,/,A70,/,'*',28X,E12.3,28X,'*',/,A70)
 1100  FORMAT(A6,58X,A6,/,A6,58X,A6,/,A8,E12.3,30X,
      1E12.3,A8,/,A6,58X,A6,/,A6,58X,A6)
       RETURN
       STOP
       END
C*****************************************************
```

```
C*******************************************************
C      LAMDA FUNKTION
C
C      this function has to be set to the value real
C      in each subroutine it is used
C      this represents the pipe friction factor for any
C      Reynolds number, for
C      smouth pipe surfaces (expected for e.g. copper)
C      the used formula is for laminar flow 64/Re and
C      for turbulent after the correlation of Prandtl
C      and Karman
C
       REAL FUNCTION LAMDA(RE)
       REAL LAM0,LAM
       IF (RE.LT.0.0) STOP "FUNCTION SUBROUTINE
      1STOP: REYNOLDS < 0"
       IF (RE.GT.2320.0) GOTO 100
       IF (ABS(RE).LT.1.E-30) RE=SIGN(1.E-30,RE)
       LAM=64./RE
       GOTO 200
C
C      first guess for lamda
  100  LAM=.309/((LOG10(RE/7.))**2)
C
C      iteration to find lamda
       J=0
       DO
       J=J+1
       LAM0=LAM
       LAM=1./((2.*LOG10(RE*SQRT(LAM)/2.51))**2)
       EXIT DO IF(ABS((LAM0-LAM)/LAM).LT.1.E-6)
       UNTIL (J.GT.100)
  200  LAMDA=LAM
       RETURN
       STOP
       END
C*******************************************************
```

```
C*******************************************************
C      RO FUNKTION
C
C      this represents the density of water as a
C      function of temperatur
C      temperatur is always in degC ! !
       REAL FUNCTION RO(T)
       TEM=T
       RO=1002.41+.00702*TEM-.0057585*TEM*TEM+1.8153E-5*
      1TEM*TEM*TEM-3.2366E-8*TEM*TEM*TEM*TEM
       RETURN
       STOP
       END
C*******************************************************


C*******************************************************
C      ETA FUNKTION
C
C      this represents the dynamic viscosity of water
C      as a function of temperatur
C      temperatur is always in degC ! !
C
       REAL FUNCTION ETA(T)
       TEM=T
       ETA=1.71676E-3-3.6179E-5*TEM+3.17478E-7*TEM*TEM
      1-1.19919E-9*TEM*TEM*TEM+1.6141E-12*TEM**4
       RETURN
       STOP
       END
C*******************************************************


C*******************************************************
C      NUE FUNKTION
C
C      this represents the dynamic viscosity as a
C      function of temperatur
C      temperatur is always in degC ! !
C
       REAL FUNCTION NUE(T)
       REAL RO,ETA
       TEM=T
       NUE=ETA(TEM)/RO(TEM)
       RETURN
       STOP
       END
C*******************************************************
```

APPENDIX E: Listing of Controller Routines

This listing contains the code of the controller subroutines. They do not include the on/off differential controller, which was simulated by a standard TRNSYS routine. Variable names etc. are explained in the routines.

```
C=================================================C
C*-*-*-*-*-*-*-*-*-*-*-*-*-*-*-*-*-*-*-*-*-*-*-*-*C
C                                                 C
      SUBROUTINE TYPE21(TIME,XIN,OUT,T,DTDT,PAR,INFO)
C                                                 C
C*-*-*-*-*-*-*-*-*-*-*-*-*-*-*-*-*-*-*-*-*-*-*-*-*C
C
C-------------------------------------------------C
C     PROPORTIONAL CONTRTOLLER FOR SDHW SYSTEM     C
C     CONCOMITANT WITH AN ON/OFF CONTROL DECISION  C
C     AND A COUNTING ROUTINE TO CHECK FOR CYCLING  C
C     PARAMETER DESCRIPTION SEE BELOW              C
C-------------------------------------------------C
      DIMENSION XIN(10),PAR(15),OUT(20),INFO(10)
      REAL ML,MH,MDOT
      SAVE IXCON1,IXCON2,IX
      IF (INFO(7).GE.0) GO TO 1
C-------------------------------------------------C
C  FIRST CALL OF SIMULATION                       C
C-------------------------------------------------C
      INFO(6)=2
      INFO(9)=1
      CALL TYPECK(1,INFO,4,5,0)
      IXCON1=0
      IXCON2=0
C-------------------------------------------------C
C  DID THE ON/OFF CONTROLLER CHANGE ITS           C
C  OUTPUT SINCE THE LAST TIME                     C
C-------------------------------------------------C
    1 IF (INFO(7).GE.1) GOTO 10
      IF (IXCON1.NE.IXCON2) THEN
         IX=IX+1
         IXCON2=IXCON1
      ENDIF
C-------------------------------------------------C
C  SET PARAMETER AND INPUT VARIABLES              C
C-------------------------------------------------C
C  LOWEST FLOWRATE
   10 ML=PAR(1)
C  HIGHEST FLOWRATE
      MH=PAR(2)
C  FLOWRATES RATIO
      FRR=MH/ML
C  DEVIATION STEP SIZE FOR CHANGE IN CONTROL DECISION
      DS=PAR(3)
C  SET TEMPERATURE FOR THE CONTROL DECISION
      TSET=PAR(4)
C  OVERHEAT TEMPERATURE TO ALLOW SOME EXTRA DEGREES
      DTOVHE=PAR(5)
```

```
C  SUMMATION SETTING FOR ON/OFF CONTROLLER SWITCHES
      IXCON1=INT(XIN(1)+.1)
C  ON/OFF CONTROLLER OUTPUT
      X1=XIN(1)
C  OLD CONTROL VARIABLE
      X2=XIN(2)
C  CONTROL TEMPERATURE (COLLECTOR OUTPUT TEMPERATURE)
      TCO=XIN(3)
C  FLOWRATE WITH LAST CONTROLLER SETTING
      MDOT=XIN(4)
C-------------------------------------------------------C
C  COMPUTE THE PROPORTIONAL CONTROLLER SETTING          C
C  IN DEPENDANCE OF THE PREVIOUS SETTING AND            C
C  RESTRICT THE OUTPUT TO NUMBERS OF 1-FRR OR 0         C
C-------------------------------------------------------C
C  THEORETICAL LOW FLOWRATE TEMPERATURE
        TTHEORY=(TCO-DTOVHE)*MDOT/ML
C  CONTROLLER DECISION
        X=TTHEORY/TSET
C  CONSTRAINTS
      IF(X2.GT.0.0)
        IF(ABS(X/X2).LT.(1.+DS)) X=X2
      ENDIF
      IF(X.GT.FRR) X=FRR
      IF(X.LT.1.) X=1.
      X=X*X1
C-------------------------------------------------------C
C  SET OUTPUTS --                                       C
C-------------------------------------------------------C
      OUT(1)=REAL(IX)
      OUT(2)=X
      RETURN
      STOP
      END
C=======================================================C
```

```
C=====================================================C
C*-*-*-*-*-*-*-*-*-*-*-*-*-*-*-*-*-*-*-*-*-*-*-*-*-*-*C
C                                                     C
      SUBROUTINE TYPE21(TIME,XIN,OUT,T,DTDT,PAR,INFO)
C                                                     C
C*-*-*-*-*-*-*-*-*-*-*-*-*-*-*-*-*-*-*-*-*-*-*-*-*-*-*C
C
C-----------------------------------------------------C
C     INTEGRAL/PROPORTIONAL CONTROLLER FOR SDHW        C
C     SYSTEM                                          C
C     PROPORTIONAL CONTRTOL DOMINANT OVER INTEGRAL    C
C     CONTROL FOR HIGHER OUTPUT                       C
C     CONCOMITANT WITH AN ON/OFF CONTROL DECISION     C
C     AND A COUNTING ROUTINE TO CHECK FOR CYCLING     C
C     PARAMETER DESCRIPTION SEE BELOW                 C
C-----------------------------------------------------C
C
      DIMENSION XIN(10),PAR(15),OUT(20),INFO(10)
      REAL ML,MH,MDOT
      SAVE IXCON1,IXCON2,IX,ALPHA,COLM
      IF (INFO(7).GE.0) GO TO 1
C-----------------------------------------------------C
C  FIRST CALL OF SIMULATION                           C
C-----------------------------------------------------C
      INFO(6)=2
      INFO(9)=1
      CALL TYPECK(1,INFO,4,8,0)
      IXCON1=0
      IXCON2=0
C-----------------------------------------------------C
C  DID ON/OFF CONTROLLER CHANGE ITS                   C
C  OUTPUT SINCE THE LAST TIME                         C
C-----------------------------------------------------C
    1 IF (INFO(7).GE.1) GOTO 10
      IF (IXCON1.NE.IXCON2) THEN
         IX=IX+1
         IXCON2=IXCON1
      ENDIF
C-----------------------------------------------------C
C  SET PARAMETER AND INPUT VARIABLES                  C
C-----------------------------------------------------C
C  LOWEST FLOWRATE
   10 ML=PAR(1)
C  HIGHEST FLOWRATE
      MH=PAR(2)
C  FLOWRATES RATIO
      FRR=MH/ML
C  DEVIATION STEP SIZE FOR CHANGE IN CONTROL DECISION
      DS=PAR(3)
```

```
C  SET TEMPERATURE FOR THE CONTROL DECISION
      TSET=PAR(4)
C  OVERHEAT TEMPERATURE TO ALLOW SOME EXTRA DEGREES
      DTOVHE=PAR(5)
C  SIMULATION TIME STEP
      DELT=PAR(6)
C  TOTAL COLLECTOR RUNNING TIME PER DAY
      TCT=PAR(7)
C  WUESTLING FACTOR
      WF=PAR(8)
C  SUMMATION SETTING FOR ON/OFF CONTROLLER SWITCHES
      IXCON1=INT(XIN(1)+.1)
C  ON/OFF CONTROLLER OUTPUT
      X1=XIN(1)
C  OLD CONTROL VARIABLE
      X2=XIN(2)
C  CONTROL TEMPERATURE (COLLECTOR OUTPUT TEMPERATURE)
      TCO=XIN(3)
C  FLOWRATE WITH LAST CONTROLLER SETTING
      MDOT=XIN(4)
C-------------------------------------------------------C
C  COMPUTE INTEGRAL CRITERIA FOR CONTROLLER SETTING   C
C  IN DEPENDANCE OF THE PREVIOUS SETTING, TIME OF DAY C
C  AND ACTUAL FLOWRATE                                C
C-------------------------------------------------------C
C  TIME OF DAY
      DTIME=(TIME/24.-INT(TIME/24.))*24.
C-------------------------------------------------------C
C  SET ALL DAILY INTEGRATED VALUES                    C
C  TO 0 FOR TIME < 1am                                C
C-------------------------------------------------------C
      IF(DTIME.LT.1.0) THEN
         COLM=0.0
         ALPHA=0.0
      ENDIF
C-------------------------------------------------------C
C     CALCULATE ALPHA                                  C
C-------------------------------------------------------C
      SPO=0.0
      IF(DTIME.GT.(12.-TCT/2.).AND.
     1DTIME.LT.(12.+TCT/2.)) SPO=1.0
      ALPHA=ALPHA+SPO*DELT/TCT
C-------------------------------------------------------C
C  INTEGRAL OF DAILY COLLECTOR FLOW SO FAR            C
C-------------------------------------------------------C
C  COLLECTOR FLOWRATE INTEGRAL
      COLM=COLM+MDOT*DELT
C  FLOWRATE FACTOR BETA1
      BETA1=0.0
```

```
      IF(COLM.GT.0.0)THEN
         BETA1=ALPHA*260.*WF/COLM
      ENDIF
C-----------------------------------------------------C
C  COMPUTE THE PROPORTIONAL CONTROLLER SETTING        C
C  IN DEPENDANCE OF THE PREVIOUS SETTING              C
C-----------------------------------------------------C
C  THEORETICAL LOW FLOWRATE TEMPERATURE
      TTHEORY=(TCO-DTOVHE)*MDOT/ML
C  CONTROLLER DECISION BETA2
      BETA2=TTHEORY/TSET
C-----------------------------------------------------C
C  CONSTRAINTS:                                       C
C  RESTRICT THE OUTPUT TO NUMBERS OF 1-FRR OR 0       C
C-----------------------------------------------------C
      X=MAX(BETA1,BETA2)
      IF(X2.GT.0.0)
        IF(ABS(X/X2).LT.(1.+DS)) X=X2
      ENDIF
      IF(X.GT.FRR) X=FRR
      IF(X.LT.1.) X=1.
      X=X*X1
C-----------------------------------------------------C
C  SET OUTPUTS --                                     C
C-----------------------------------------------------C
      OUT(1)=REAL(IX)
      OUT(2)=X
      RETURN
      STOP
      END
C=====================================================C
```

REFERENCES

[1] Wuestling, M.D., "Investigation of Promising Control Alternatives for Solar Water Heating Systems", M.S. Thesis in Mechanical Engineering, University of Wisconsin-Madison (1983).

[2] van Koppen, C.W.J., Thomas, J.P.S. and Veltkamp, W.B., "The Actual Benefits of Thermally Stratified Storage in a Small and a Medium Size Solar System", Eindhoven University of Technology, Eindhoven, The Netherlands (1980).

[3] Lunde, P.J., "How To Improve DHW Performance", Solar Age, Aug. 1985.

[4] Hollands, K.G.T., Richmond, D.A. and Mandelstam, D.R. "Re-Engineering Domestic Hot Water Systems for Low Flow", ISES International Congress 1985, Montreal, Poster Session A-11.

[5] Sharp, K., "Thermal Stratification in Liquid Sensible Heat Storage", M.S. Thesis in Mechanical Engineering, Colorado State University, Ft. Collins (1978).

[6] Karaki, S., Loef, G.O.G., Brisbane, E.T., Wiersma, D. and Cler, G., "A Liquid-Based Flat-Plate Drain-Back Solar Heating and Cooling System for CSU Solar House III", DOE Report No. SAN-11927-29, May 1985.

[7] Solar Energy Intelligence Report, 11, No. 29, p. 251, July 22, 1985.

[8] Fanney, A.H. and Klein, S.A., "Thermal Performance Comparisons for Solar Domestic Hot Water Systems Subject to Various Collector Array Flow Rates", ISES International Congress 1985, Montreal, Poster Session A-11.

[9] Solar Energy Labratory, "TRNSYS - A Transient System Simulation Program", Version 12.1, University of Wisconsin - Madison, 1983.

[10] Duffie, J.A. and Beckman, W.A., Solar Engineering of Thermal Processes, Wiley, New York, 1980.

[11] Fanney, A. H. and Klein, S.A., "Performance of Solar Domestic Hot Water Systems at the National Bureau of Standards - Measurements and Predictions", Journal of Solar Energy Engineering 105, 311-321, August 1983.

[12] Morrison, G.L. and Braun J.E., "System Modelling and Operation Characteristic of Thermosyphon Solar Water Heaters", Solar Energy Labratory, University of Wisconsin-Madison, 1983.

[13] Malkin, M.P., personal communications, Madison, WI, (1984,85).

[14] Cole, R.L. and Bellinger, J.O., Solar Energy Group, "Natural Stratification in Tanks", Argone National Labratory, IL, February 1982.

[15] Veltcamp, W.B. and van Koppen, C.W.J., "Optimization of the Flows in a Solar Heating System", Eindhoven University of Technology, Eindhoven, The Netherlands, September 1982.

[16] Lavan, Z. and Thompson, J., "Experimental Study of Thermally, Stratified Hot Water Storage Tanks", Solar Energy 19, 519-524, 1977.

[17] Sunstrip International Corp., ISES International Congress 1985, Intersol 85 Exhibition.

[18] Fanney, A.H., personal communications, Gaithersburg, MD, (1984, 1985).

[19] Karaki, S., personal communications, Ft. Collins, CO, (1985).

[20] Duffie, J.A. and Klein, S.A., personal communications, Madison, WI, (1984, 1985).

[21] Armstrong, P. Research Associate CSU and Winn, C.B., Principal Investigator CSU, correspondence, Ft. Collins, CO, July 1985.

[22] Dunkle, R.V. and Davey, E.T. "Flow Distribution in Solar Absorber Banks", ISES International Congress 1970, Melburne.

[23] Davey, E.T. and Rodgers, A. "Flow Distribution in Forced Circulation Solar Water Heater Banks", Report CISRO Division of Mechanical Engineering, 1974.

[24] ASHRAE, Standard 93-77, American Society of Heating, Refrigeration, and Airconditioning Engineers, "Methods of Testing to Determine the Thermal Performance of Solar Collectors", New York, 1977.

[25] Siemens, A.G., Technische Tabellen, Ausgabe 1984.

[26] Zeitz, M., "Analog- and Digital-Simulation Technicts", Lecture, University of Stuttgart (1984).

[27] Fanney, A.H., correspondence, Gaithersburg, MD, (Jan. 1985).

[28] Beitz, W. und Kuettner, K.-H., Dubbel, Taschenbuch fuer den Maschinenbau, Springer-Verlag, Berlin, Heidelberg, New York, 14 Auflage, 1981.

[29] Karaki, S., Brisbane, E.T. and Loef, G.O.G., "Performance of the Solar Heating and Cooling System for Solar House III Summer Season 1983 and Winter Season 1983-84", DOE Report No. SAN-11927-15, July 1984.

[30] ACE 2.3, "Analysis of Collector Efficiency", Energy Management Analysis of Madison, J. Braun, Madison, WI, 1984.

[31] Fanney, A.H., correspondence, Gaithersburg, MD, (Aug. 1985).

[32] Winn, B.C., "Controls in Solar Energy Systems", in "Advances in Solar Energy", American Solar Energy Society Inc., 1983.

[33] Solar Energy Research Institute, "Controllers for Solar Domestic Hot Water Systems", Report under Subcontract No. AH-9-8189-1, Golden, CO, Oct. 1981.

[34] Mumma, S.A., "Field Testing of Systems Using Controls to Enhance Thermal Stratification During Solar Collection", ASHRAE Transactions 1985, 91, Pt. 2.